MECHATRONIC DEVICES FOR THE INVESTIGATION OF FIBROBLAST POPULATED COLLAGEN LATTICES AND THE APPLICATION OF PRECISE MECHANICAL LOADS

Thesis submitted for the Degree of

Doctor of Philosophy

in the

Faculty of Medicine

at the

University of London

by

Mark Eastwood

Department of Surgery

University College and Middlesex Hospitals Medical School

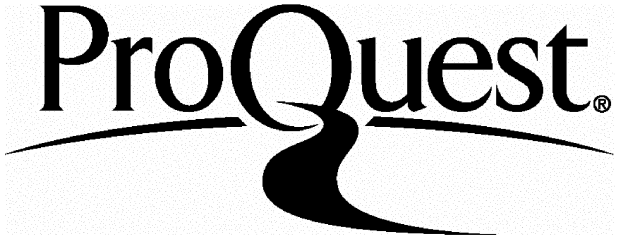

Abstract.

In this study mechatronic devices have been designed and developed that enable quantitative analysis of fibroblast populated collagen lattices (FPCL) to be made. The Culture Force Monitor (CFM) enables forces as low as 1 dyne (1×10^{-5}N) to be made of the contraction of FPCLs whilst growing in culture.

The CFM has enabled the force of contraction to be quantified over a range of cell lines and types. Each normal human dermal fibroblast can produce an average force of approximately 10^{-10}N. The contraction process can be divided into 3 distinct phases during the initial 24 hrs. These phases are hypothesised to be due to the processes of cell attachment and spreading. This has been tested using the CFM in conjunction with a stereoscopic microscope to relate the initial phase of contraction (0-8hrs) with the morphological changes in the cells. There was a positive correlation between development of force with time and the shape and extension of cell processes.

Disruption of cytoskeletal elements can either increase or decrease the measured force. Disruption of microtubules with colchicine or vinblastine elicited an immediate rise in force, whilst disruption of microfilaments with cytocholasin B caused an immediate fall in force. Based on these observations a hypothesis has been proposed for cytoskeletal function based on a 'balanced space frame' model within the cell.

The tensioning-Culture Force Monitor (t-CFM) was developed from the CFM. This instrument utilises a computer controlled microdriver to apply precise loads to FPCLs, whilst simultaneously measuring the actual force applied. Mechanically loading fibroblasts by approximately 20% above the endogenous force elicited an opposite mechanical response. This may represent a form of 'tensional homeostasis' within cells in a 3D matrix or tissue. Mechanically loaded fibroblasts appear to adjust matrix tension back towards the pre loading levels. Cellular orientation and

morphology is also altered by mechanical loading, leading to a hypothesis that cells become orientated with iso-strains to reduce the perceived loading.

Contents.

Index to figures and tables.

Chapter 2

Chapter 3

Chapter 4

Chapter 5

Chapter 6

Acknowledgements

I would like to thank my project supervisor, Dr. Robert Brown for many things, for being enthusiastic with new ideas, for being supportive of not so new ideas, for being kind with my stupid ideas, for answering biologically fundamental questions with patience, and, above all, for being my friend.

I would also like to thank Professor Gus McGrouther for enduring a mechanical engineer in the department of plastic surgery, and most importantly, for supporting me and my work for the past 3 years with a constant supply of enthusiasm and encouragement.

My eternal gratitude is extended to my wife, Sally, and my children Jennifer, Naomi, Rachel and Anna for allowing to become an 'absent father and husband' whilst completing this work.

I would like to thank Miss Rebecca Porter for preparation of TEM specimens and proof reading this thesis, Miss Kirsty Smith for SEM preparation and microscopy and photography. Dr Umraz Khan for the supply of rabbit tendon fibroblasts, Dr Adel Wilson for normal human fascia cells, Dr David Lee for bovine articular chondrocytes, and Mr Zubair Ahmed for imunohistochemical analysis.

This work was funded by the Phoenix trust and Pearl Assurance.

Chapter 1: General Introduction.

1.1) Wound Closure.

The rapid closure of a wound is a basic biological process common to all high order mammals. The closure prevents the escape of body fluids and stops the ingress of bacteria (Rudolph et al, 1992). Much of this rapid closure is due to wound contraction where the edges of a wound are drawn to the centre (Abercrombie et al, 1956, 1960, Highton and James 1964, Van Winkle 1967 Peacock 1984, Clark 1988). The closure of a wound is thought to be a cell mediated event, however it is unclear whether the contractile forces involved are generated by the locomotion of fibroblasts, tractional forces (Harris et al 1980, 1981), or by the contraction of a differentiated fibroblast, the myofibroblast (Gabbiani et al, 1972). In this study experimental equipment has been devised to enable the quantitative analysis of both fibroblast derived collagen gel contraction and the assesment of mechanical stimulation of fibroblasts whilst seeded in a collagen gel.

1.2) The Fibroblast.

The fibroblast is a mesenchymal cell that is responsible for normal connective tissue turnover and if not engaged in this activity is a

quiescent fibrocyte situated in the connective tissue (Grinnell 1994). When a wound is created, damage occurs to the connective tissue and blood vessels, resulting in the release of plasma proteins and blood cells into the wound site, (Khaw et al, 1994). The release of these growth factors causes fibroblasts to migrate into the wound bed, proliferate, and synthesise a new collagen rich matrix comprising the granulation tissue, it is during this phase that wound contraction starts. Once the wound is closed remodelling of the granulation tissue begins, the process of remodelling occurs over a period of up to 6 weeks (Kerstein 1995, Weihrauch et al 1994), depending upon the type and depth of wound. In extreme cases of overactivety, this remodeling process can cause scar contracture. The result can be loss of function, deformity, pain, and even dislocation of joints, (Ruldolph 1984). At the end of the remodeling phase it is thought that such fibroblasts revert back to a fibrocyte phenotype (Grinnell 1994). The act of migration may also cause some of the tension to be generated (Harris et al, 1981) and it has been elequently argued that this initial tension may be the cause of the differentiation of a fibroblast into a myofibroblast (Grinnell 1994).

1.3) The Myofibroblast.

The myofibroblast is a differentiated form of the fibroblast, this cell type is identified by the presence of α smooth muscle actin in the form of stress

fibres and ruffles in the nucleus. The name "myofibroblast" was given since these cells were able to exhibit a smooth muscle like contraction in vivo (Gabbiani et al, 1972).

1.4) Cytoskeleton, Fibroblast Shape and Function.

Fibroblast shape whilst within a 3D matrix or a Fibroblast Populated Collagen Lattice (FPCL) is controlled by its cytoskeletal elements within the cell (Tomosek and Hay 1984). The acquisition of bipolarity and the elongation of cell is dependant on microtubules and microfilaments (Tomasek and Hay 1984). Microtubules are one of the main structural components of the cell, these are tubes of about 25nm outside diameter normally composed of 13 protofilaments (Chen et al 1995, Afzelius et al 1995) the principle component being tubulin monomer. Microtubules are not fixed or permanent structures within the fibroblast, but change in length and number depending on the internal state of the cell. A variety of functions are performed by the microtubules; cell movement, maintenance of cell shape, and the intracellular transport of granules and vesicles (Akalin et al 1995,Rasmussen et al 1992, lampidis et al 1992).

Microfilaments are polymers of the protein α-actin monomer (outside diameter 6nm) (Schwienbacher et al 1995). Microfilaments can grow or

shrink depending on the internal state of the cell. They appear to act in close association with the microtubules, the internal energy balance in the cell is dependant on the co-operation of microtubules and the microfilaments. Microfilaments connect to the extra-cellular matrix through the cell membrane receptors (integrins) for specific sites on so called adhesion proteins. The contractile properties of the microfilaments comes from the involvement of the protein myosin, which forms actomyosin complex (Bershadsky and Vasiliev 1988, Trinkaus 1984, Pollard et al, 1976, Danowalski 1989). The mechanical tension generated by the actomyosin interaction is thought to be responsible for the ability of fibroblasts to move and ultimately to contract a collagen lattice.

1.5) Collagen.

Collagen is the main structural protein of connective tissue, indeed 25% of the total body protein is collagen (Bell 1995). To-date 18 or 19 genetically different types of collagen have been identified (Mayne and Brewton 1993), 90% of the total body collagen content is comprised of type I, being the major collagen species found in skin, tendon, bone, cornea, annulus fibrosus, lung, liver and muscle (Weiss 1982).

Soluble collagen was first extracted by Nageotte (1927) from rat tails by the action of dilute acetic acid. This method extracts intact tropocollagen, in contrast to the more recent pepsin extraction techniques where teleopeptides are lost, (Cockburn and Barns 1991) fibril formation is altered in the absence of such telopeptides, (Leibovich and Weiss 1970). The formation of fibrils from soluble collagen solution has been extensively studied (Wood 1960, Wood and Keetch 1960) in the hope that studies of the in vitro process would provide some insight into fibrillogenesis observed in vivo. In effect, at neutral pH, acid soluble collagen rapidly aggregates to form fibrils at 37^0C which will give a gel or 3D collagen lattice.This can be reversible and will re-disolve at 4^0C.

1.6) Previous Models of Fibroblast Contraction.

Fibroblast growth when suspended in a reconstituted collagen lattice was studied nearly 40 years ago (Ehrmann and Grey 1956), more recent studies (Elsdale and Bard 1972) also observed fibroblasts in a collagen lattice, when they reported that the collagen gel had been reduced to a "dense opaque body less than 1/10 of the original size". Bell et al, (1979) began studying the collagen reorganisation as an in-vitro model of wound contraction and produced the now classic paper on the production of a tissue like structure by contraction of collagen by fibroblasts. Since that

time many models of fibroblast generated forces have been reported. Fibroblasts when grown on a thin film of silicon rubber substrata will cause wrinkling, apparently due to tractional forces produced by cell locomotion, (Stopak, Harris and Wild, 1980, Harris 1981). In this model a thin layer of silicon is put onto a glass coverslip, and cross-linked by the action of heat. Fibroblasts can then be seeded and cultured on the silicon layer, the contraction by the fibroblasts eventually produces wrinkling of the silicon film.

This experimental model was first devised by Carter (1967), and then elaborated by Harris (1973) and Letourneau (1975). The main drawback with this model is that quantitative measurements of forces generated by fibroblast traction are not accurate. The wrinkles observed by fibroblast traction have been correlated with the number of wrinkles generated in the silicon rubber by known externally applied mechanical loads to produce estimates of the forces generated. Difficulties include variability in thickness of the silicon film, adhesiveness of the silicon film to fibroblasts due to its limited wetability, and restriction to fibroblast monolayer cultures. Cells under these conditions do not behave as their in vivo counterpart in the extra-cellular matrix or as the fibroblast suspended in 3D collagen lattice. Consequently comparisons are difficult to make between the FPCL, and its connective tissue counterpart, and the silicon rubber membrane technique. However for all its technical

limitations this model is in widespread use today as a quick assay of fibroblast generated tension (Khaw et al, 1994, Danowalski 1988).

Models that investigate the behaviour of fibroblasts whilst suspended in a 3D matrix have also been used. The technique of Bell, Iversson and Merrell (1979) of fibroblast contraction of a free floating collagen lattice is still in widespread use (Bellows et al, 1982, Farsi and Aubin 1984, Guildry and Grinnell 1985, Tranquillo and Murray 1992, Ehrilch and Rajarathan 1990, Finesmith et al, 1990, Garner et al, 1995) The diameter of the gel is measured optically over the major and minor axis, or the total area estimated by image analysis. From this data graphs can be constructed that show the relationship between the reduction in gel diameter or area with time. This system is limited in that it relies on operator dependant measurements of size and assumes that the gel remains a flat disc. In a variant of this method deformation of the gel is visualised by measuring the diameter of a ring of cells as the gel contracts. Computer based image analysis (Finesmith, Broadley and Davidson 1990) improves the analysis where the FPCL is placed over a grid and photographed. Image analysis allows an extremely accurate measurement to be made of the gel surface area.

All these systems suffer from two major flaws (i) no direct measurement of force is made, and (ii) the gel is fully floating and so not subjected to

the restraining effects of the surrounding connective tissue. In vivo any contraction is subject to a reactive force from the wound margins, i.e. the tissue is mechanically tethered. Also the number of collectable data points is limited, restricting the ability of the system to distinguish any short term effects, possibly making graphs unreliable.

Free floating gels have a disadvantage over tethered gels in that the fibroblasts are unstressed. It is argued that the fibroblast under these conditions is more representative of the fibrocyte than the fibroblast, in that the cell is stellate and quiescent, i.e. not producing collagen or proliferating (Nishiyama et al, 1989, Nakagawa et al, 1989). These features are similar to those found in dermis whereas in the anchored or tethered gel the morphological and proliferative features of the cells is more representative of granulation tissue (Nishiyama et al, 1989, Nakagawa et al, 1989). The absence of such reactive mechanical loadings is particularly important as fibroblasts are widely believed to respond in a complex manner to tensile forces in their matrix (Eastwood et al, 1994, 1996).

Tethered forms of the FPCL systems have been developed (Guidry and Grinnell 1986). Collagen lattices were cast and allowed to remain tethered to the petri dish, reductions in gel thickness were then measured using a microscope at the centre of the petri dish over a period of days as

the fibroblasts contract down the collagen matrix. Forces generated by the contraction of a tethered FPCL whilst floating in culture medium have been measured directly (Vandenberg, 1988,1989,1995, Kasugai et al, 1990, Kolodney and Wysolmerski, 1993, Eastwood et al, 1994, 1996). In the system of Kasugai et al, (1990) a FPCL was attached between two stainless steel meshes, one fixed to the side of a petri dish and the other supported by two fishing floats. An attachment was made to a force transducer and force measurements made and recorded as the FPCL contracted. This system relied on analogue technology with data being logged on a chart recorder. More recently a description of an instrument was made, that again relied on analogue technology, but had the advantage of being contained with its own mini incubator (Delvoye et al, 1991). The collagen gel was attached to glass rods via Velcro strips. The two glass rods were immobilised and so an isometric force measurement system was achieved, however the small movements required for transmission of the strain to the strain gauges was subject to high frictional losses. This system is relatively insensitive, calibration was with masses that ranged from 1g to 5g.

An instrument by Kolodney and Wysolmerski (1992) circumvented many of these problems, in that entire FPCL and attachments to the measuring device were floated. In their system the FPCL was cast between the microporous polyethylene bars in a silicon elastomer well, which when

filled with culture medium caused the FPCL to float and so provided a friction free measurement device. The force transducer was based on capacitance difference which required very little movement to transmit the strain and so could be described as an isometric measurement device.

1.7) Disruption of the Cytoskeleton

The CFM provides a powerful method to assess the process of fibroblast contraction of a collagen gel since it produces a continuous and precise, computer-based record of force output from living cells as they interact with the collagenous substrate. Previous work with the CFM has shown that contractile forces are generated almost immediately after the collagen gel has formed and correspond most closely with cell attachment to the collagen and extension of processes into the matrix (Eastwood et al, 1996). Since this interaction clearly involves the participation of cytoskeletal elements of the fibroblasts, the CFM can also be used as a tool for quantitative, experimental assessment of the part played by individual cytoskeletal elements. A range of cytoskeletal disrupters have been used in previous studies in attempts to examine this question, in both quantitative and qualitative systems (Luduena and Roach, 1981, Danowski and Harris, 1988). These have included microtubule disrupting agents such as colchicine and vinblastine and the

microfilament poison, cytochalasin B. In free-floating FPCL's each of these classes of agent inhibit contraction (Rudolph, 1980) though the relevance of this, to cells in a tethered system (i.e. subject to a reactive mechanical response) remains in question. Both increases and decreases in contraction of collagen lattices have been reported following microtubule disruption (Kolodney and Wysolmersky, 1992; Delvoye et al, 1991; Danowski, 1989). These were explained either through a mechanical mechanism (Kolodney and Wysolmersky, 1992), based on cytoskeletal loading and the tensigrity model (Ingber, 1993) or by biochemical regulation of motor elements in the cell (Kolodney and Elson, 1995). Clearly, though, the detailed mechanism is not understood and the role of microtubules remains unclear. A better understanding of cytoskeletal function, in particular the action of microtubules, would appear to be pivotal, therefore, in explaining events during collagen contraction. Detailed, quantitative data on force changes from the CFM have been used here as the basis for a new concept describing the role of microtubules in regulating forces within fibroblasts and their potential importance in contraction and collagen organisation.

1.8) Cytotoxic Drugs.

1.81) Colchicine.

Colchicine is a naturally occurring drug extracted from the meadow saffron, whilst colcemid is a synthetic analog with similar actions. This antimitotic alkaloid drug works by binding onto the tubulin molecule so that it cannot polymerise (Hennessey et al 1991). This drug has no effect on polymerised tubulin, and only binds to the depolymerised tubulin or the protein monomer rendering it unable to participate in the microtubule formation. As the process of de-polymerisation continues (i.e treadmilling) as normal, but with the re-assembly blocked the microtubules eventually become completely fragmented.

1.82) Vinblastine Sulphate.

Vinblastine sulphate is a naturally occuring drug that is extracted from the plant Vincra rosea. Other members of the vinca alkaloid group of drugs extracted from this plant include vincristine sulphate, and vindisine sulphate. These drugs work by interfering with the microtubule assembly, all these drugs have similar activity but the predominate site for the toxicity varies. By interfering with the microtubule assembly these drugs have the same net effect as colchicine and colcemid. The process of

treadmilling continues as normal, so eventually the microtubules become completely fragmented (Parry 1993).

1.83) Taxol.

Taxol is a drug, extracted from the bark of the Pacific yew tree, Taxus brevifolia, with the effect of stabilising the microtubules by binding tightly to the polymerised tubulin and reducing its rate of depolymerisation. Taxol also has the effect of causing the free tubulin pool to polymerise reducing it to polymerised segments (Slichenmyer and Von Hoff, 1990).

1.84) Cytochalasin B.

Cytochalasin B is a drug of fungal origins, it has the net effect of depolymerising the microfilaments by binding to the end of the microfilament that is responsible for polymerisation. The minus end still de-polymerises so the actin microfilament over a period of time gets reduced (Lewis-Alberti 1989).

1.9) Mechanical Stimulation.

Mechanical stimulation is known to have a direct effect on scar formation, pressure bandages are in common use for victims of deep burns (Ward

1991, Kischer et al 1975), and have therapeutic effects during the healing of chronic venous ulcers (Herrick et al, 1992). In the latter, it was reported that after 2 weeks of pressure bandage therapy major histological changes had occured. Incorrect methods of suturing a wound can lead to an increase in scar tissue formation. All these effects are presumed to be due to mechanical stimulation of fibroblasts whilst remodelling the connective tissue of a wound.

The effect of mechanical stress on fibroblast populations in collagen matrix has been studied previously. These studies have ranged from the stress effect on cyclic AMP pathway (He and Grinnell, 1994), the up-regulation of Tenascin C (Chiquet-Ehrismann et al, 1994), to the effect on the free intercellular calcium ion concentration, (Arora, Bibbly and McCulloch 1994). Margolis and Popov (1991) reported that the application of a local force to mouse embryo fibroblasts caused an induction of cell processes. The effect of mechanical load on collagen expression was studied by Carver et al, (1991), who found that the ratio of collagen type III to collagen type I increased in response to mechanically stretched cells. Lambert et al, (1992) found that a modulation of the function of fibroblasts could be effected by the application of mechanical stress. Butt et al, (1995) reported that fibroblasts in a collagen gel that was subjected to external mechanical stress resulted in increased cell growth and proliferation.

Methods for the application of mechanical stimulation differs. Sudden release of the loading across an attached lattice causes an effect known as strain recovery, or stress relaxation, (Mochitate et al, 1991, He and Grinnell, 1994.) In these experiments the collagen lattice was allowed to remain attached to the culture well for a number of days, (fibroblasts become stellate, contracted the gel thickness, and produced an internal strain). When the gel was released from the culture well a rapid contraction of the gel was seen. This has been likened by Grinnell (1994) to the transition from granulation tissue to dermis. Morphologically, the fibroblasts change during this strain recovery from large stellate or bipolar cells to rounded cells with the retraction of pseudopodia and the collapse of actin bundles, (Tomasek et al, 1992, Mochitate et al, 1991, Grinnell 1994).

Mechanical loading of fibroblasts growing as a monolayer on a silicon rubber film has been studied, (Butt et al 1995, Arora et al, 1994). The silicon rubber membranes are distorted by reducing the pressure beneath the rubber bottomed membranes the cells. The deformation causes a strain to be generated in the rubber which is transmitted to the adherent fibroblasts. Devices to generate such forces are available commercially (Flexcell Corp. McKeesport PA), with sophisticated controls to determine the level of vacuum and hence the level of distortion and the frequency of the force cycle. A similar model has been reported using a mechanical

plunger. Movement of the plunger causes a deformation of the silicon membrane which is passed onto the adherent fibroblasts. All these systems result in a strain gradient being created, which is greatest on the outside edge of the culture well, reducing towards its centre. A more constant strain gradient can be created when a piece of silicon rubber is stretched in a unidirectional fashion in a single plane. The most complex system produced, and the most repeatable in terms of mechanical loading, of cells on an elastic silicon film has been achieved by Vandenburgh (1988,1989,1995). This model uses a computer controlled linear actuating stepping motor that has high positional accuracy. This system has been employed to quantitate the effect of mechanical loading on skeletal muscle cells

1.10) The Culture Force Monitor.

In this study a Culture Force Monitor (CFM) has been designed and developed. This model facilitates the quantitative measurements of fibroblast induced collagen gel contraction from the point of initial collagen gel polymerisation, and can be used over short and long time periods (Eastwood et al, 1994,1996, Brown et al, in press). The CFM employs a floating tethered FPCL and is therefore more representative of granulation tissue than normal dermis (Grinnell 1994). Also because the

FPCL and the attachment system is floating in culture medium the model is not subject to frictional losses.

1.11) The tensioning-Culture Force Monitor.

The tensioning-Culture Force Monitor (t-CFM) is a development of the CFM that enables precise mechanical loads to be applied to the FPCL in a controllable and repeatable manner by a computer controlled microstepping motor. The accurate repeatable mechanical loading of a teathered 3-dimensional collagen lattice has not to the authors knowledge been achieved prior to this study. Delvoye et al, (1991) applied a load to a tethered collagen lattice by manually altering the matrix tension with the aid of a micrometer drive screw, normally used for the adjustment of the culture position during the initial set-up of the experiment.

Chapter 2: Methods.

2.1) The Culture Force Monitor (CFM)

The central measuring beam of the CFM was manufactured from 0.15mm thick Copper-Beryllium sheet, (Goodfellow Metals Ltd, Cambridge, UK) cut into strips of 100 x 10mm. These strips were precipitation hardened at a temperature of 330°C for 1 hour 10 minutes. Transducer class strain gauges (Wellyn Strain Measurement, Basingstoke, Hants, UK) were attached to the CFM beam in a full bridge network, 20mm from one end, to give maximum lever arm and hence the maximum sensitivity. A hook was soft soldered onto the opposite end of the CFM to facilitate connection to the culture through a stainless steel wire "A" frame. Transducer class strain gauges with a resistance of 5000 ohms in each leg were used, and since very little deflection of the CFM was expected, a high input signal was applied by means of a ripple free 12v power supply (RS Components, Rugby, UK). The output signal was increased with a strain gauge amplifier (RS Components, Rugby, UK). The output from the amplifier was channelled into a digital autoranging voltmeter, to give a constant visual reading, and into an analogue to digital converter (Bytronic Ltd, Sutton Coldfield, UK) installed into a PC (520Mb hard disc, 8Mb RAM) with a 486 processing chip. Data was collected at a rate of one reading per second of force and time. Post processing of the

experimental data was performed with purpose written software, which averaged 600 readings to produce acceptable smoothing, and then stored this value against time. A flow diagram of the process is shown in figure 2.1. For the system to be able to measure a force, it was reacted against a "ground" position, provided by connection of the second attachment bar to a rigid post. The whole apparatus was mounted on a base of 316 Stainless steel 150 x 180 x 75mm ground and polished for ease of cleaning and sterilisation. Two posts were set into the base plate, 10 x 10 x 150mm to carry the force transducer, and a 150mm long bar of 10mm square section which acts as the "ground" post for the fibroblast induced contraction to react against.

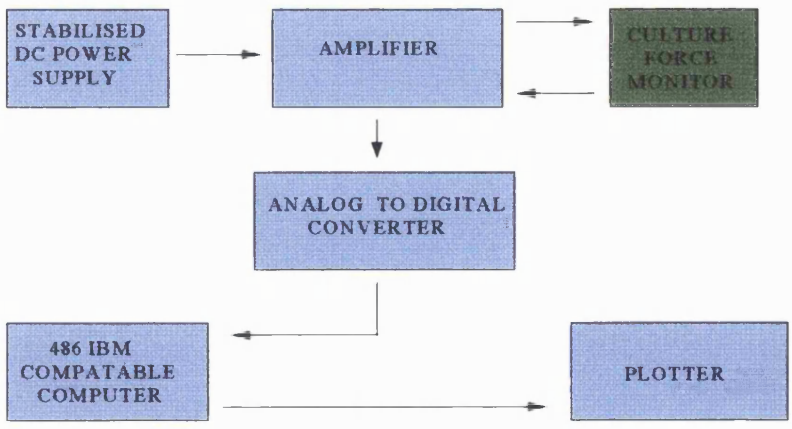

Figure 2.1) The system layout of the Culture Force Monitor.

2.2) Culture Chamber.

A cell chamber (modified from the work of Kolodney and Wysolmerski 1993) was constructed by casting silicone elastomer (Dow Corning, Milton Keynes, UK)) into a polymethylpentene petri dish around a rectangular mould of dimension 75 x 25 x 15mm. The silicone elastomer was degassed for thirty minutes prior to casting and for twenty minutes after casting. The petri dish and silicone elastomer casting were then placed into an incubator at 37°C for 24 hrs to harden. After setting the mould was removed to leave a channel of 25 x 75 x 15mm in the silicone block within the petri dish. This channel was hydrophobic in nature, to inhibit cell attachment.

2.3) Cell Attachment Bars.

Attachment bars to form a physical connection to the culture were made from hydrophillic microporous Vyon (Porvair Ltd, Kings Lynn, Norfolk, UK). 5mm thick sheets, were cut into strips of 5 x 70mm, one side of each Vyon attachment bar was roughened with a scalpel. Sterilisation of these bars by autoclaving at 120°C for 20 minutes also removed any volatile residues. The hydrophillic nature of the Vyon encouraged cell and substrate attachment. The attachment bars were connected to the CFM through two "A" frames of stainless steel suture wire, 0.35mm diameter.

The "A frame" configuration with a loop at one end provided easy connection to the hook on the CFM, and removed any sine error. Holes were pressed into the Vyon bars with a 0.35mm hypodermic needle. The stainless steel wires were then easily connected into the Vyon attachment bars, which were sufficiently buoyant to support the mass of the wire "A" frames. Since the attachment bars then floated in the culture medium an efficient, near friction-free bearing surface was produced. The complete CFM system is shown in figure 2.2.

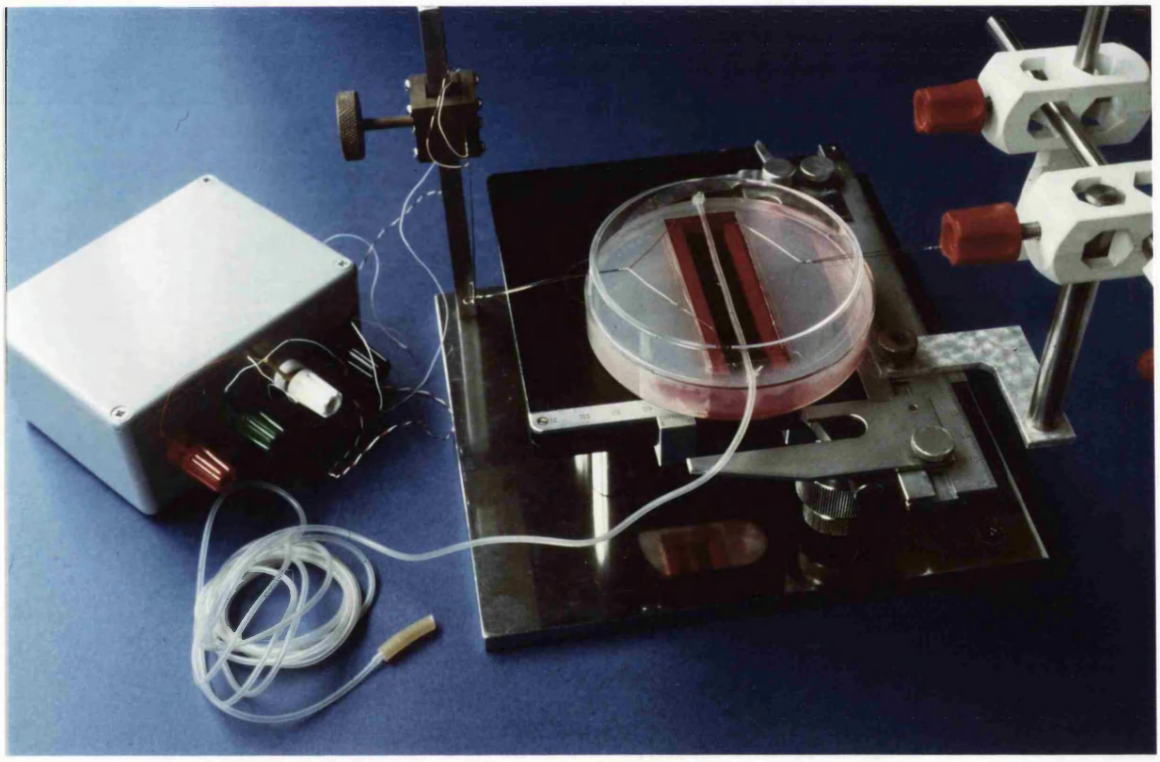

Figure 2.2) The Culture Force Monitor.

2.4) Cell Culture.

2.41) Explant Extracted Cells.

Human dermal fibroblasts were obtained from explants grown from skin taken directly from the operating theatre, (Burt and McGrouther 1992). 2-4mm cubes of tissue were plated into 25cm^2 culture flasks, with 5 ml of Dulbecco's Modified Eagle's Medium (DMEM), (Gibco, Paisley, Scotland), supplemented with 10% foetal calf serum, Streptomycin/Penicillin (Gibco, Paisley, Scotland) and gassed with 5% CO_2 prior to incubation at 37°C. Fibroblasts were grown to confluent monolayers and extracted from the culture flasks by trypsinisation (Gibco, Paisley, Scotland). Extracted cells were centrifuged at 400g for 5mins, then counted with the use of a haemocytometer (BDH, Leicestershire, UK.), prior to suspension in prepolymerised collagen gel. Rabbit tendon fibroblasts were also grown from explants by the same method.

2.42) Collagenase Extracted Cells.

Collagenase digested fibroblasts were prepared by the digestion of a whole tissue sample taken directly from the operating theatre. Small pieces of tissue were incubated for 4 hours with bacterial collagenase, (Sigma, Poole Dorset, UK), in Liebowitz 15 medium, (Gibco, Paisley, Scotland) at 37°C. Cells were then centrifuged down (400g for 5 min) to remove collagenase solution and plated into 25cm^2 culture flasks with

5ml of DMEM supplemented with 10% foetal calf serum, Streptomycin/Penicillin (Gibco, Paisley, Scotland) and gassed with 5% CO2 prior to incubation at 37°C. Bovine articular chondrocytes were prepared by the same method (kindly provided by Dr David lee, Institute of Orthopedics, Stanmore, UK.).

2.5) Collagen Gel Preparation.

The collagen gel (Advanced Protein Products Ltd, West Midlands, UK) was prepared by mixing 4ml of NATIVE acid soluble type I rat tail collagen with a concentration of 2.28mg/ml, with 0.5ml of 10x strength Dulbecco's Modified Eagle's Medium, DMEM, (Gibco, Paisley, Scotland), a balanced pH was achieved by the dropwise addition of 5M NaOH.

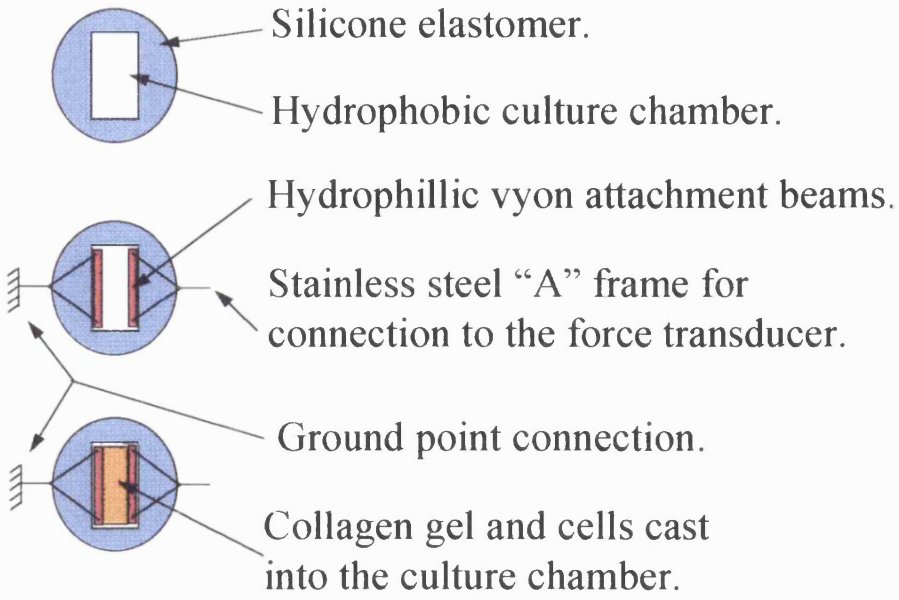

Figure 2.3) Culture well experimental set up. (Low aspect ratio).

Suspensions of human dermal fibroblasts were prepared as described previously, 2.41,2.42 prior to addition to the neutralised collagen solution, (final collagen concentration 1mg/ml), and poured into the silicone elastomer culture chamber over the two Vyon attachment bars, and allowed to set. The collagen/cell suspension formed a provisional gel within five minutes, and the cell chamber was then topped up with a further 15ml of culture medium, to which was added 2.5μg/ml of Amphotericin B (ICN CELLect, Flow, Scotland). The process is shown diagramaticaly in figure 2.3.

2.6) CFM Set Up and Operation.

Once the collagen gel had polymerised the culture well was attached to the CFM. One of the stainless steel "A" frames was connected to the ground point. The other "A" frame was attached to the force transducer as shown diagramatically in figure 2.4.

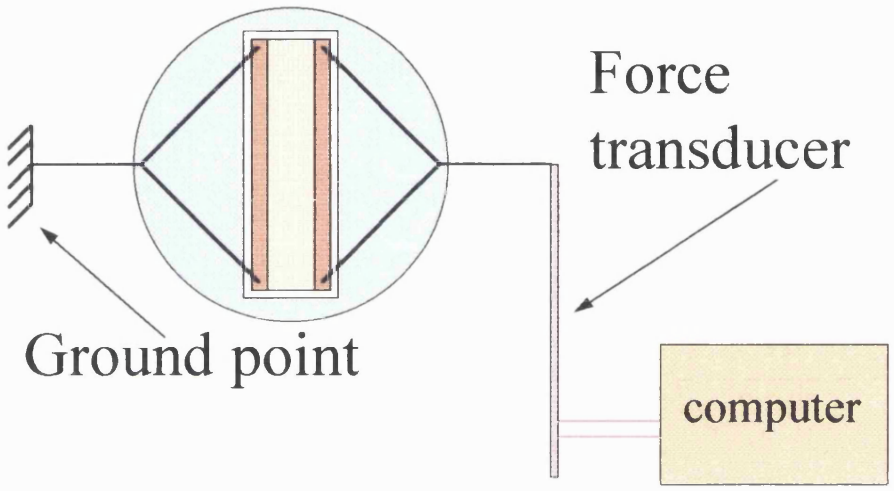

Figure 2.4) Diagram of the CFM operation.

Contraction of the collagen gel caused the two Vyon beams to be pulled together, but as one of them was fixed all the movement was transferred to the moveable beam, i.e. the one attached to the force transducer. The Copper Beryllium (Cu/Be) beam acted as a long lever arm, with the strain

gauges mounted at their furthest possible distance away from the point of connection to the "A" frame. Minute movements of the collagen lattice, i.e. the contraction of the FPCL, were then detected. Deflection of the Cu/Be causes the resistance of the strain gauges to alter in proportion to the strain detected. Alterations in the resistance in the strain gauges causes the current, and hence the output to alter. The signal from the strain gauges was then converted from its analog form to a digital pulse, at a rate of one every second, so that it could be read into the computer for later processing.

2.7) Tensioning Culture Force Monitor (t-CFM).

The t-CFM utilises the same force transducer, data collection system, and culture well as the CFM, the experimental setup for this part of the t-CFM was identical to the experimental proceedure as described in 2.06. Tension was applied to cultures via a microprocessor controlled microstepping motor, (Micromech, Braintree, UK).

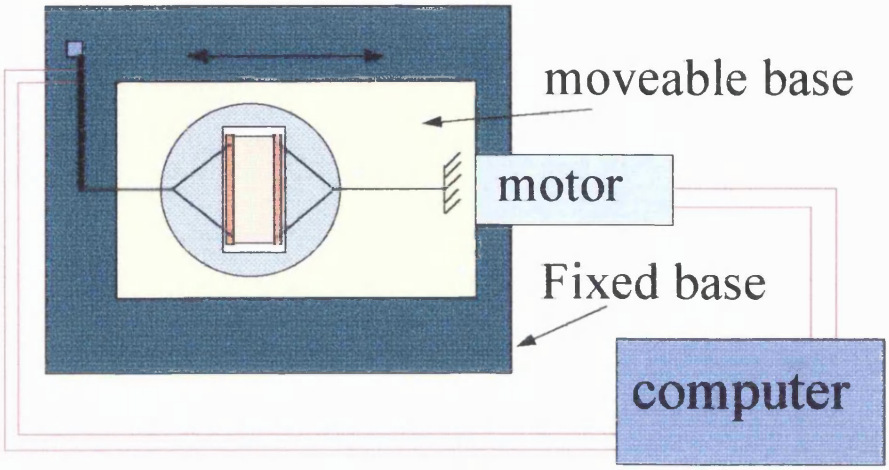

Figure 2.5) Diagrammatic representation of the t-CFM.

The stepping motor drives a precision ground leadscrew with a pitch of 0.508mm which through attachment to the table via a recirculating ball nut, enables precise movement of the table to be achieved. The microstepping motor and table are mounted onto a base of dimensions 200 x 180 x 10mm constructed of perspex, a stainless steel post of 180 x 10 x 10mm facilitates attachment of the force transducer in the same way as the CFM. The culture well is attached to the t-CFM via a cradle constructed from perspex. A locking screw "nips" the petri dish and secures it in position. Initial positioning of the culture well during the

experimental set up is through the moveable "X-Y" table mounted onto the motorised base. Movement is available by the use of micrometer thimble drives mounted in the "X" and "Y" direction. The SX6 microprocessor controller (Micromech, Braintree, UK) enabled a resolution of up too 50800 pulses per revolution of the microstepping motor. This, in conjunction with the precision ground leadscrew enabled a positional accuracy of $1x10^{-8}$m to be achieved.

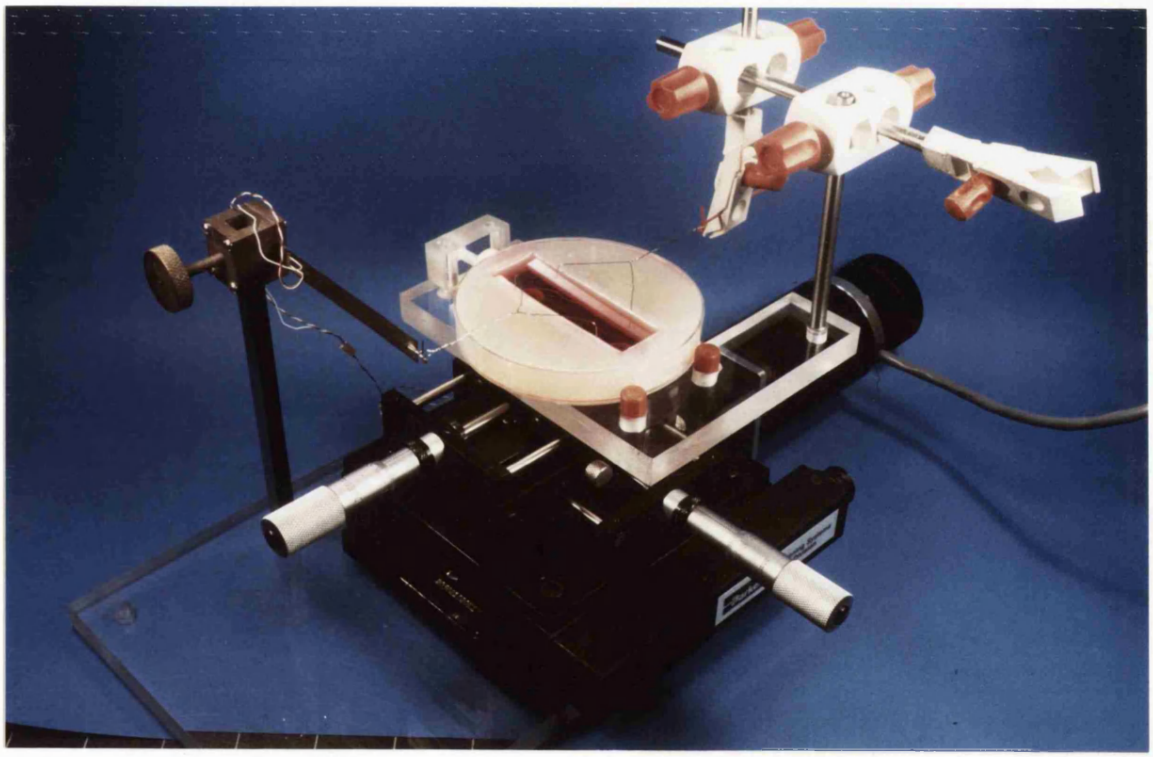

Figure 2.6) The tensioning Culture Force Monitor.

The IBM compatible computer, (520Mb hard disk, 8Mb RAM, 486 processor) enabled a force feed back loop to be established by the use of

purpose written control software, the software enables the t-CFM to respond to the cell induced changes in matrix tension. Independent control of the microstepping motor is achieved by the programming of the SX6 (Micromech, Braintree, UK) controller in "X-ware4" via the IBM computer. The code can be activated or deactivated by the RP240 instructional set, (Micromech, Braintree, UK), which is run independently of the main computer. The t-CFM is shown in figure 2.6.

The t-CFM can be used in a number of different modes. I) as a CFM with no mechanical load being applied to the culture. II) with pre-programmed motion (hence loads) being applied to the culture. III) with the force-feed back control system operative, where the fibroblast generated tension is the determining factor for the table motion and associated load. In this mode the mechanical load is either applied or removed to maintain a set matrix tension. The options for the t-CFM operational modes are shown digrammatically in figure 2.7.

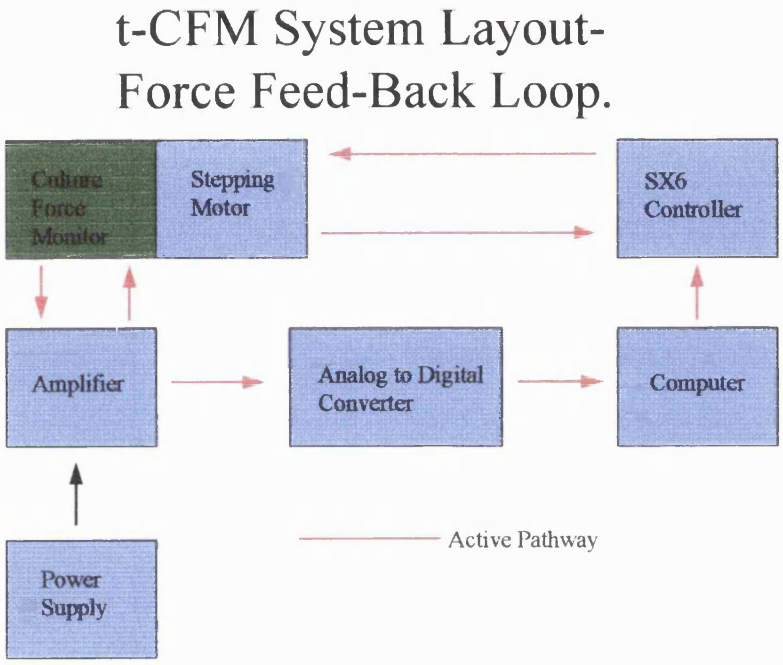

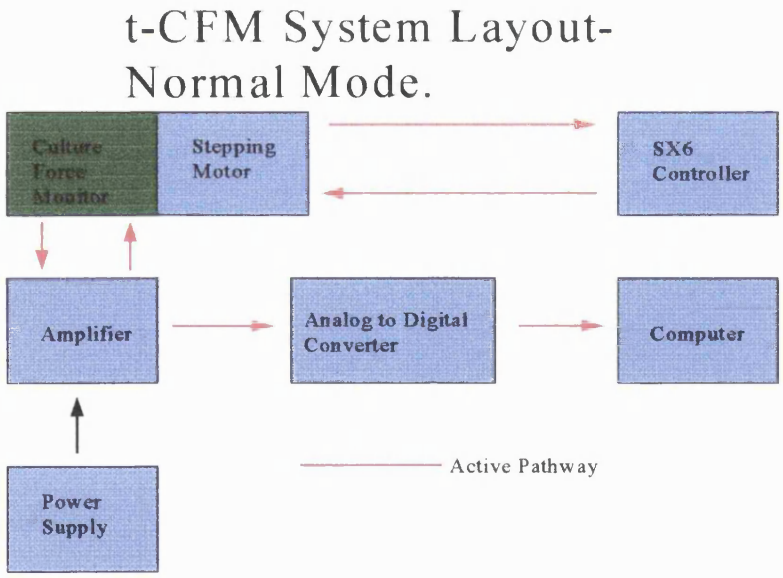

Figure 2.7) Operational system configurations for the t-CFM.

2. 8) Drug Preparations.

To avoid mechanical disturbance of the force transducer small volumes of drug solutions were administered remotely, from outside the incubator, through a millibore tube set into the lid of the CFM culture well. The drugs (all from Sigma Chemicals, Dorset, UK) were administered in 0.5 ml of complete DMEM to give a final concentration in the gel + media as follows: 0.1mM Colchicine, 2uM Cytochalasin B, 0.1mM Vinblastine Sulphate. 0.1 mM Taxol was added to cultures in a vehicle of 400ul ethanol with 100μl DMSO.

2.9) Morphological studies.

Direct observation of collagen gels after 24 hours in the CFM involved fixation, (and subsequent processing, see below) by replacement of medium in the CFM culture chamber with 2.5% gluteraldehyde at 4^0C in phosphate buffer, without the release of tension (Tomasek et al, 1992). Tethered gels for timed morphological examination rather than CFM analysis were prepared as described above but poured into 4 well plates. These gels remained tethered, or attached to the culture wells i.e. the gels were not free floating. After increasing contraction periods these gels were fixed by the addition of 2.5% gluteraldehyde in 0.1M phosphate buffer, pH 7.5 at 4^0C, for 1hr followed by washing in phosphate buffer, pH

7.5 at 4°C. The gels were stained with 1% toludine blue, (destained with distilled water) for routine light microscopy and stereomicroscopic examination on an Edge High Definition Stereo Light Microscope (Edge Scientific Instrument Corporation, LA, USA), (Greenberg and Boyde, 1993). For transmission electron microscopy gels were post-fixed in osmium tetroxide (Agar Scientific, Stansted, Essex. UK) for 45 minutes, dehydrated and embedded in Spurrs resin, (Agar Scientific, Stansted, Essex, UK). Sections stained with lead citrate and uranyl acetate (BDH Milton Keynes, UK) before being examined on a Phillips CM12 electron microscope. For scanning electron microscopy fibroblast populated collagen gels were fixed as above, dehydrated, critical point dried and sputter coated before examination on a Joel 35C electron microscope. For the studies of fibroblast alignment in response to mechanical loading the fibroblast populated gels were fixed as above then rapidly cooled in liquid N_2. After freezing the gels were fractured along predetermined planes, dehydrated, then processed in the same manner as previously described for scanning electron microscopy.

2.10) Finite Element Analysis (FEA).

Strain analysis of the collagen lattices was performed using the RASNA software suite of programs (California USA). The collagen lattice was

modelled in both the high aspect ratio of 3:1 (load and cell generated tension being measured along the short aspect) and the short aspect ratio of 0.33:1. A load was applied that was representative of the force magnitude applied by the t-CFM. The model consisted of 20 noded isoparametric elements connected through a P-Shell formulation, restraints were applied by the removal of the ux, uy, uz, ϕx ϕy and ϕz degrees of freedom along the side of the model representing the ground point edge. The load was applied as uniform pressure acting out from the model edge. The total model consisted of 20 elements with 98 degrees of freedom. The analysis was computed on Sun Sparkstation running a Unix operating system.

Chapter 3): Methods Development.

3.1) Calibration of the CFM

The CFM was calibrated against known dead weights which ranged between 0.5g and 30mg. Prior to calibration the force transducers were set into the clamping block and energised. Transducers were left to thermally soak for a period of 24h in the incubator, which was set to run

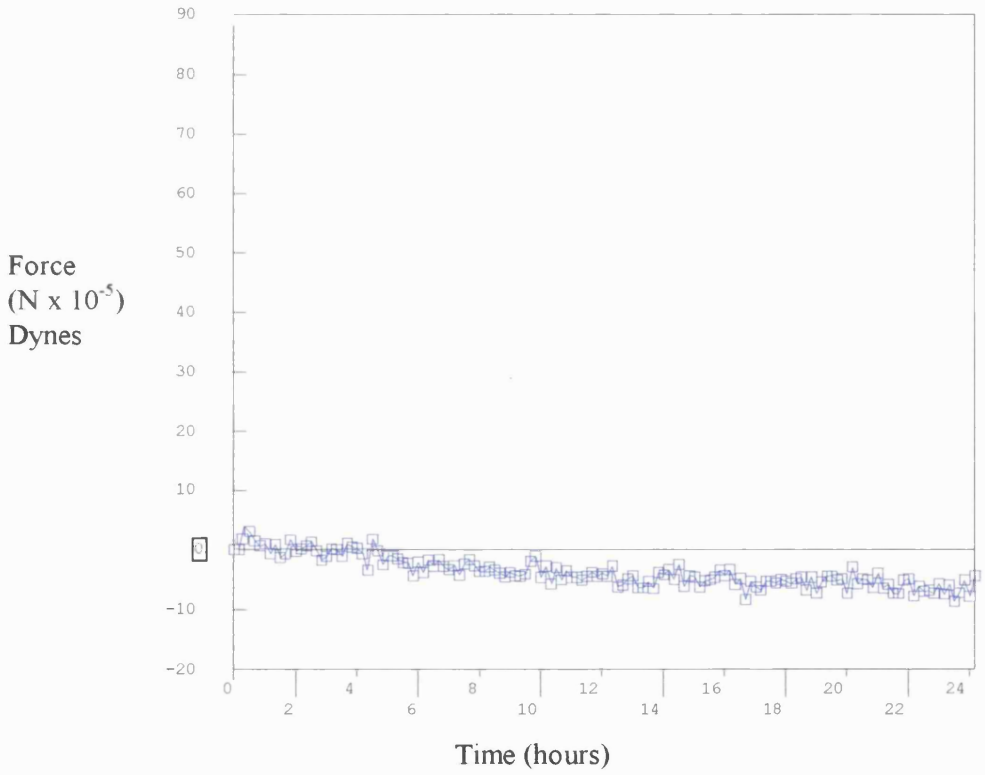

Figure 3.1) Thermal drift of the force transducer.

at the normal operational temperature, humidity and CO_2 content. After the initial 24h period had expired normal data collection was performed to check the thermal stability of the force transducer over the following 24h. Figure 3.1 shows a typical thermal analysis, with the force transducer unrestrained and load free. The slight drift is caused by the self heating of the strain gauges, this data was subsequently deducted from all graphs shown in this thesis. The data collection rate was set to 1 reading per second. Each mass was set onto the force transducer via the attachment hook and the system allowed to settle, then data was collected for a period of 10 minutes. The following 600 readings were averaged to obtain the data point, and the process continued over the complete range of the force transducer. This calibration was carried out on every force transducer used, and re-calibration performed on every occasion when either the system was serviced, or component parts changed.

Figures 3.2-3.5 show the initial calibration curves, of mass against the ADC reading, for the force transducers used in the course of this study. The conversion factors shown on the graphs are used in subsequent data processing to convert the ADC reading stored on computer to dynes (a function performed in a Lotus 123 spread sheet). A curve fitting option has been used that clearly shows the high linearity of the force transducers over the complete working range. A high co-efficient of

accuracy (r^2=1 in all cases) would be expected in a system such as this because the force transducer is acting as a spring. The addition of mass to the force transducer increases the spring energy contained within the system. Removal of the mass results in the recovery of the energy with minimal loss to heat and friction. The loading applied to the force transducer are within the elastic limit of the Cu/Be beams and so there is no loss due to plastic deformation.

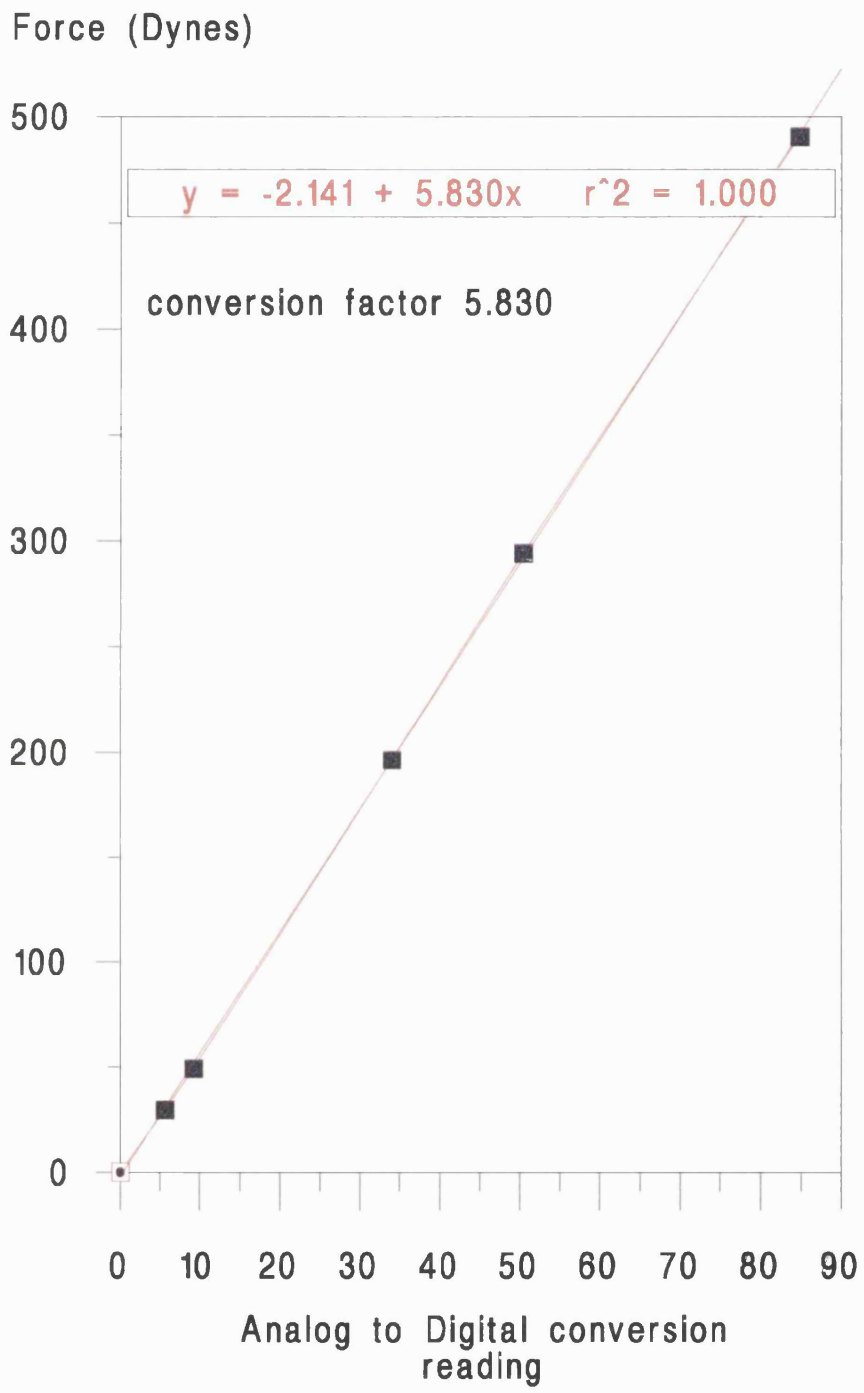

Figure 3.2) Calibration curve of force transducer 1. Multiplication factor of 5.83 to convert ADC reading into dynes.

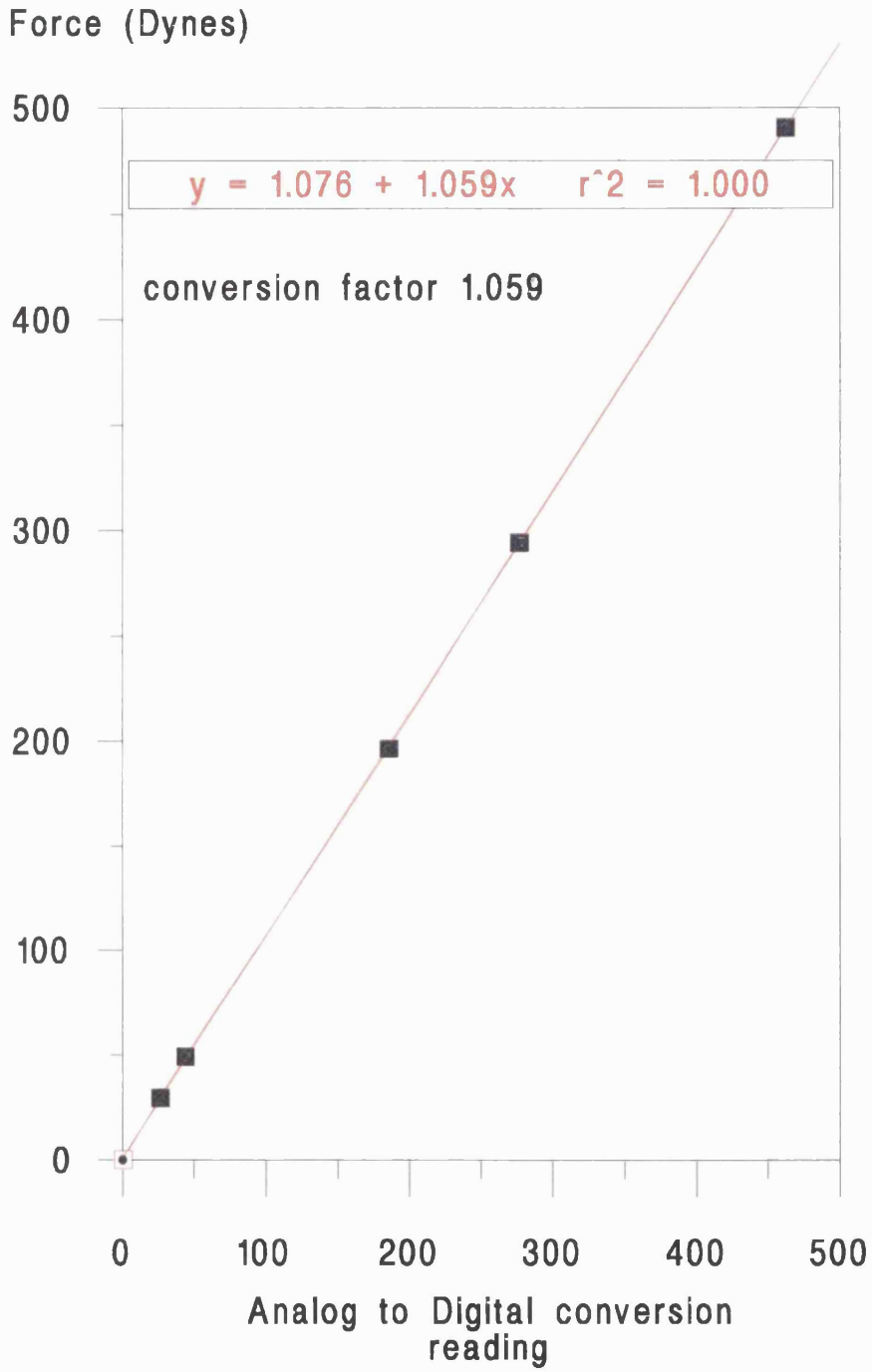

Figure 3.3) Calibration curve of force transducer 2. Multiplication factor of 1.059 to convert ADC reading into dynes.

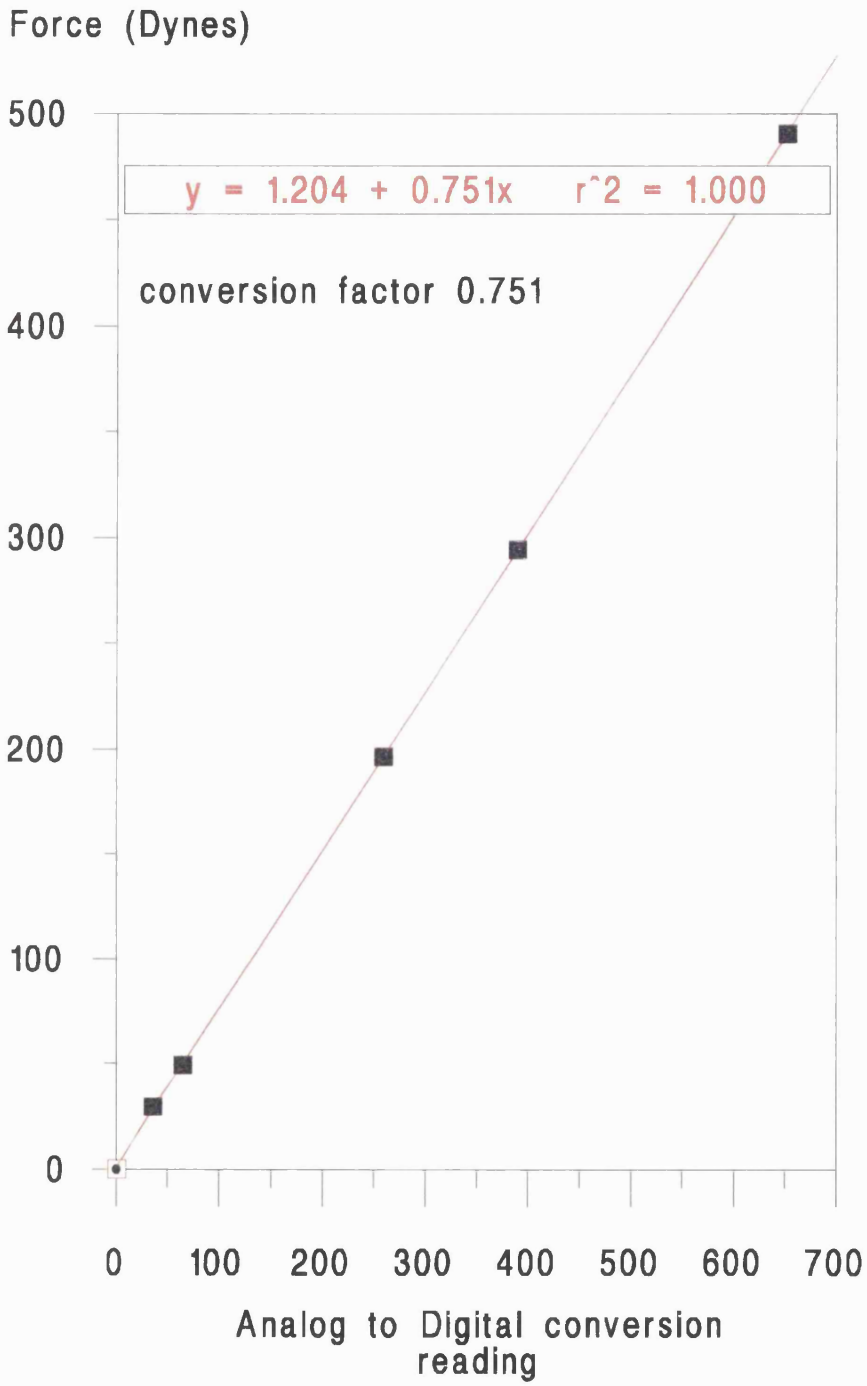

Figure 3.4) Calibration curve of force transducer 3. Multiplication factor of 0.751 to convert ADC reading into dynes.

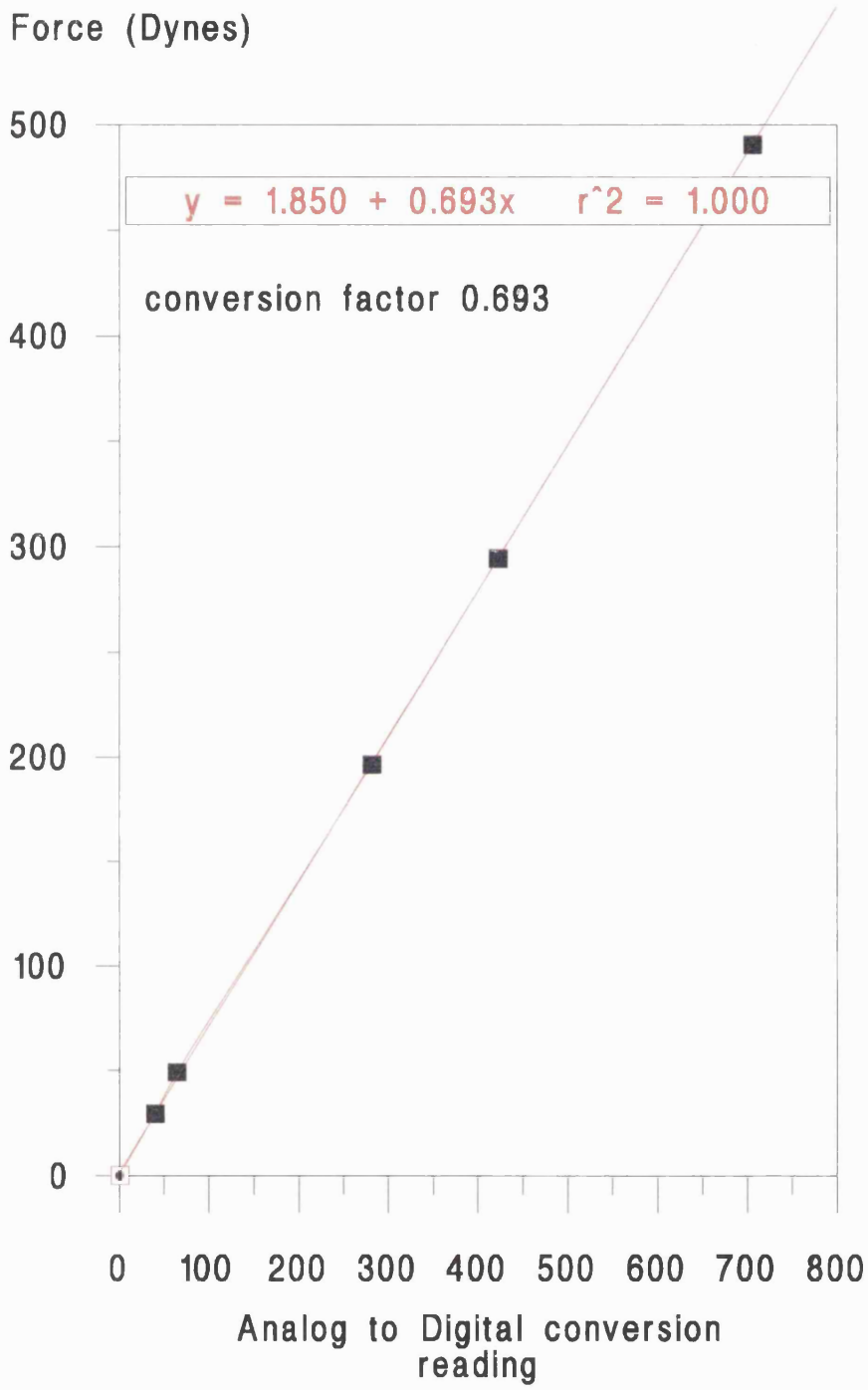

Figure 3.5) Calibration curve of force transducer 4. Multiplication factor of 0.693 to convert ADC reading into dynes.

3.2) Calibration of the tensioning-Culture Force Monitor.

The motion of the culture platform was calibrated against the force transducer, this was achieved by connecting a rigid link between the two components. The programmed motion was activated, and the data recorded. Since the force transducer has a linear response, i.e. F=kx, where F is the applied force, k is the spring constant for the force transducer and x is the known displacement, the relationship between force and movement was easily ascertained. All the mechanical loading cycles used in this study were initiated after 8 hrs, during which time the fibroblasts became attached into the collagen matrix (Eastwood et al, 1996).

3.21) Cyclical Over Loading (COL).

This cycle is shown in figure 3.7. The cycle consisted of loading the FPCL above the resident cell population generated force by 120 dynes over a 15 min time period, (loading rate 480 dynes/hr) followed by a 15 min rest period. Unloading was at the same rate as the loading, again followed by a 15 min resting period, the complete cycle was repeated 15 times.

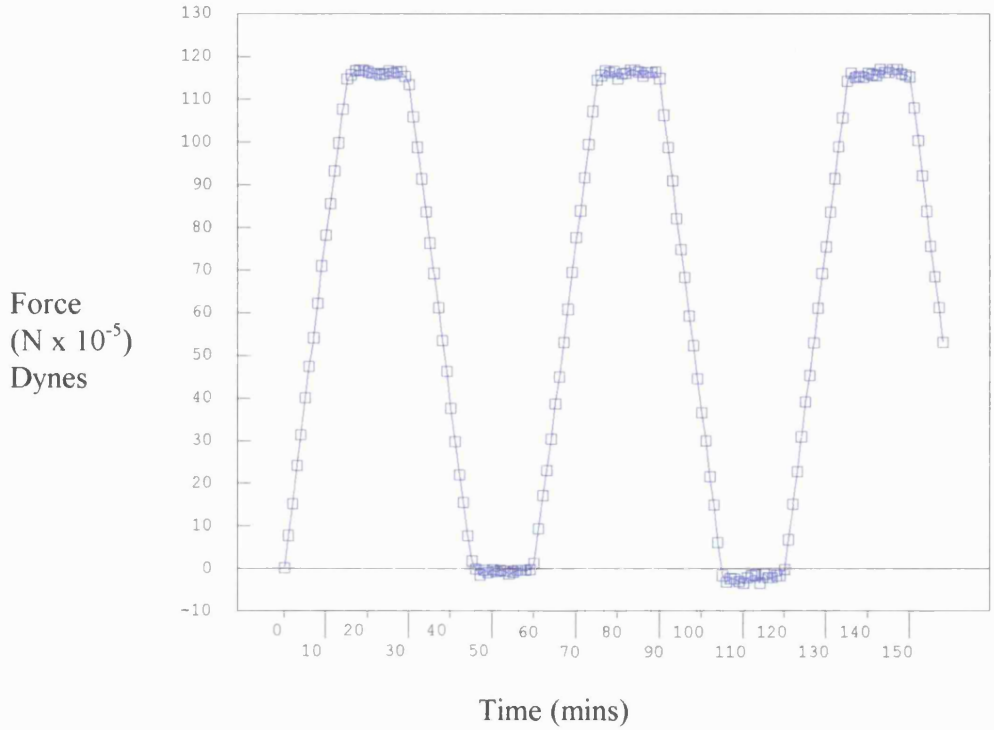

Figure 3.6) Loading above the mean point (COL).

3.22) Cyclical Under Loading (CUL).

This was the reverse of cycle 1. The FPCL was unloaded initially, this resulted in the FPCL being constantly under-loaded about the mean point. This cycle is shown in figure 3.7.

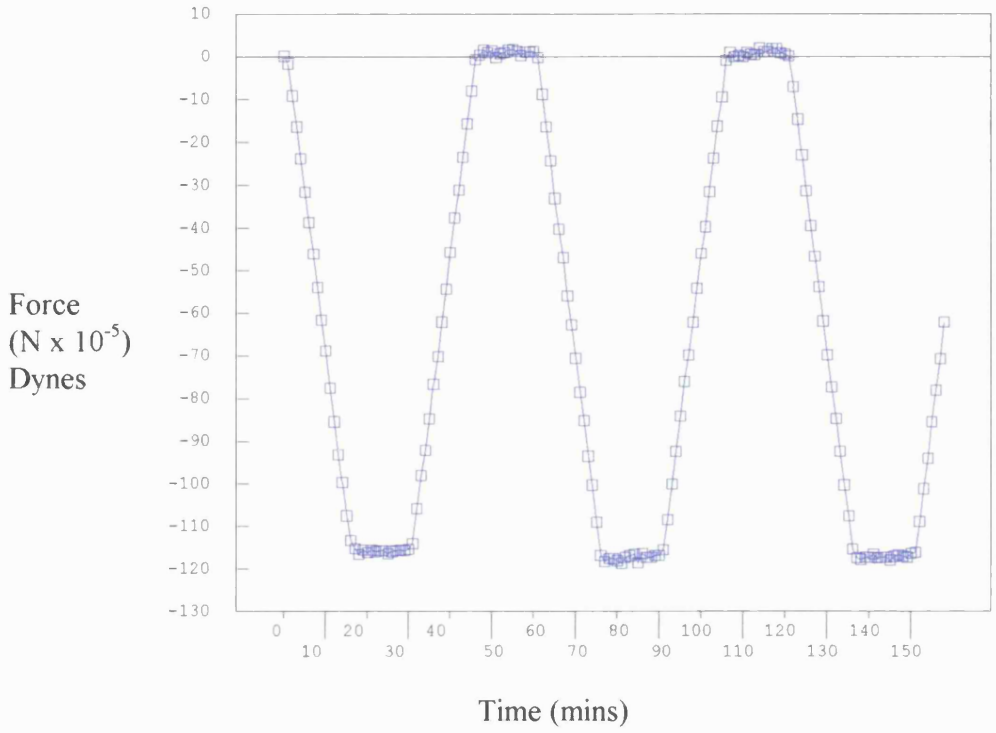

Figure 3.7) Loading below the mean point (CUL).

3.23) Cyclical Median Loading (CML)

In this cycle the initial loading was a half cycle i.e. only 60 dynes, followed by a 15 min. resting period. From this point the loading followed the same loading, resting, then unloading as in cycle 1 and 2. Figure 3.9, shows that the loads were centred about the mean force generated.

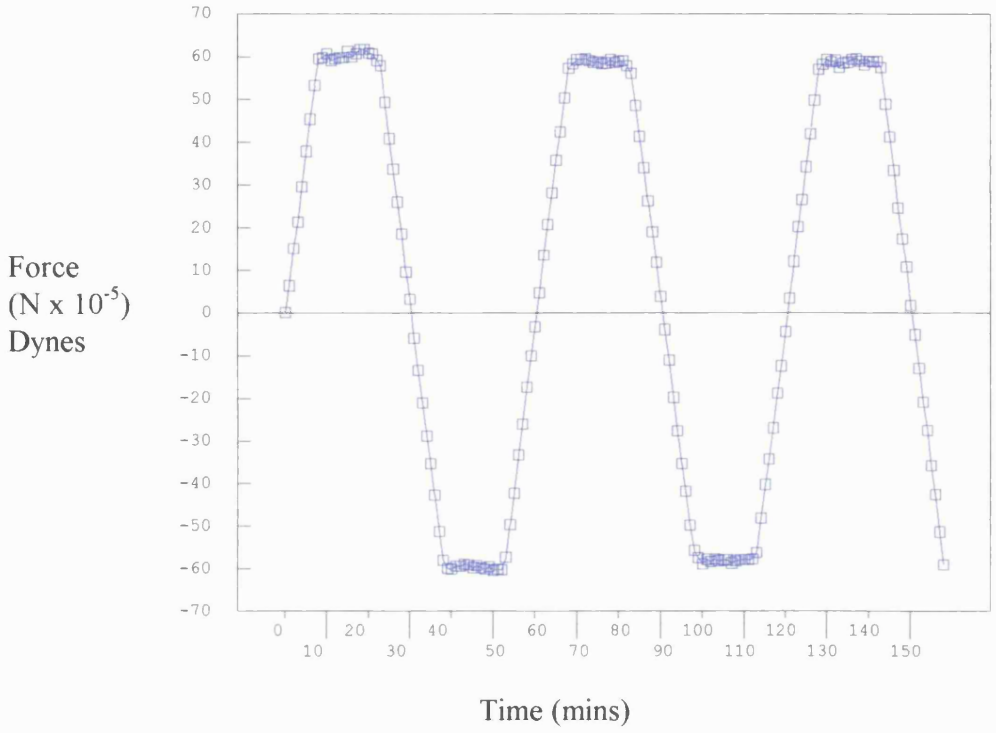

Figure 3.8) Loading about the mean point. (CML)

3.24) Cyclical Incremantal Loading (CIL)

This loading cycle was employed to determine the threshold of cellular response to mechanical stimulation. The loading pattern used a constant loading and unloading rate of 200 dynes/hr. Between loading and unloading, 30 minute rest periods were used to observe any cellular response. The initial loading cycle stimulated the FPCL by 15 dynes. Subsequently the loading increased by 10 dynes every cycle, the final

cycle applying a mechanical load of 75 dynes. Figure 3.9 shows four of the seven cycles, the remaining cycles have been omitted for clarity.

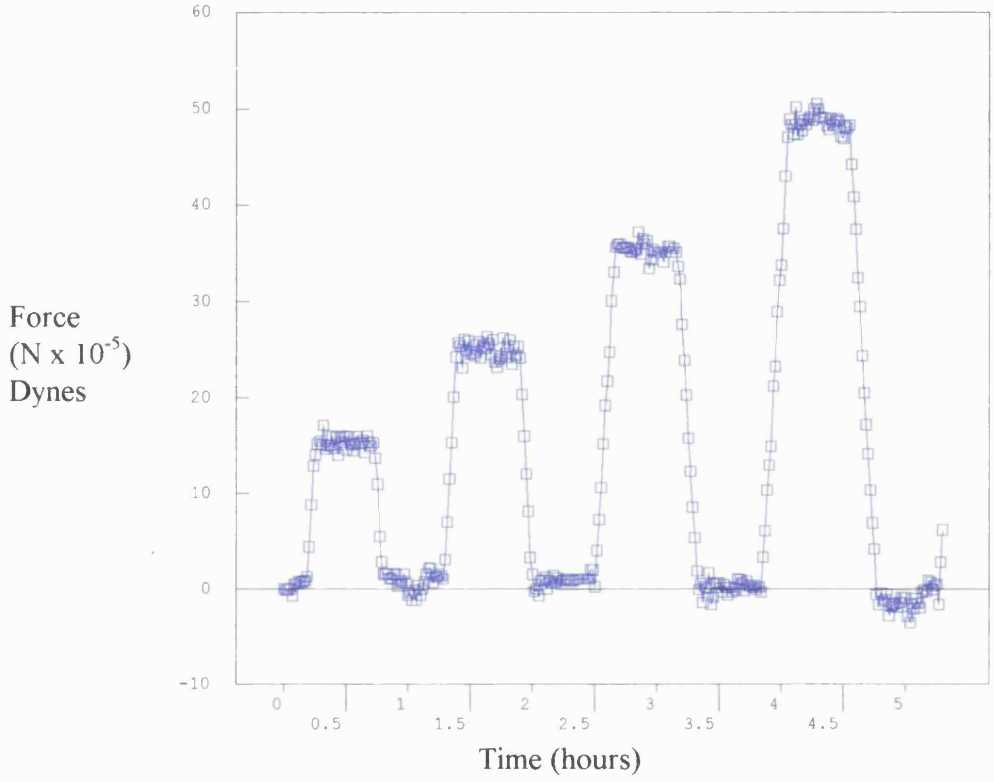

Figure 3.9) Cyclical Incremental Loading (CIL). Note: For clarity only four of the seven cycles have been shown.

3.3) Remote Drug Application.

Drugs were applied to the culture system via a remote application device. A petri dish cover had two small holes (1.5mm) bored diametrically through the rim. Through these holes a millibore tube was passed which was sealed at one end. Small holes were made in the tube over the culture well area so that the drug and vehicle would only drop into the

culture well. The tube was extended through the incubator wall and a syringe was attached to the other end. This enabled drugs to be administered to the CFM with no mechanical disturbance of the system from opening the incubator door etc.

Experiments were performed to determine the residue of drug left in the millibore tube so that accurate calculations could be made as to the final concentration of drug applied to the culture well. The petri dish cover and millibore tube were weighed along with a 1ml syringe. 0.5ml of water was added to the syringe and then weighed again, a collecting dish for the water was also weighed. The water in the syringe was pumped out into the collecting dish through the millibore tube. The collecting dish and water were then weighed so that the total mass of water left in the millibore tube could be determined.

This was double checked by weighing the syringe and millibore tube again after the water had been pumped through. From this the total mass of water left in the millibore tube and syringe could be accurately determined. This was considered to be representative of the mass of the drug and vehicle that would be left in the syringe and millibore tube. From the results it was determined that 2.33% of the total volume would be lost.

In some of the studies multiple doses of the drug were applied. A further set of experiments were performed to determine if a "wetted" drug application system resulted in an increased mass of drug becoming lost to the system. Indeed the results showed that the total volume lost had increased to 2.75%.

Chapter 4): The Culture Force Monitor (CFM), contraction of Fibroblast Populated Collagen Lattices (FPCL) and the role of fibroblast sub-populations.

4.1) Materials and Methods.

All materials and methods used were as described in chapters 2 and 3.

Results

4.2) System Stability and Mechanical Damping.

The stability of the CFM in an undisturbed incubator was excellent. A high level of mechanical damping was provided by the connection of the force transducer to the collagen gel.

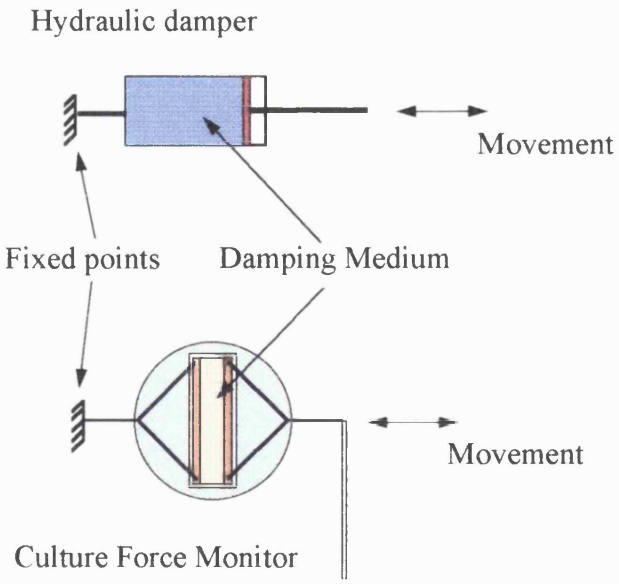

Figure 4.1) Mechanical analogy between the CFM and a hydraulic damper.

The collagen gel in effect acted as the equivalent of the oil in a hydraulic damper. In this type of component movement is permitted but sudden motion is damped therefore vibration did not effect the performance of the CFM. Figure 4.1 shows a diagram of a hydraulic damper and the analogy with the CFM.

4.2) Cell Free Collagen Gel Contraction.

In order to determine the net effect of cells in a FPCL contraction, cell free collagen gels were cast into the culture well and attached to the CFM. The results from these experiments formed controls which were subsequently mathematically subtracted from FPCL contractions. Figure 4.2 shows a typical baseline response of cell-free collagen gel. The distinct and reproducible increase in force as the collagen gel underwent maturation was of particular interest. The collagen gel contracts over the initial 3h period, from this point on no further increase in the contraction is evident and a steady state force is maintained.

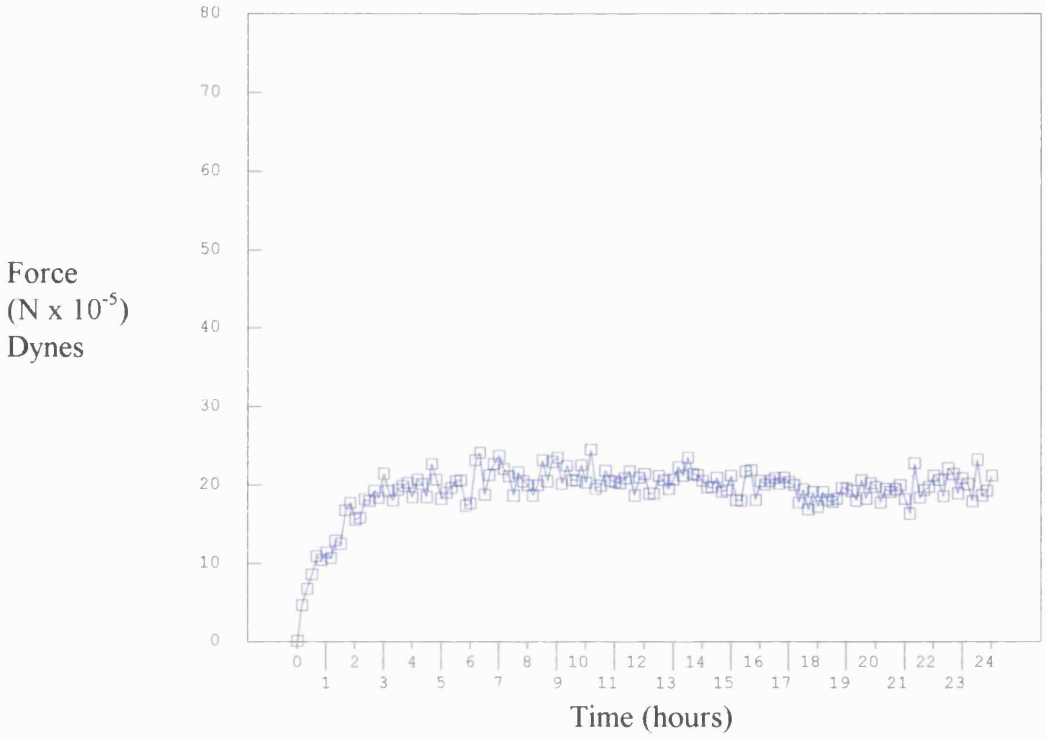

Figure 4.2) Typical cell free collagen gel contraction. This control is subsequently computationally removed from the results.

4.3) FPCL Contraction.

Contraction force data was generated and compared for a range of cell types in the CFM over 24 hour periods. All graphs presented in this study show the net contractile force generated per 10^6 cells in culture, i.e. the thermal drift of the force transducer plus the contractile force generated by the collagen gel itself has been removed and the results standardised for 10^6 cells. It is important to note that these measurements represent

the earliest cell and matrix changes, (i.e. there was no pre-incubation of the gel in which maturation of collagen fibrils or cell attachment might occur).

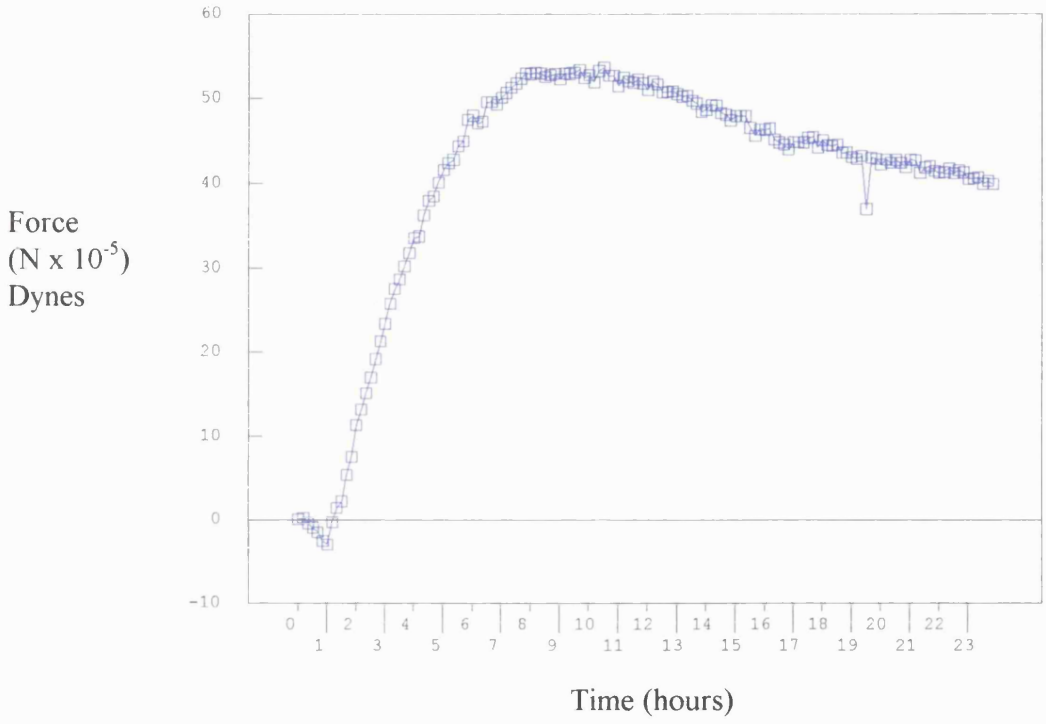

Figure 4.3) Typical contraction of collagen gel by fibroblasts. The graph shows the net force/million cells

Figure 4.3 shows a typical contraction developed by human dermal fibroblasts over a 24 hour period. The force generated began to increase within the first hour after collagen gel formation and peaked after approximately 7 hrs. Over a number of experiments cells with different

contractile patterns began to emerge, in which definite phases of contraction could be identified.

4.4) The Three Phases of Contraction in a 24 Hour Period.

Contraction of the FPCL could be broken down into 3 distinct phases. The initial phase, (1), between 0 and 7 hours, consisted of near linear increase in force. It was in this phase that the greatest rate of increase in force was observed. Analysis of the phase 1 curve showed that the rate of force generated was between 5.3 and 7.3 dynes/hour/million cells, depending on the cell line used. Although different lines of human dermal fibroblasts produced different rates of contraction in this phase the force generated was highly reproducible within cell lines. Phase 2, between 7 and 15 hours, consisted of a minor contractile force in some cell lines that resulted in the maintenance of the peak contractile force generated. In effect this phase showed that the contraction was maintained, since most of the contractile force applied to the beam continued to be exerted. Contraction in phase 3, 15-24 hours, was not always present, but when it occurred, took the form of a further contraction to another peak value.

4.5) Detailed Analysis of the 3 Phases of Contraction.

A detailed analysis of the 3 phases of the patterns of contractile force generated over 24 hours is shown in figures 4.4-4.12. These figures show

the variability between cell lines in the gradient and maximum force generated. In these nine examples shown of different cell lines peak phase 1 contractile force was generated between 3.4 and 11 hours (average 7.14 hrs +/- 1.76 hrs). The peak force ranged between 18.3 to 61 dynes (average 40.4 dynes +/- 14.33 dynes) This produced a relatively constant rate of force generation within a range of 3.05 to 8.41 dynes/hour/million cells, averaging at 5.78 (+/-1.98) dynes/hour/million cells (total overall gradient to peak force).

Phase 2 variations were more striking than those seen in phase 1. Figures 4.4-4.12 shows progressively less evidence of a maintenance of contraction in phase 2. Hence phase 2 varied from an increase in force (figure 4.4) of 38.6% to a decrease of 57% of the phase 1 contraction (figure 4.12).

The variations in the phase 3 contraction are also shown in figures 4.4-4.12. The graphs show that phase 3 could vary from maintenance of force of an actively relaxing FPCL (figure 4.9, 4.10) to an active contraction (figures 4.4-4.6, 4.11,4.12). Figures 4.11,4.12 show the ability of some cell lines to produce patterns of alternating relaxation and contraction from different phases in the 3 phase model. Included with each of the graphs is a summary of the contractile data generated. A summary of the data is shown in figure 4.13.

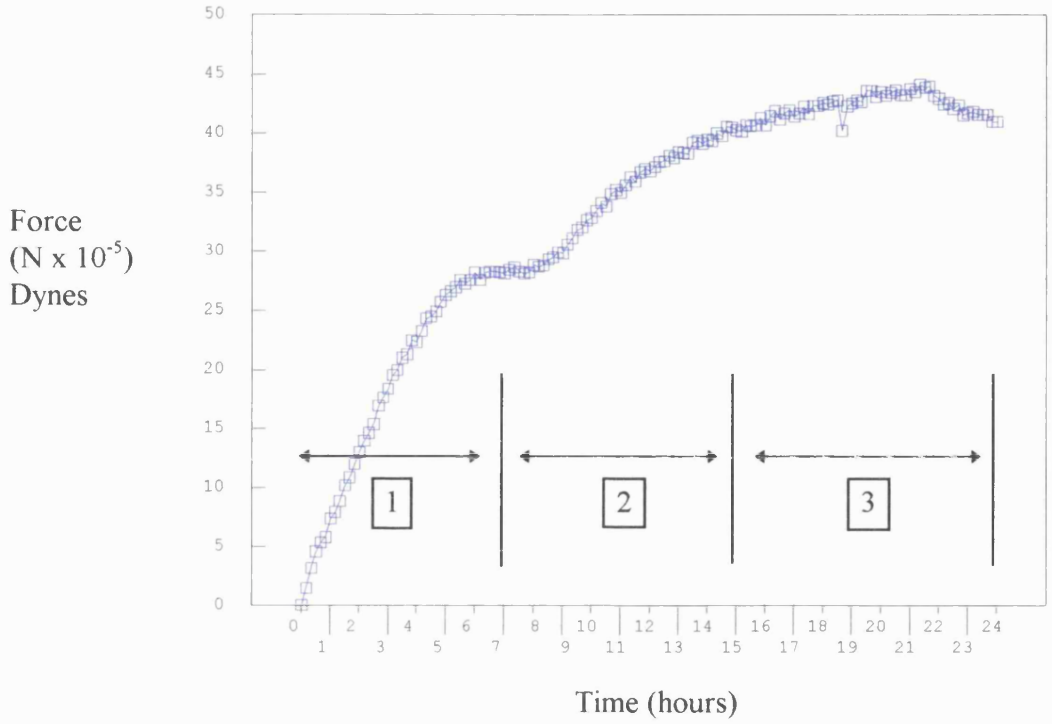

Figure 4.4) Graph of net force/million cells, showing all the phases of contraction.

Table 4.1 Graph statistics

Peak force generated in phase 1	27 dynes
Time to phase 1 peak	6.75 hours
Rate of force increase	4 dynes per hour
Phase 2 contraction	yes
Phase 3 contraction	yes
Overall peak value	44 dynes per million cells

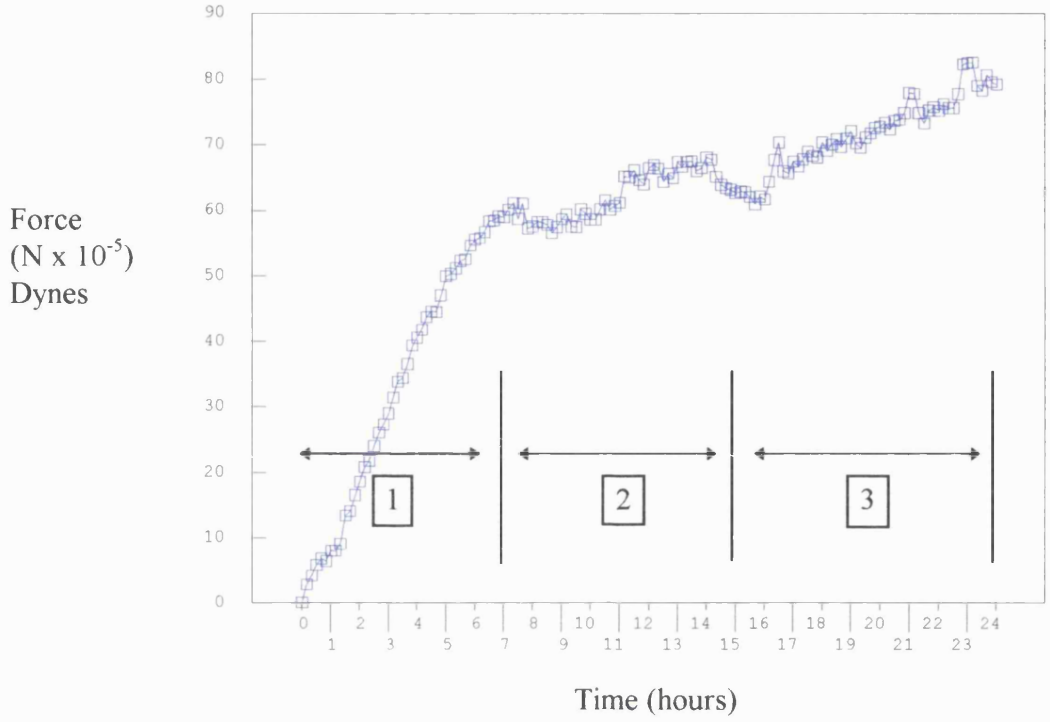

Figure 4.5) Graph of net force/million cells. Indicated are the 3 phases of contraction.

Table 4.2 Graph statistics

Peak force generated in phase 1	61 dynes
Time to phase 1 peak	7.25 hours
Rate of force increase	8.41 dynes per hour
Phase 2 contraction	yes
Phase 3 contraction	yes
Overall peak value	80 dynes per million cells

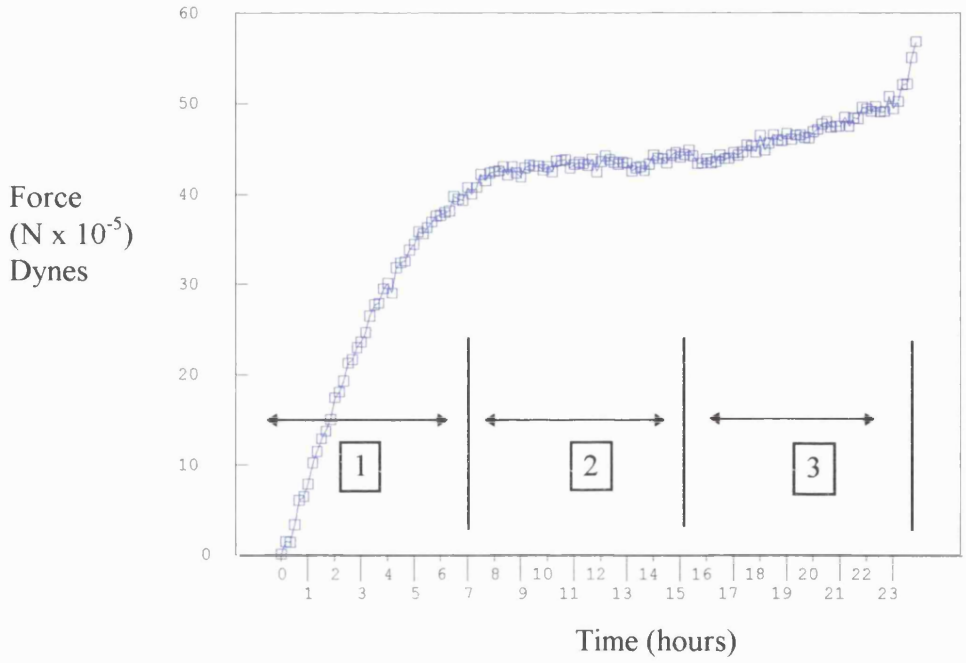

Figure 4.6) Graph of net force/million cells, showing phase 1, 2 and 3 contraction.

Table 4.3 Graph statistics

Peak force generated in phase 1	42 dynes
Time to phase 1 peak	8.1 hours
Rate of force increase	5.18 dynes per hour
Phase 2 contraction	yes
Phase 3 contraction	yes
Overall peak value	55 dynes per million cells

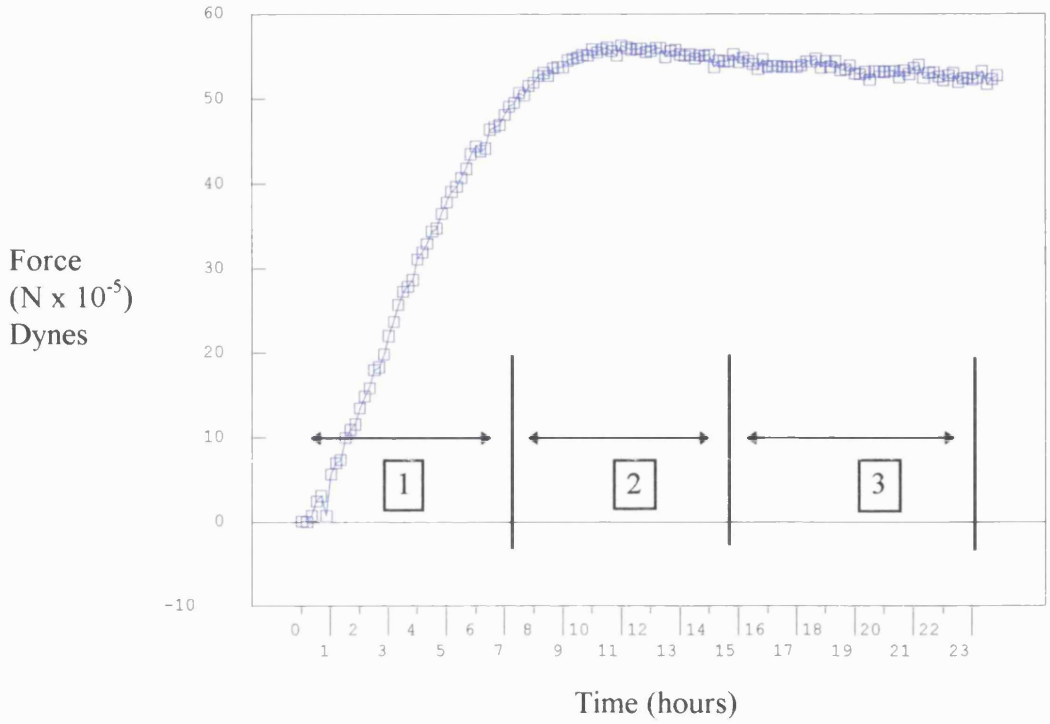

Figure 4.7) Graph of net force/million cells. Contractile curve shows phase 1 and 2 contraction only.

Table 4.4 Graph statistics

Peak force generated in phase 1	57 dynes
Time to phase 1 peak	11 hours
Rate of force increase	5.18 dynes per hour
Phase 2 contraction	yes
Phase 3 contraction	no
Overall peak value	57 dynes per million cells

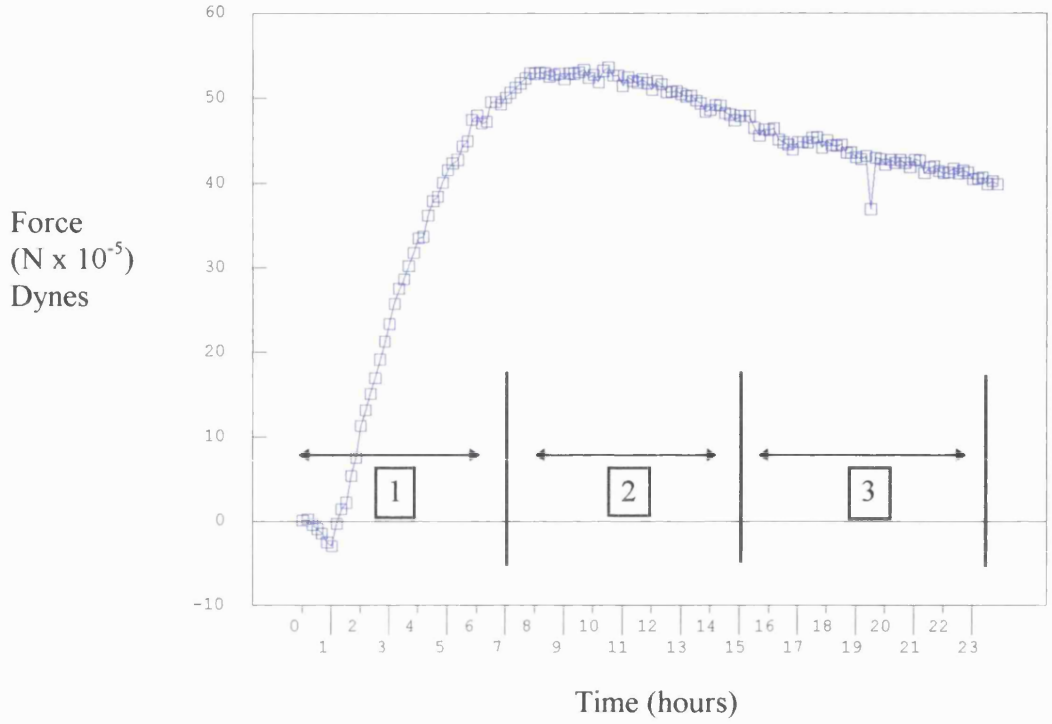

Figure 4.8) Graph of net force/million cells. Contraction shows a phase 1 contraction only.

Table 4.5 Graph statistics

Peak force generated in phase 1	54 dynes
Time to phase 1 peak	8.2 hours
Rate of force increase	6.58 dynes per hour
Phase 2 contraction	no
Phase 3 contraction	no
Overall peak value	54 dynes per million cells

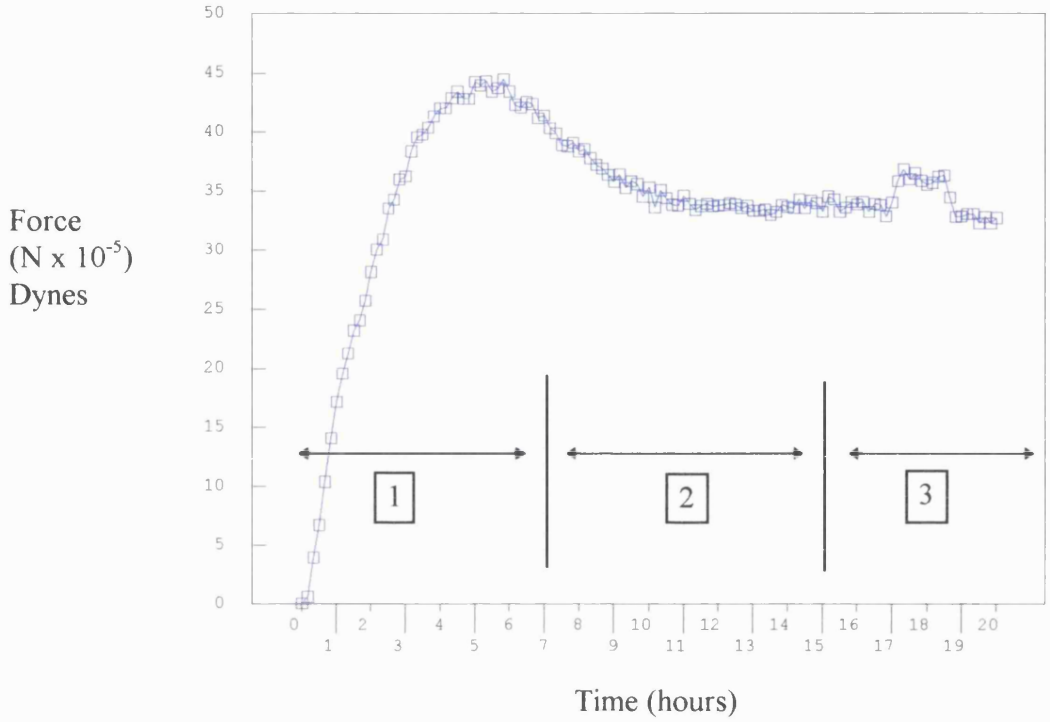

Figure 4.9) Contraction showing primary and a delayed secondary contraction.

Table 4.6 Graph statistics

Peak force generated in phase 1	44 dynes
Time to phase 1 peak	5.5 hours
Rate of force increase	8 dynes per hour
Phase 2 contraction	yes
Phase 3 contraction	no
Overall peak value	44 dynes per million cells

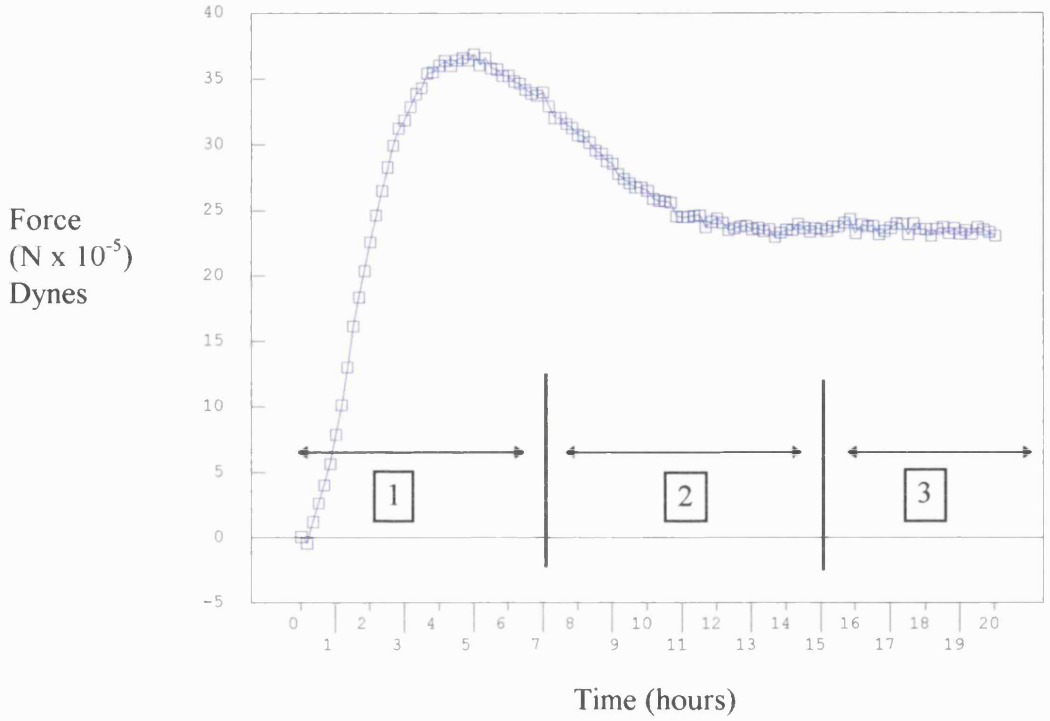

Figure 4.10) Graph of net force/million cells, showing a phase 1 contraction, no phase 2 and a small phase 3 contraction.

Table 4.7 Graph statistics

Peak force generated in phase 1	37 dynes
Time to phase 1 peak	4.5 hours
Rate of force increase	48.22 dynes per hour
Secondary contraction	no
Tertiary contraction	yes
Overall peak value	37 dynes per million cells

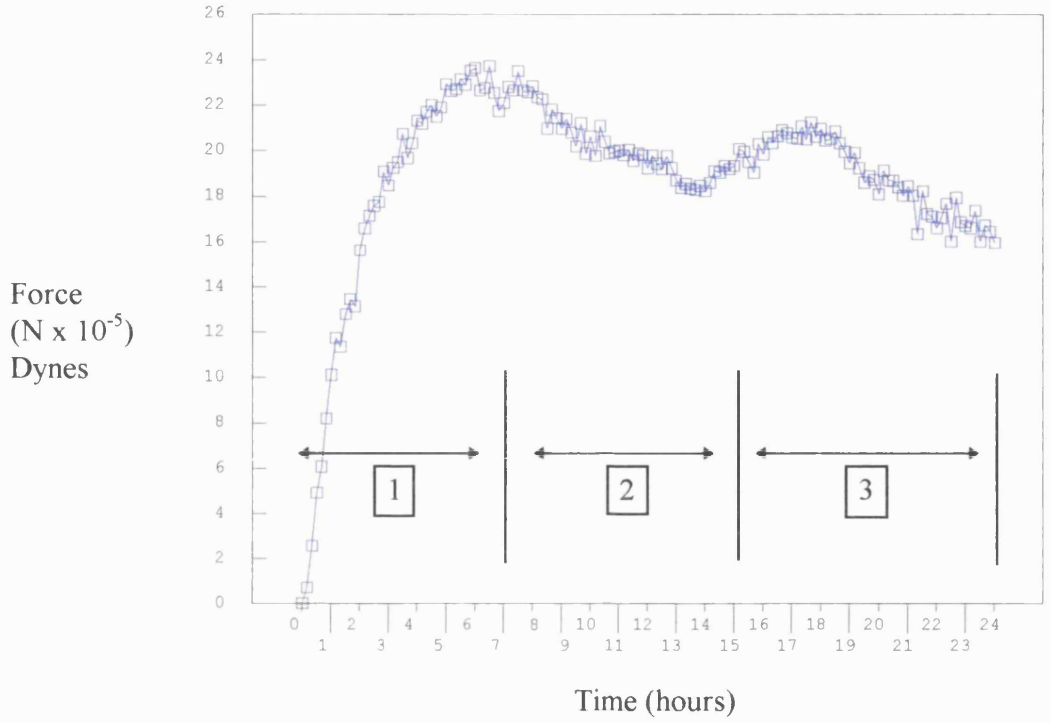

Figure 4.11) Graph of net force/million cells. The contractile curve shows a phase 1 contraction no phase 2, and a small phase 3 contraction.

Table 4.8 Graph statistics

Peak force generated in phase 1	24 dynes
Time to phase 1 peak	7 hours
Rate of force increase	3.43 dynes per hour
Phase 2 contraction	no
Phase 3 contraction	yes
Overall peak value	24 dynes per million cells

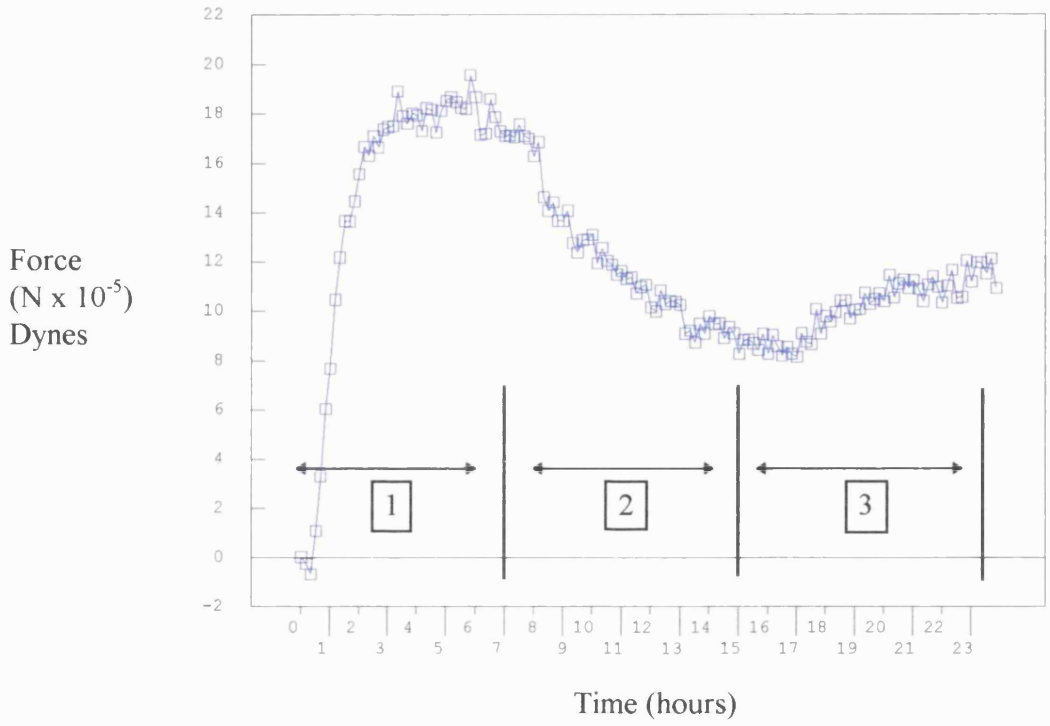

Figure 4.12) Graph of net force/million cells. The graph shows phase 1 and 3 contractions only.

Table 4.9 Graph statistics

Peak force generated in phase 1	18.3 dynes
Time to phase 1 peak	6 hours
Rate of force increase	3.05 dynes per hour
Phase 2 contraction	no
Phase 3 contraction	yes
Overall peak value	18.3 dynes per million cells

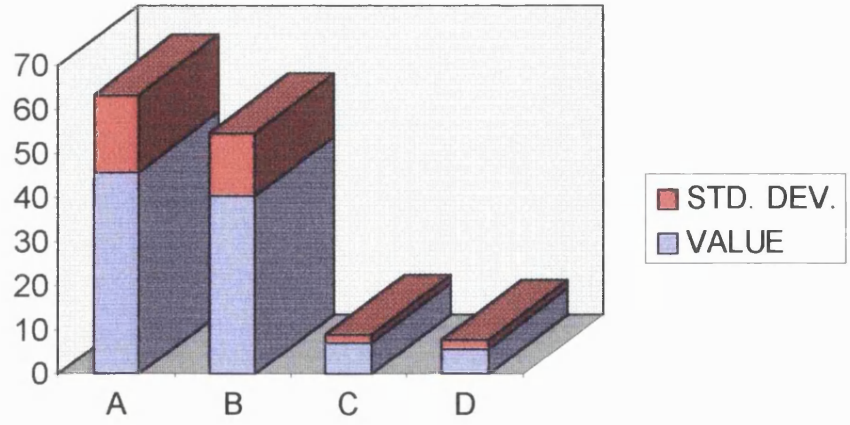

Legend.
A = Overall contraction. (Dynes/million cells)
B = Peak phase 1 contraction value. (Dynes)
C = Time to phase 1 peak value. (Hours)
D = Contraction rate during phase 1. (Dynes/hour/million cells)

Figure 4.13) Results of processed data from figures 4.4-4.12. Shown are the average values (in blue), and the standard deviation (in red).

4.7) Bacterial Collagenase v Explant Cell Extraction.

Figure 4.14 compares the profiles of contractile force generated by two populations of human dermal fibroblasts from the same specimen of skin. Both were extracted from a single piece of human dermis split into two sections. The first cell preparation (curve A) was prepared conventionally by growth from explants and isolation of the outgrowing fibroblasts. This was assumed to be a self-selected cell population, based on their ability

to migrate out of the tissue. The second preparation, (curve B), was from a total

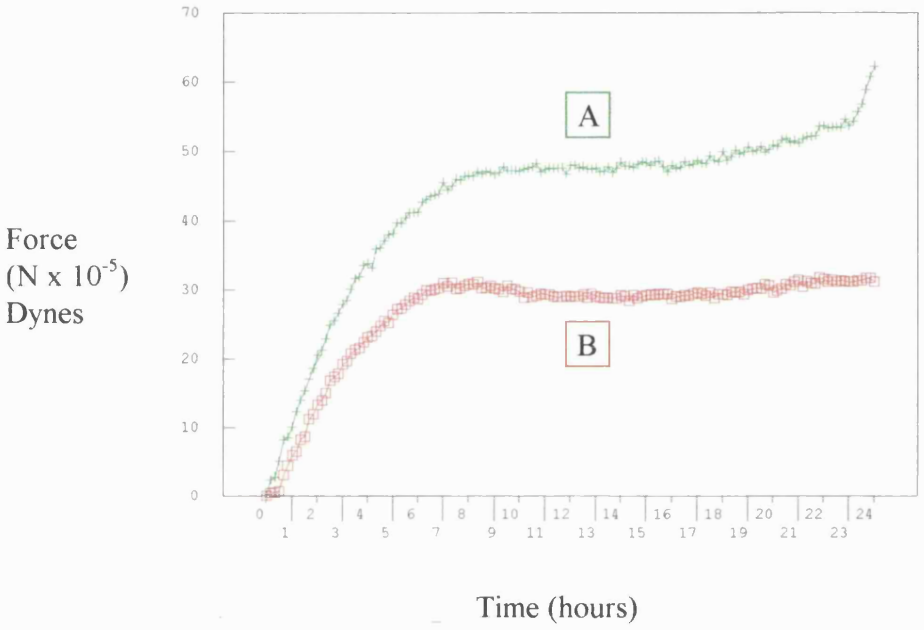

Figure 4.14) Collagenase digestion v explant migration. (Data shows net force/million cells)

digestion of tissue with bacterial collagenase, releasing all there fibroblast sub-populations with no selective bias towards emigration. Each was analysed on the CFM at passage number 1. Although the overall pattern of contraction was similar for both populations, the peak phase 1 contractile force was 60% greater for explant-selected cells and further contraction was evident in phase 3. The difference between the

two curves clearly indicates that cells from the explant culture system produced a greater net contractile force, i.e. they reached a higher equilibrium constant, than the total enzyme extracted population.

More evidence for fibroblast sub-populations can be seen in figure 4.13. This figure shows that there is a large variation in the total force generated from a range of cell lines (45.9 +/-17.5 dynes). Figure 4.13 also shows the time taken for the phase 1 peak contraction to be reached is reasonably constant at 7.14 +/-1.76 hrs, as is the contraction rate of 5.78 +/-1.98 dynes/hr/million cells.

4.8) Fibroblasts From Other Tissue Sources.

Fibroblasts from tissues other than human dermis, (rabbit tendon and human Dupuytrens nodule tissue), gave quite distinct patterns of contraction within the 3 phase model. Rabbit tendon fibroblasts, ((a):sheath and (b):endotenon) contracted late in the sequence seemingly missing the phase 1 and 2 contraction and then producing a phase 3 contraction from the 15 hour time point, (figure 4.15). In both cases, total contraction was small even by 24 hours. Human Dupuytrens nodule fibroblasts, (figure 4.16), again produced a characteristic profile. A

normal phase 1 contraction was followed by a dramatic phase 2 contraction.

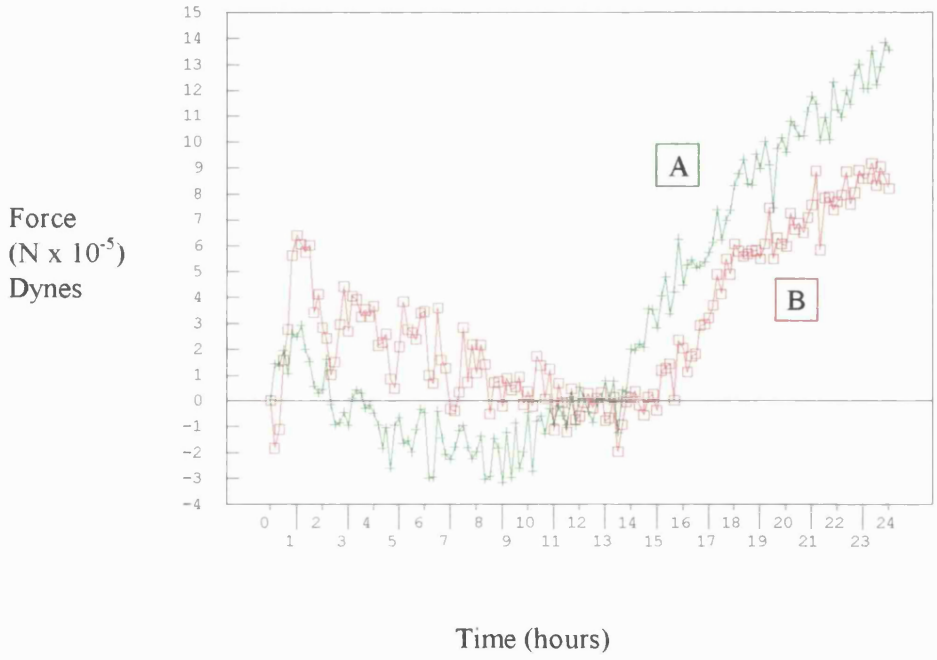

Figure 4.15) Contractile profile produced by rabbit tendon fibroblasts: curve A sheath: curve B endotenon. (Cells kindly provided by Dr. U. Khan)

Overall rates of contraction were 7 dynes/hour/million cells for phase 2 with a clear inflexion point, but there was no phase 3 contraction. Maximum force generated was 16% and 76% (rabbit tendon and human Dupuytrens tissue respectively) of the strongest contractile force generated by human dermal fibroblasts. In contrast to these cell lines, bovine articular chondrocytes (passage No 2), produced a peak net force

of only 14 dynes over phases 1 and 2 under the same conditions (figure 4.17).

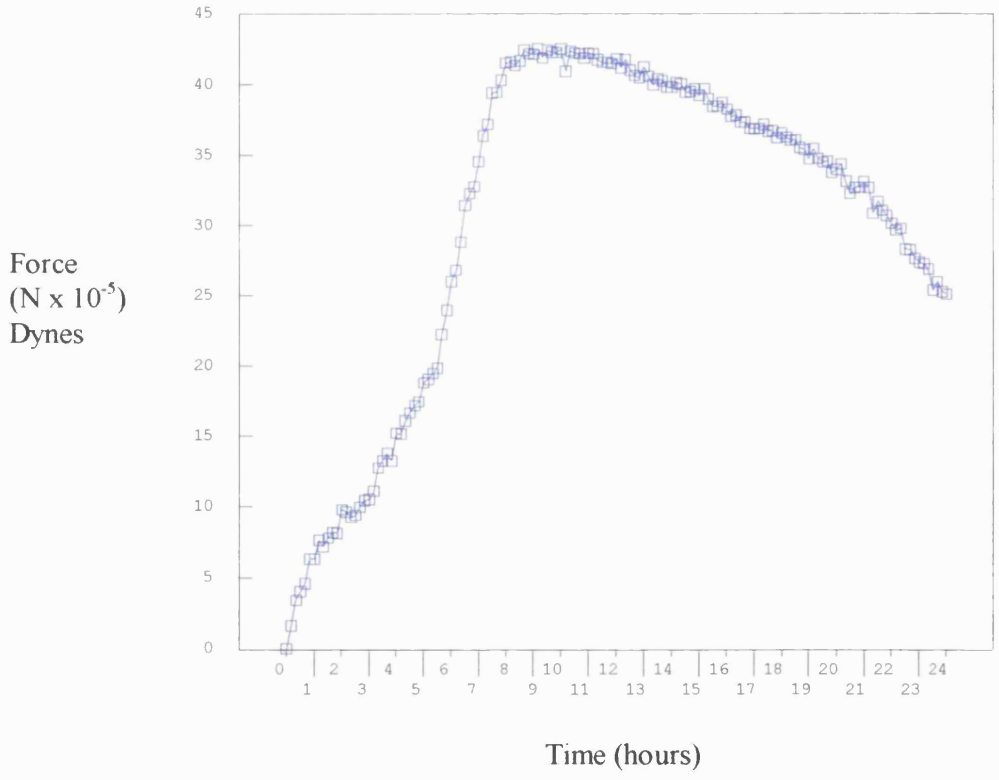

Figure 4.16) Net contractile force/million cells produced by Dupuytrens tissue fibroblasts.

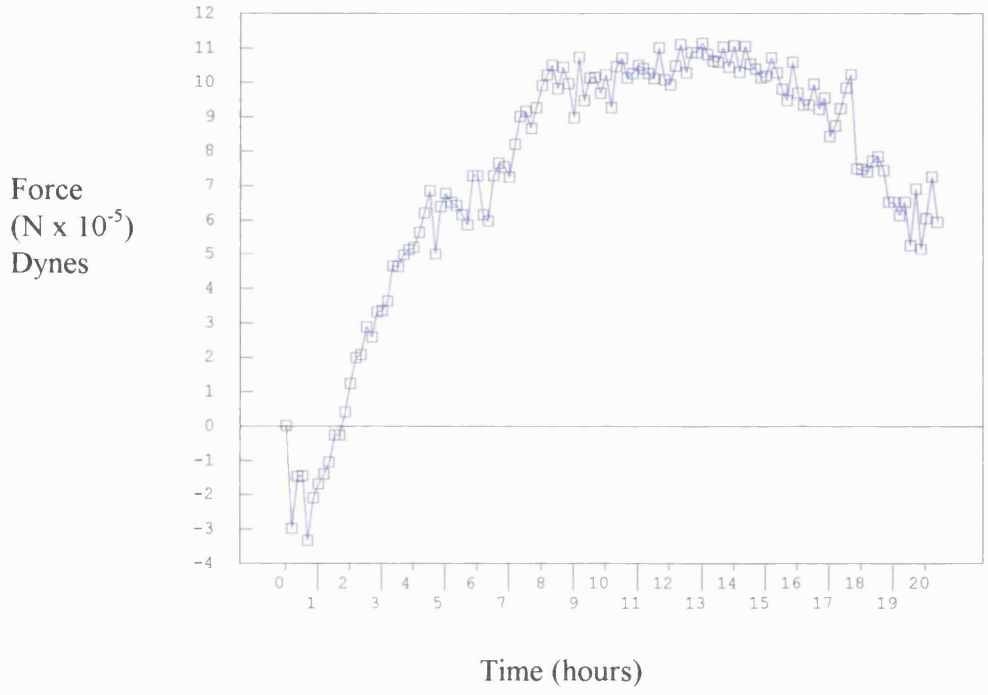

Figure 4.17) Net contractile force/million cells produced by bovine articular chondrocytes (Cells kindly donated by Dr. D. Lee)

4.9) Morphological appearance.

The morphological appearance of the human dermal fibroblasts and the extracellular matrix was monitored at various stages throughout the contraction, (0,1,2,4 and 8 hours), and related to the contractile force generated. These morphological stages relate directly to the time points indicated in figure 4.18, which represents a contraction profile for the same cell line and passage number. Since most of the force was generated during phase 1 of the contraction, four of the time points were

in this phase. The intention was to relate the changes in cell shape and attachment to the patterns of contractile force generated.

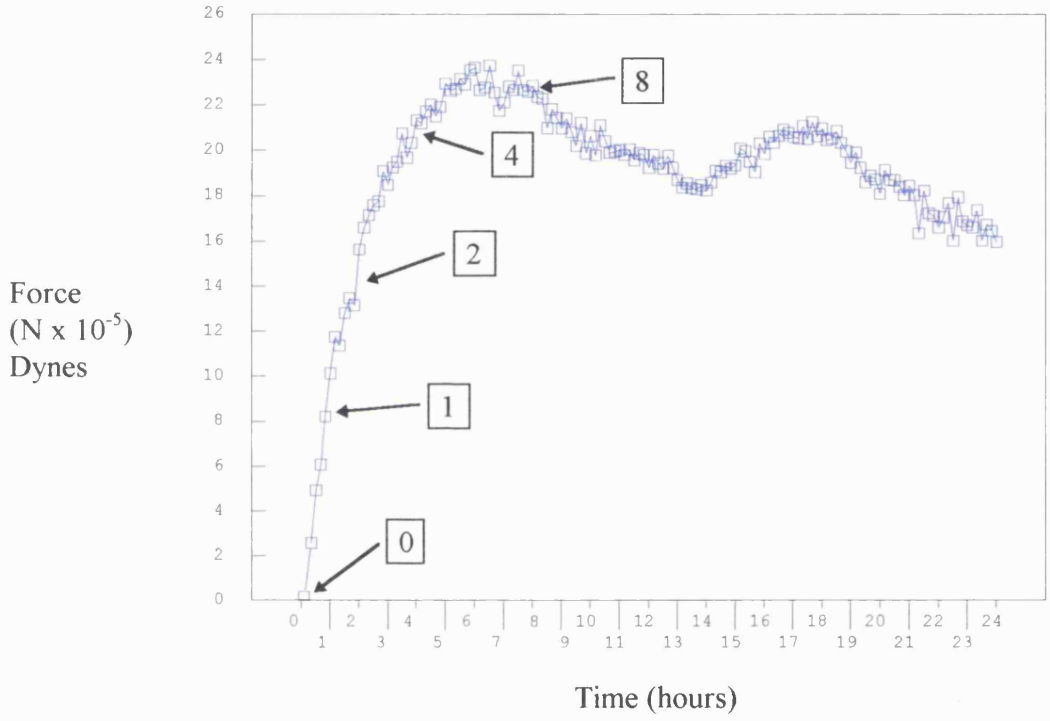

Figure 4.18) Contractile curve, indicated on the curve of net force/million cells are the time points for the morphological studies.

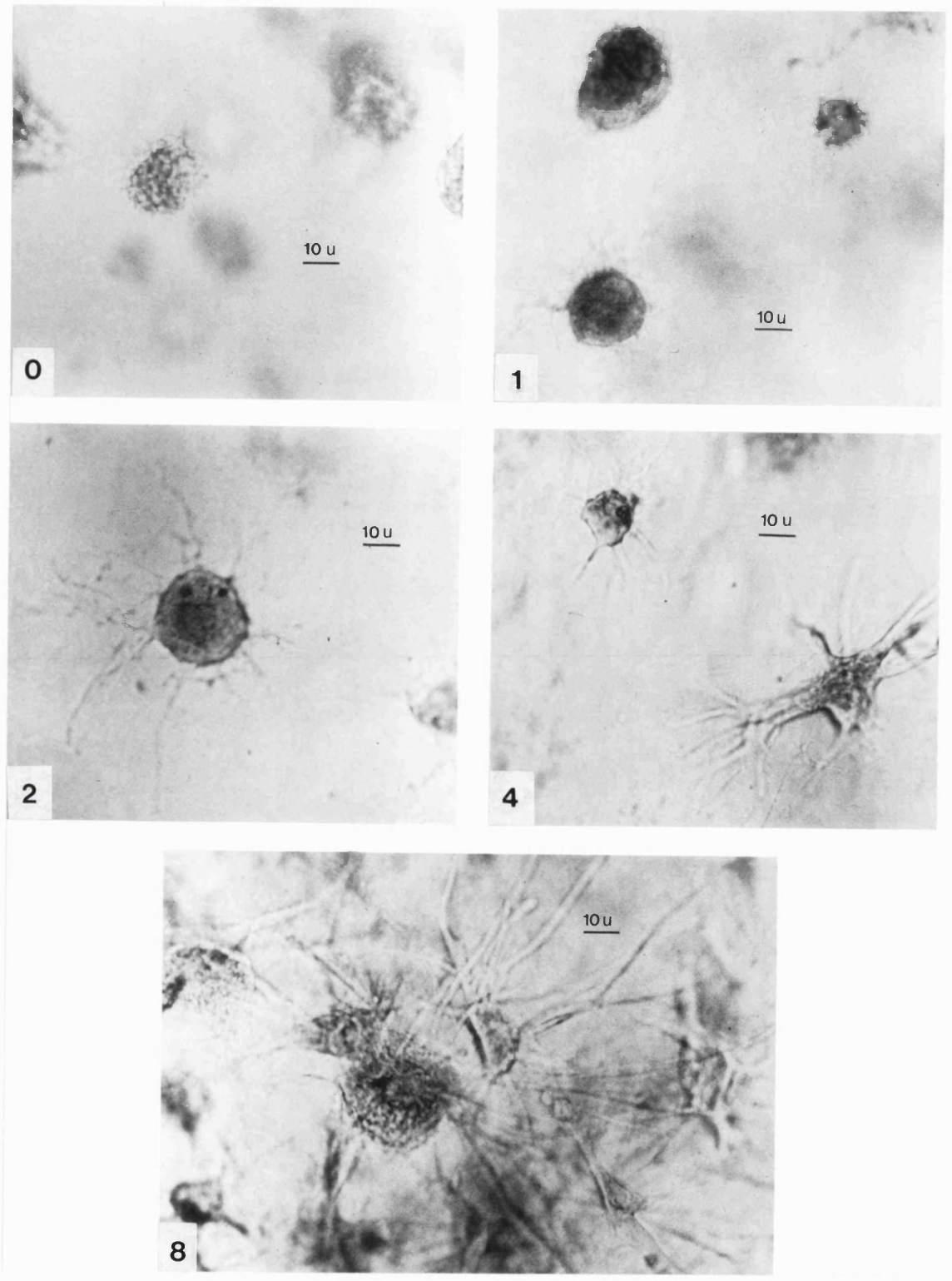

Figure 4.19)... Morphological studies of the fibroblasts taken from the time points indicated in figure 4.18.

Time point 0 (FPCL fixed immediately after gel formation) viewed in a stereoscopic microscope shows that the cells were generally rounded with only a few small surface projections, (figure 4.19a). Cells were dispersed randomly throughout the gel with little clustering and cell-cell contact. At 1 hour the force had increased to 8.5 dynes/million cells, or 35% of the gross maximum force generated in this case. Cells at this time point had begun to take on a more complex shape with the initiation of cell process formation and progressive entanglement at some distance into the surrounding collagen lattice, (figure 4.19b).

By 2 hours 70% of the peak force had been generated and cell processes had further extended in number and distance into the collagen lattice, (figure 4.19c). Continued entanglement of cell processes had brought cells lying in close proximity into direct contact, the main body of many cells had spread to almost twice their original size. These changes continued through the 4 hour stage when contraction had attained 90% of the peak contractile force, (figure 4.19d). Some cells at this stage had assumed a bipolar shape with long processes extending considerable distances from the main cell body, although the majority of the cells, sometimes adjacent to the elongate bipolar cells, were stellate in appearance.

At 8 hours (figure 4.19e) the contraction had peaked and was reducing slightly (approximately 4%). The span of the fibroblasts (across the processes), had increased by a factor of about 4 or 5 since time point 0. In addition cell processes were more extensively interlocked with other cells in their vicinity than at previous time points. At this time point the cells were divided in approximately equal proportions between stellate and bipolar morphologies.

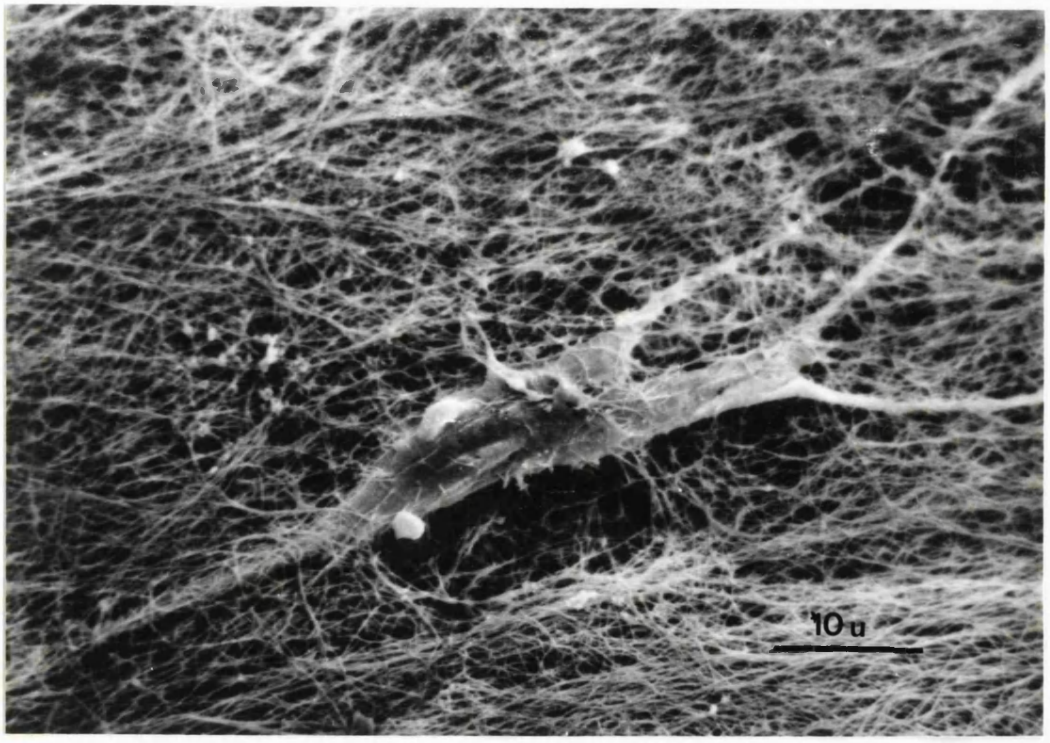

Figure 4.20) Scanning electron micrograph of a fibroblast in a collagen matrix. (SEM preparation and processing courtesy of Miss K. Smith).

Figure 4.20 shows the appearance in the scanning electron microscope of collagen matrix surrounding a single fibroblast after a 24 hour contraction. The cell shown was clearly intimately bound into the collagen lattice over a large portion of its cell body. To one side of the cell there was no attachment to the adjacent matrix where a cavity had been formed. The remains of the ECM could clearly be seen still attached to the side of the cell. This view is consistent with the idea that the cell had broken away from this area of the collagen lattice. Interestingly the cavity was bordered by a region of densely packed, aligned collagen suggesting that fibril bundling had resulted in the cell pulling away from the matrix, leaving a collapsed layer of collagen.

The ultrastructural appearance of the cells from these collagen gels, taken at 0, 8 and 24 hour stage is shown in figure 4.21a-c. These were consistent with the stereoscopic appearance, showing rounded cells with few short processes at time point 0 (figure 4.21a) and dramatically increased numbers and extent of cell process formation by 8 and 24 hours, (figure 4.21b and 4.21c). None of the classical features of myofibroblastic differentiation, (folds in the nucleus or dense microfilament bundles), were seen at these stages.

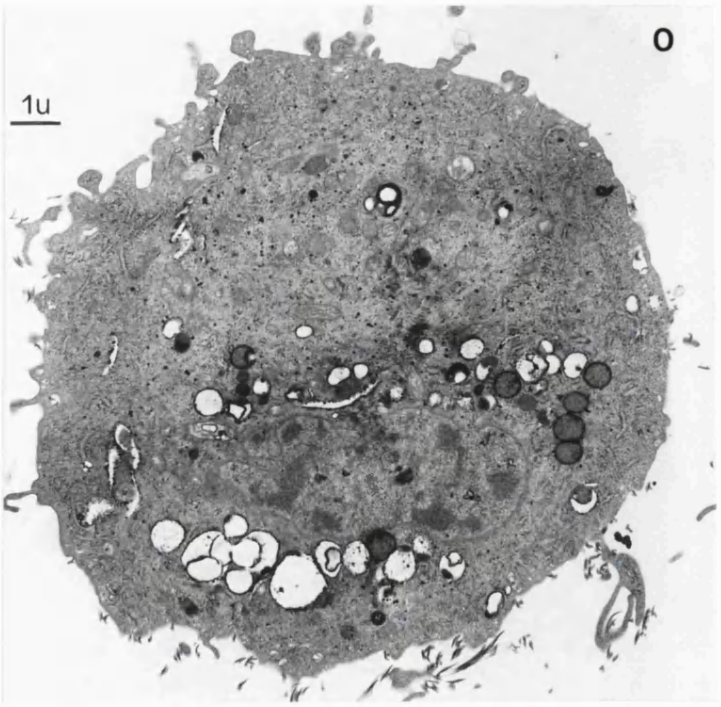

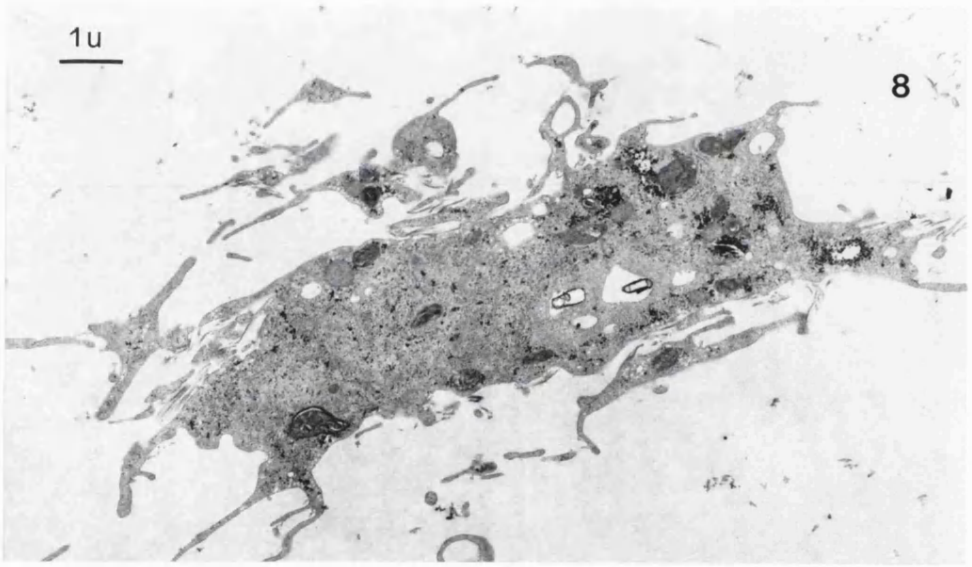

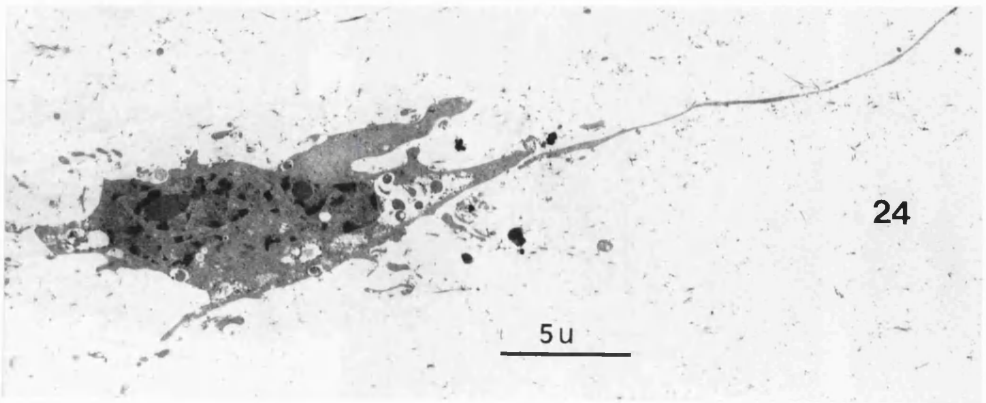

Figure 4.21 Ultrastructural appearance of fibroblasts from 0, 8, and 24 hours in culture. (TEM preparation and processing courtesy of Miss R. Porter.)

4.10) Discussion.

In this study we have analysed the very earliest contractile forces generated by human dermal fibroblasts in a model system designed to quantitate contraction in collagen gels. The primary design considerations for this model were:

A. To accurately measure the forces generated in culture by non-contractile cell types over short intervals and long time courses.

B. To represent, as closely as possible, normal cell behaviour in dermal wound contraction. In particular the resistance of the beam is intended to represent the restraining effect of surrounding wound margins to the contraction.

It is important that the FPCL is restrained as the tensional condition of the matrix dictates the morphology and function of the resident cells. A free floating FPCL will cause the resident cells to behave as if they were in normal dermis, i.e. the fibroblasts become stellate and quiescent systems (Nishiyama et al, 1989). In a tethered FPCL the resident fibroblasts are reported to behave as if they are in granulation tissue, becoming bipolar, actively synthesising collagen and proliferating (Grinnell 1994).

Kolodney and Wysolmerski (1992), have described a comparative approach to measurement of fibroblast and endothelial cell contraction in mature collagen gels. The system described by Kolodney and Wysolmerski (1992) records the changes in a mature collagen gel, i.e. the gel was incubated with cells prior to connection to the force measurement device, so the early changes described here were not recorded. Since the CFM model produces quantitative data on culture contraction it is most comparable with that of Kolodney and Wysolmerski (1992). However, in this comparison the present instrument has the following advantages.

1. Data capture is onto a personal computer, permitting rapid rates of collection, improving subsequent analysis, and allowing for correction due to gel changes and thermal drift in the instrument. Avoidance of an analog chart recorder for data capture in the CFM greatly improved sensitivity, reproducibility and data analysis.

2. It uses hydrophillic, vyon attachment bars to support the culture, eliminating the need to treat these surfaces.

3. Contraction is not perfectly isometric (max. displacement 0.5mm or 3.3% of total gel length), but this better represents tissue contraction than

either unrestrained collagen gel shrinkage (Bouvard et al, 1992) or a fully isometric model (Kolodney and Wysolmerski, 1992).

4. Due to the high sensitivity of the CFM instrument in this model modest cell numbers were required to obtain accurate measurements.

Delvoye et al, (1991), have described an apparatus capable of measuring forces of collagen gel contraction but the instrument used analogue technology so the removal of basal response was outside of the scope of the device, which also suffered from high background noise, obscuring the subtle, but important, fluctuations in force. The ability of the present system to measure very early force generation with great accuracy, reproducibility and with little background noise makes it ideal for investigating the mechanisms by which force is generated by cells in this system.

The nature of the collagen gel is clearly important to contraction. Use of anomalous substrate such as pepsin extracted collagen (hence free of telopeptide) (Nishiyama et al, 1988), make such comparisons difficult. Collagen gel concentration influences both the force and the rate of contraction, Delvoye et al, (1991). Similarly, other factors affect collagen fibrillogenesis, such as the removal of telopeptides by protease digestion (Hodges et al, 1960, Rubin et al, 1963) and the addition of

glycosaminoglycans (Wood 1960). Comparisons were therefore best made only between similar gel preparations. Delvoye et al, (1991), using similar gel and cell types to that reported here, recorded forces equivalent to a range of $1x10^{-8}$ to $1x10^{-9}$ Newton/cell using their apparatus. Kasugi et al, (1990), found forces of around $5x10^{-8}$ Newton/cell although their collagen gels were 2.4 times higher in concentration, and the experiments were conducted on periodontal fibroblasts. These average forces were in the order of 10 times greater than those measured in the present study of $4.5x10^{-10}$ +/- $0.175x10^{-10}$ Newton/cell, (assuming participation of all cells present) and by Kolodney and Wysolmerski (1992). In both cases (Delvoye et al, 1991, and Kasugai et al, 1990), the measurement device appeared to be less sensitive than the device described here. Instruments described previously were calibrated between 0-5gm whereas in the present study calibration was between 30mg and 0.5gm.

The observation reported here that cell-free collagen generates a small force of contraction during a phase corresponding to maturation and growth of collagen fibrils, (Wood and Keech 1960), has not, to our knowledge, been reported before. The molecular basis of this effect is unclear at present but may reflect increasing entanglement and intermeshing of collagen fibrils during this accretion stage. Though small

in the present system, this force may become significant for fibroblasts synthesising their own collagen in granulation tissue.

The three phases of contraction from human dermal fibroblasts over 24 hours represent a framework for interpretation of the cell behaviour. In human dermal fibroblasts the first phase included most of the cell contraction and this was consistent for all cell lines studied. Examination of tethered gel contraction at time points over phase 1 showed that the rapid increase in force generated corresponded with cell attachment and the extension of cell processes which are a prerequisite to any form of cell migration.

The very early onset, (<1 hour), of contraction and rapid appearance of maxima in phase 1 is not consistent with the differentiation of specific forms of contractile fibroblasts or with the secretion of a new connective tissue matrix. However it is consistent with the idea that cell attachment, cell process elongation and movement are responsible at least with the major phase 1 contraction. This is strong evidence in support of the cell locomotion hypothesis of contraction through tractional forces (Harris et al; 1981, Stopak and Harris 1982, Ehrlich et al, 1990).

It was important to note that different cell types produce different patterns and maximal levels of contraction. This supports the idea of fibroblast

heterogeneity, (Torrey et al, 1994), though in this instance heterogeneity of mechanical function. The differences between dermal, tendon, Dupuytrens nodule fibroblasts and bovine articular chondrocytes is perhaps consistent with behaviour of these tissue cells in vivo. However, the ability to distinguish so clearly between dermal cell populations extracted from the tissue in two different ways (proteolytic digestion versus explant) does support the idea that there are contractile/migrational sub-populations of cells within any given specimen.

It would seem reasonable that the growth of cells from explanted dermis would favour the selection of those cells which migrate most strongly relative to enzyme release of all fibroblast populations. The stronger contractile force generated by explant derived fibroblasts lends further support to the idea of locomotion-generated contraction and also suggests that specific sub-populations of cells may contribute more strongly to this.

Further evidence for fibroblast sub-populations can be seen in the summary of the contractile data, (figure 4.13). The time taken to reach the phase 1 contraction equilibrium and the contraction rate are reasonably constant for a range of cell lines. The implications from this is that the mechanism for the attachment is the same (Eastwood et al, 1996).

However the variation in peak force generated is due to the sub-populations of fibroblasts within any given cell line.

The plateau of force commonly recorded following the phase 1 represents a steady state contraction against the reaction of the force transducer, (i.e. gels were tethered). This seems to be a reasonable representation of the force and the reaction which would occur in contracting wounds in vivo under the influence of continuous cell immigration and the mechanical reaction of the wound margins. Over the longer period, into phases 2 and 3, a more complex pattern of forces could be expected as resident cells produce changes in the matrix itself through collagen synthesis and cell proliferation. We have observed lysis of small areas around the cells at the ultrastructural level producing discrete channels, or cavities in the collagen mesh adjacent to migrating cells. The structural appearance of fibroblasts in the collagen matrix in these and other studies indicates that locomotion through the fibril network matrix would require local disruption of, or even complete collagen lysis. Others have identified the release of matrix metalloproteinases, (MMP), by such cells (Lambert et al, 1992) and the inhibition of contraction by the addition of tissue inhibitor of matrix metalloproteinase (TIMP), (Khaw et al, 1994, Millis et al, 1992). Such changes in the structure of the collagen lattice are likely to alter its mechanical properties in the longer term and so could CFM response. For example, it may be that the fall in contractile

force in phase 2 (some dermal fibroblast cell lines) reflects a greater tendency to produce local matrix degradation.

Bovine articular chondrocytes produced a small overall peak contraction (figure 4.17) of 11 dynes/million cells. The form of the contractile curve still followed a similar profile indicating that the cells had attached to the matrix in a similar fashion to the fibroblast cell lines. Rabbit synovial sheath and endotenon fibroblasts produced no contraction during phase 1 or 2 (figure 4.15) but did show a contraction in phase 3, (15 hours), suggesting that the whole process was delayed in this cell type, since it seems unlikely that this attachment dependant contraction is a phenomenon that is particular to dermal fibroblast or chondrocyte cell types.

In contrast to the time scale of days for contraction of un-tethered collagen gels, (Nishiyama et al, 1988), the time taken for the present response is closer to that of cellular attachment. It may be, then, that the longer term response in un-tethered gels involves a different mechanism, perhaps related to cell migration and traction (Stopak and Harris 1982, Harris 1988). Tomasek and Hayes (1984), Bellows et al, (1982), considered that fibroblasts undergo four distinct phases, over 18 to 24 hours, during the change from spherical cell to bipolar elongate shape.

The greatest rate of change of contraction also occurred over this time period, as seen in figures 4.4-4.12.

Tomasek and Hays (1984) used hydrated collagen gels with fibroblasts suspended in the gel to study the role of microtubules and microfilaments in the acquisition of bipolarity and cell elongation in fibroblasts. In their study they reported that within 15 min the cells were extending filopodia, and by 30 min almost all the cells had long thin cell processes. After 3h the firoblasts were restricting filopodia to definite regions of the cell (usually from the two opposite ends of the cell), by 6h in culture the majority of the cells had extended pseudopodia and had bipolar morphology. The contractile data from the CFM corresponded with these observations, as did the morphological study. The phase 1 contraction occurred over approximately 7h, and the morphological study showed increasing cell processes growth and entanglement (figure 4.19a-e).

The phase 2 contraction (7-15h) relates to the 6-18h observations of Tomasek and hays (1984). In their study they reported that during this time period cells extended their pseudopodia and became highly elongated. It was hypothesised that this was the final stage in fibroblast morphology before migration could occur. Scanning and transmission electronmicroscopy of collagen gels recovered from the CFM at the 24h stage also showed the highly elongated form of the fibroblasts.

Fluctuations in the level of force recorded in the phase 2 and 3 contractions may have been due to degradation of the matrix associated with fibroblast locomotion.

Chapter 5: Disruption of Cytoskeletal Components and the Effect on Contraction.

5.1) Materials and Methods

Material and methods were as described in chapters 2 and 3.

5.2) Colchicine Induced Contractions.

Contractile force was generated in the FPLC from the start of measurement, directly after the collagen gel was formed (figure 5.1).

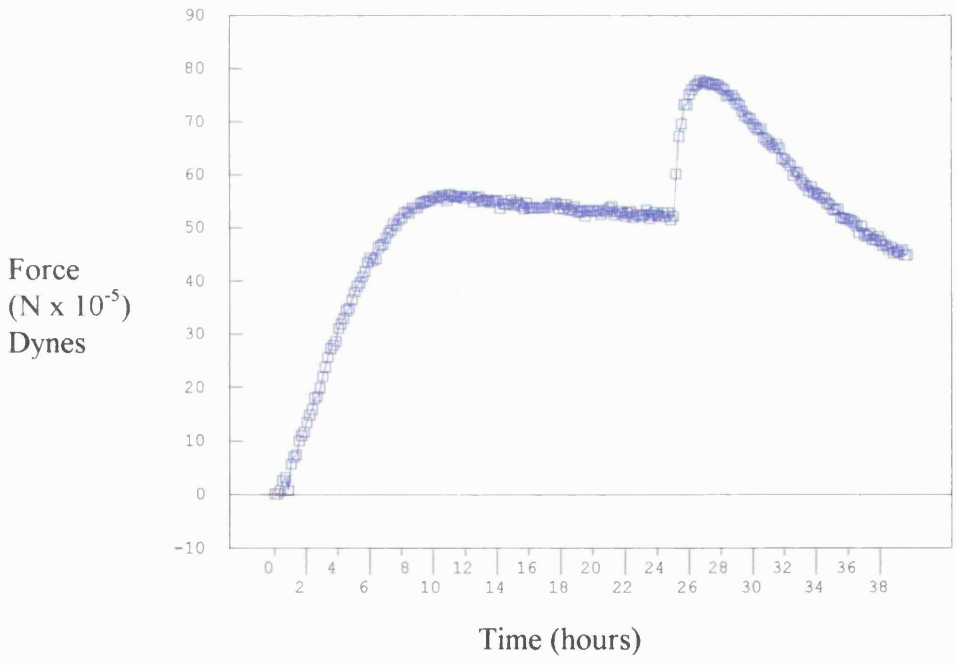

Figure 5.1) Force profile of a colchicine induced contraction. A 0.1mM dose of colchicine was applied at 25 hrs.

Cultures were monitored routinely up to the 24 hr time point during which period the contraction followed the 3 phases described previously in chapter 4 (Eastwood et al, 1996). A plateau of force was reached at approximately 7-8 hours after which time an equilibrium was established between the cellular contraction and the reaction of the CFM. In figure 5.1 the microtubule disrupter, colchicine, was added after the contraction equilibrium had been established. The effect was to elicit a rise in force of over 50% from 52 to 76 dynes/million cells over a 2 hr period. This was followed by a slow decrease in force over the following 17 hrs, at a rate of 2 dynes/hr, back to the level of force prior to drug addition.

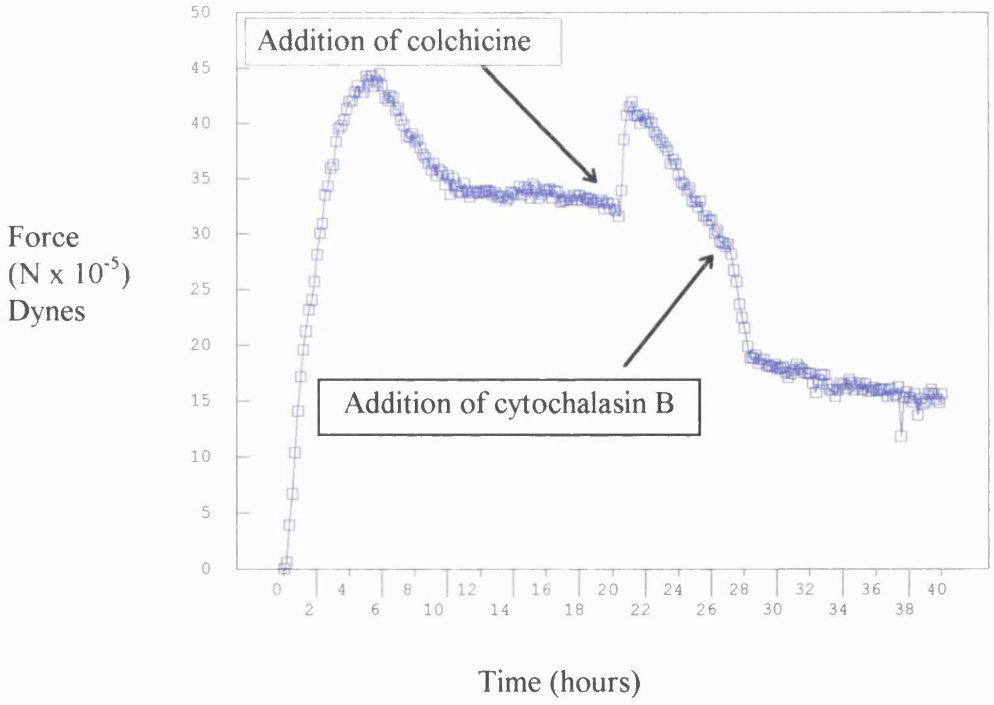

Figure 5.2) Colchicine induced contraction in another strain of human dermal fibroblasts. This was followed by the rapid reduction in force following the addition of cytochalasin B

5.3) Effect of Cytochalasin B on FPCL Contraction.

In contrast, administration of the microfilament disrupter, cytochalasin B, either after a colchicine activated contraction (figure 5.2), or during an untreated contraction, caused an immediate fall off in tension across the FPCL to only 60% of its previous level.

5.4 Addition of colchicine in the phase 1 contraction.

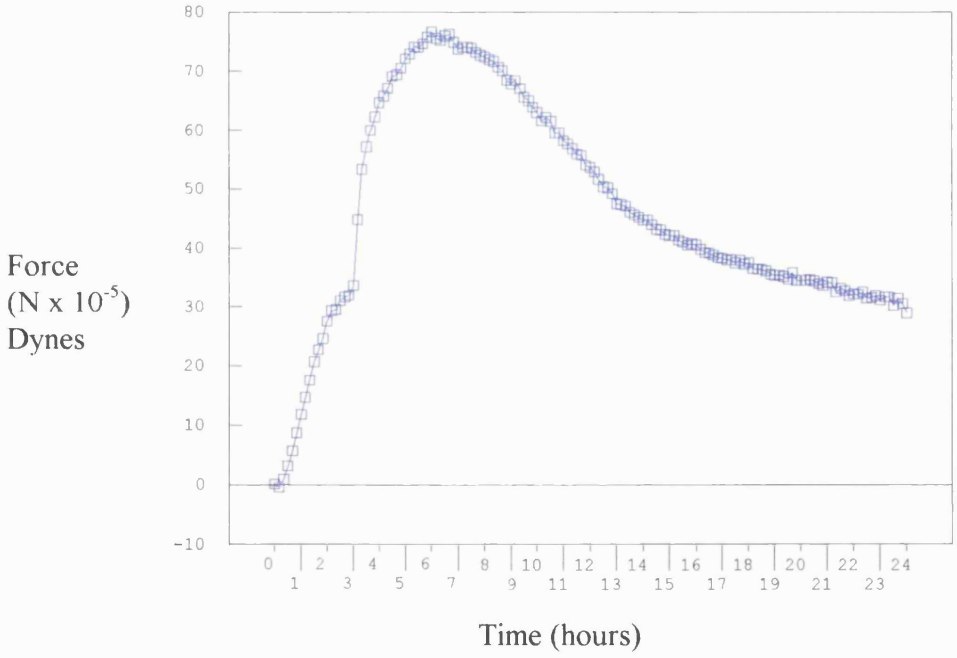

Figure 5.3) Force profile of human dermal fibroblasts treated with colchicine during the phase 1 contraction.

Figure 5.3 shows the effect of colchicine addition at a much earlier stage (3 hrs into the contraction) where the force generated was still rising rapidly (i.e. before a contraction equilibrium had been reached). Again, this produced a dramatic increase in contractile force, to more than 130% above the pre-drug level, rising over a 3 hr period from 32 to 76 dynes/million cells and then decreasing at a rate of 2.4 dynes/hr. It is notable that the final equilibrium force maintained after the drug was approximately at the level of force when the colchicine was added. This was a stable equilibrium, with little change up to the 70 hour stage. A similar return to the level of tension present prior to colchicine was seen in the late stage treatment in figure 5.1, where the original equilibrium was regained approximately 20 hours after drug treatment.

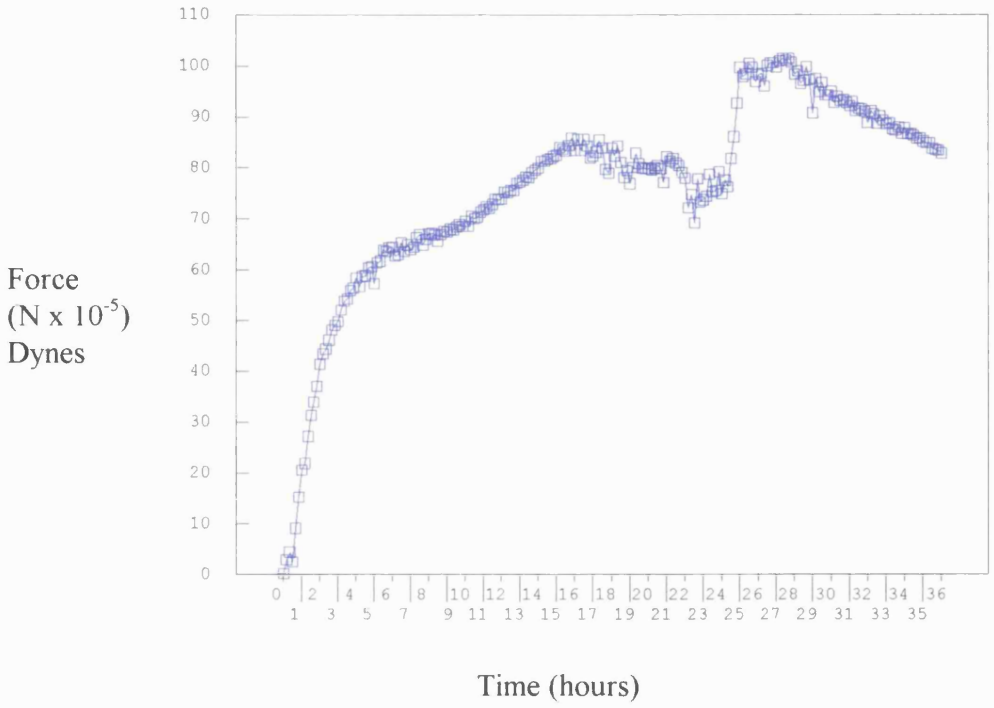

Figure 5.4) Colchicine induced contraction on Dupuytrens nodule fibroblasts.

5.5) The Effects of Microtubule Poisons on Fibroblasts from Other Sources.

Comparable increases in force were produced in all fibroblast cultures tested (i.e. from different patients), and by addition of colchicine at time points of 3, 7 and 24 hours into the contraction. Return of the tension to a

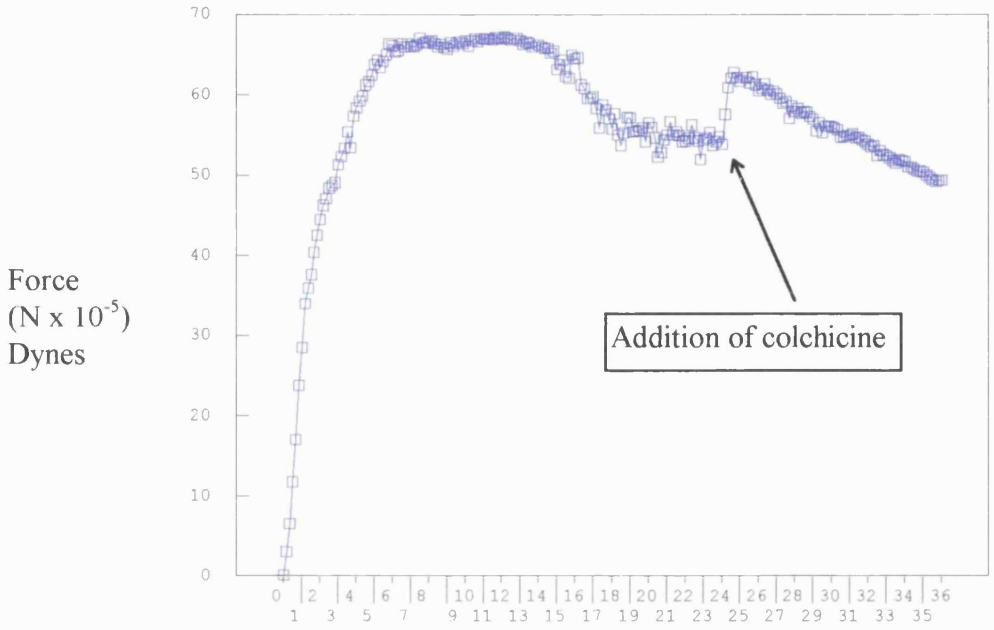

Figure 5.5) Colchicine induced contraction on normal human fascia cells. (Cells kindly provided by Dr A. Wilson).

post-treatment equilibrium was a constant feature of all the normal skin fibroblast cultures examined. Comparable colchicine-generated contraction peaks were also produced in cultures of fibroblasts from human Dupuytrens nodule and normal human fascia, though in each case the percentage activation above equilibrium differed between tissues. In no case did the subsequent addition of a second, equal dose of colchicine give any further increase in force (figure 5.6).

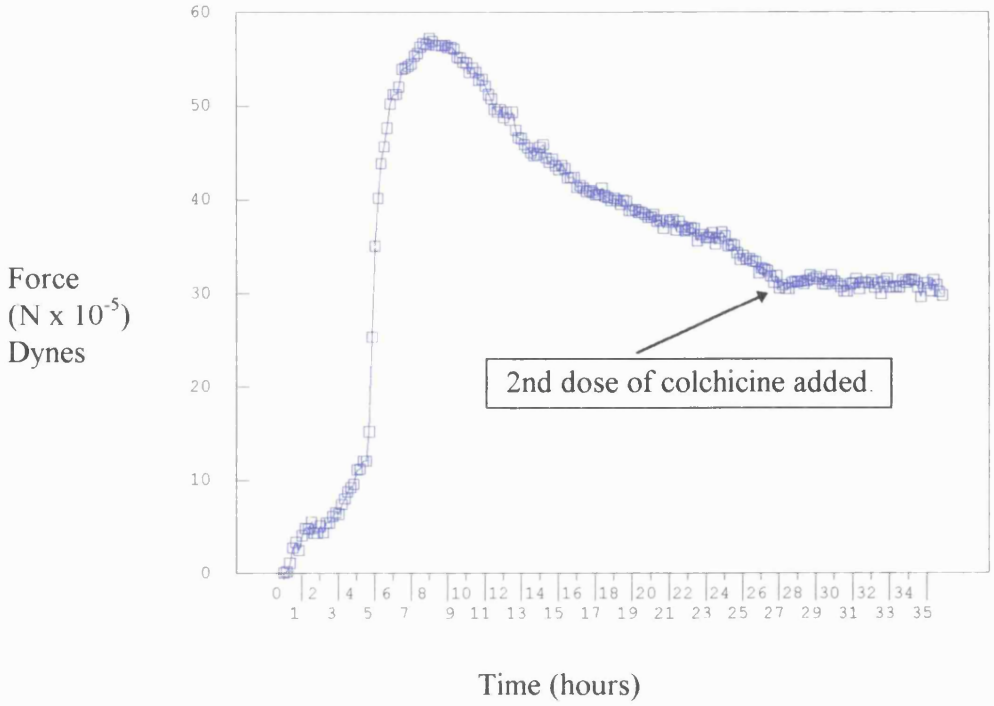

Figure 5.6) Force profile of human dermal fibroblasts with repeated doses of colchicine. The first bolus at 4.75 hrs produced the characteristic increase in force. A second equal dose at 27 hrs produced no significant change.

5.6) The Effects of Vinblastine Sulphate on FPCL Contraction.

Addition of vinblastine sulphate produced a similar profile with the characteristic immediate increase in force (figure 5.7), from 35 to 75 dynes/million cells (an increase of 114%) over a 2 hr period, with a subsequent fall-off of force of 2.33 dynes/hr. Again, addition of a second, equal dose of vinblastine produced no further change in force

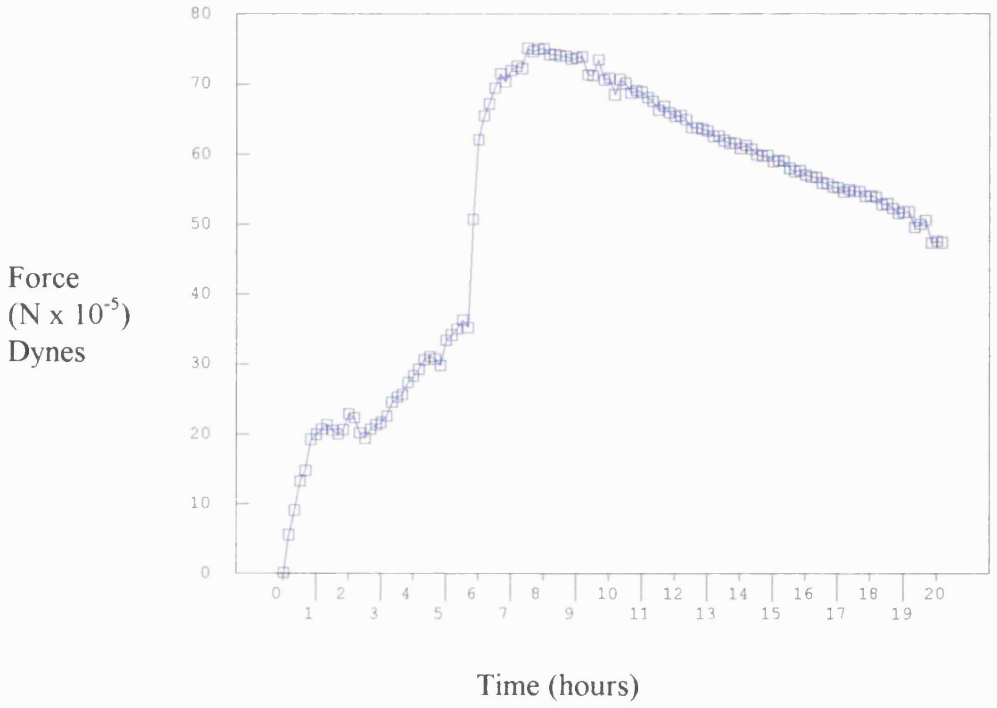

Figure 5.7) Force profile of human dermal fibroblasts showing the increase in contraction following the addition of a 0.1mM dose of vinblastine sulphate.

It is interesting to note that the drug induced peak contraction is reasonably constant for cell lines that have similar phase 1 contraction equilibrium values. Applications of microtubule disrupting drugs at early time points (i.e. within the phase 1 contraction) caused correspondingly larger rises in measured force, but the peak value was constant at 78.6 ± 1.8 dynes/million cells. Figure 5.8 shows the comparison of 3 cell lines that were treated with microtuble disrupting drugs at various time points.

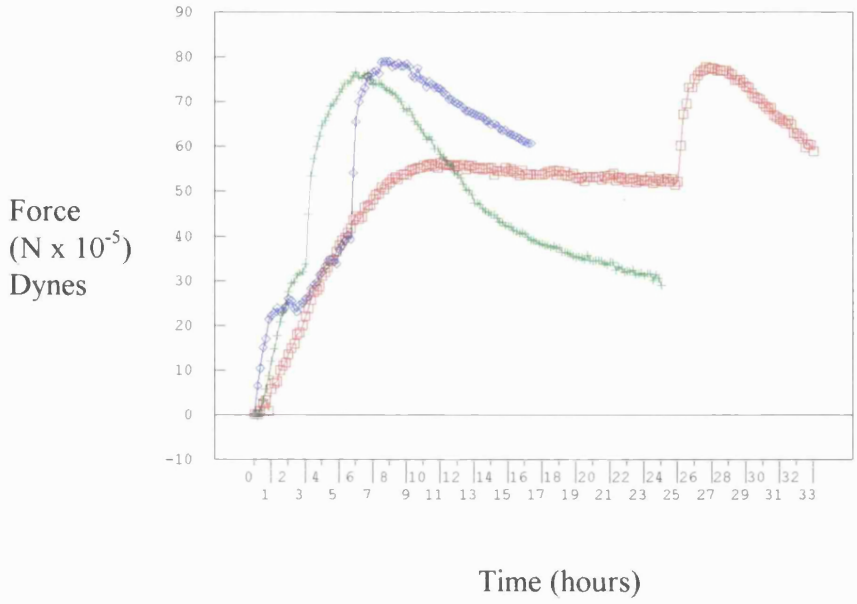

Figure 5.8) Comparison of peak induced contractions from drug applications at various time points. Note the consistent peak value achieved.

5.7) Immunohistochemical Analysis of Disrupted Microtubule Arrays.

Disruption of microtubular arrays after colchicine addition was confirmed by routine immunohistochemical analysis. In these series of experiments fibroblasts from the same cell line and passage were cast and allowed to culture in the CFM. After approximately 8 hours (when the phase 1 contraction equilibrium had been reached) a 0.1mM dose of colchicine was administered to the cultures. The experiments were stopped, fixed under tension and gels recovered from the CFM at the following time

points. Curve A, 13h; curve B, 3.5h; curve C, 0h (i.e. drug applied and immediately fixed).

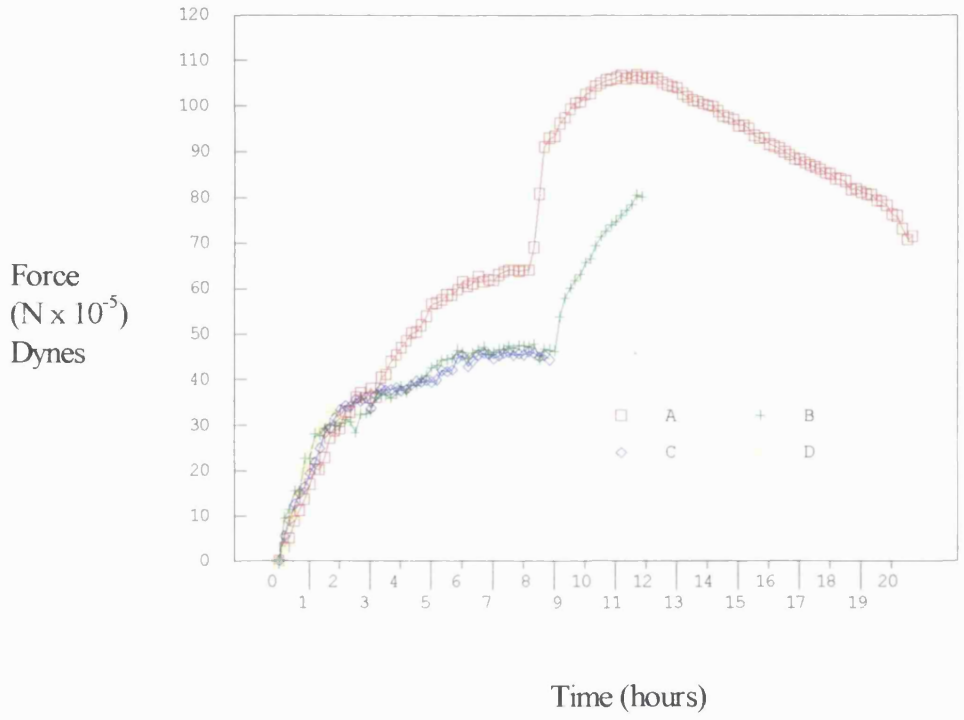

Figure 5.9) Force profiles overlaid from 4 different experiments, all human dermal fibroblasts came from the same cell line and passage number. Equal doses of colchicine were applied at approximately 8.5 hrs. (For full explanation see text).

Curve D had no drug applied and was a control. The overlaid curves are shown in figure 5.9. After fixation the gels were immunohistochemically stained for tubulin and examined under a fluorescence microscope. The results are shown in figure 5.10.

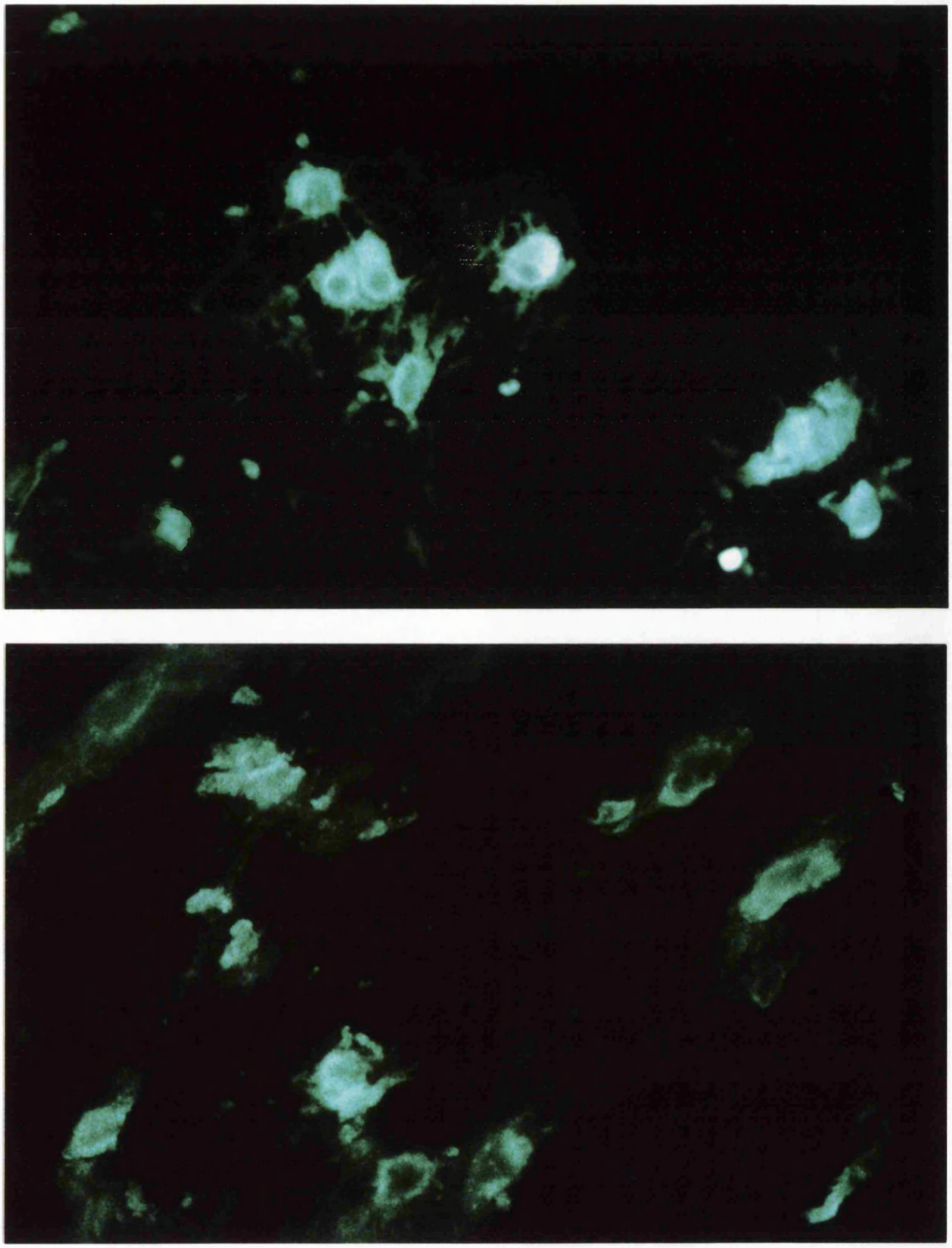

Figure 5.10) Microtubules disrupted by the action of colchicine. (Staining courtesy of Mr Z. Ahmed.)

Figure 5.10a (0 hours, curve C) shows the microtubules to be intact with dense microtubular rings around the cell nuclei, and narrow assemblages passing along the cell processes. Increasing amounts of microtubular fragmentation are evident in figure 5.10b (3.5 hours, curve B). The degree of microtubule fragmentation indicated that cell process were no longer viable. Complete fragmentation of the microtubular structure, including the dense ring around the nuclei, is evident in figure 5.10c.

5.8) Pre-treatment of Fibroblasts with Colchicine and Vinblastine Prior to Collagen Gel Formation.

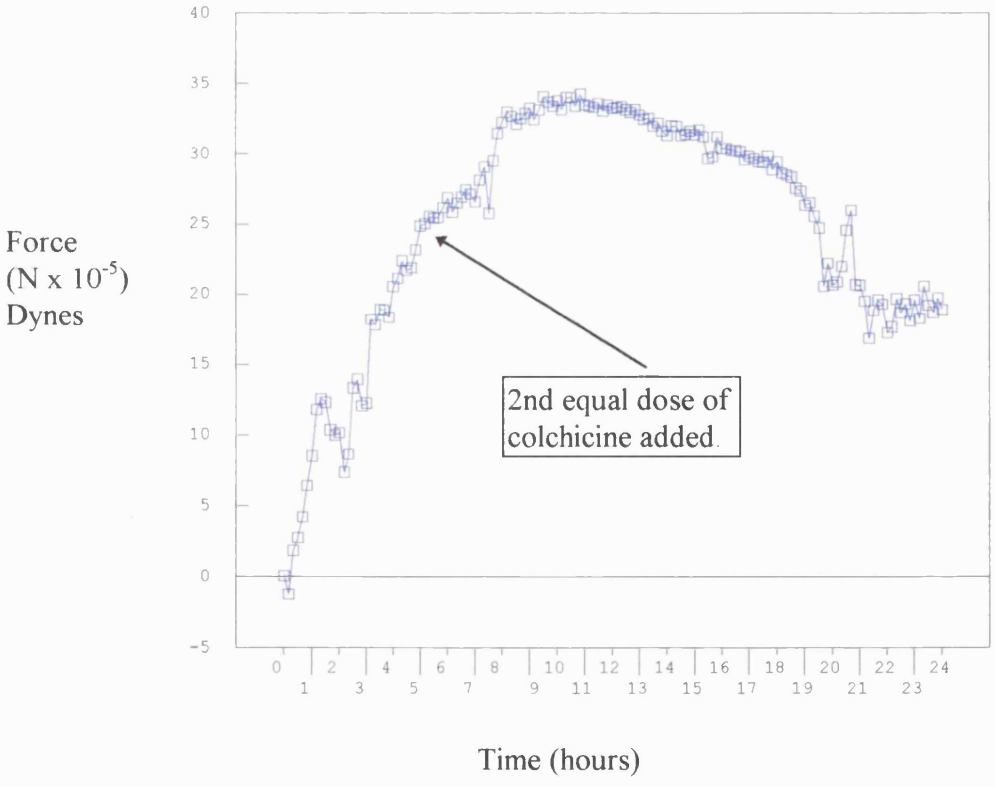

Figure 5.11) Colchicine added to culture prior to gel forming. Second equal dose of colchicine added 4.75h into the experiment.

The effects of colchicine treatment, prior to contraction, was tested by addition of the drug to the cell-collagen mixture before gel formation (figure 5.11). Contractile forces were generated in the presence of the drug at zero time, but the pattern of contraction was substantially altered, and the peak force generated was reduced by 50% from that produced by the same cell line prepared without colchicine. In addition, the force was no longer linear over the first 5 to 6 hours but included short periods of no contraction or even reductions in generated force.

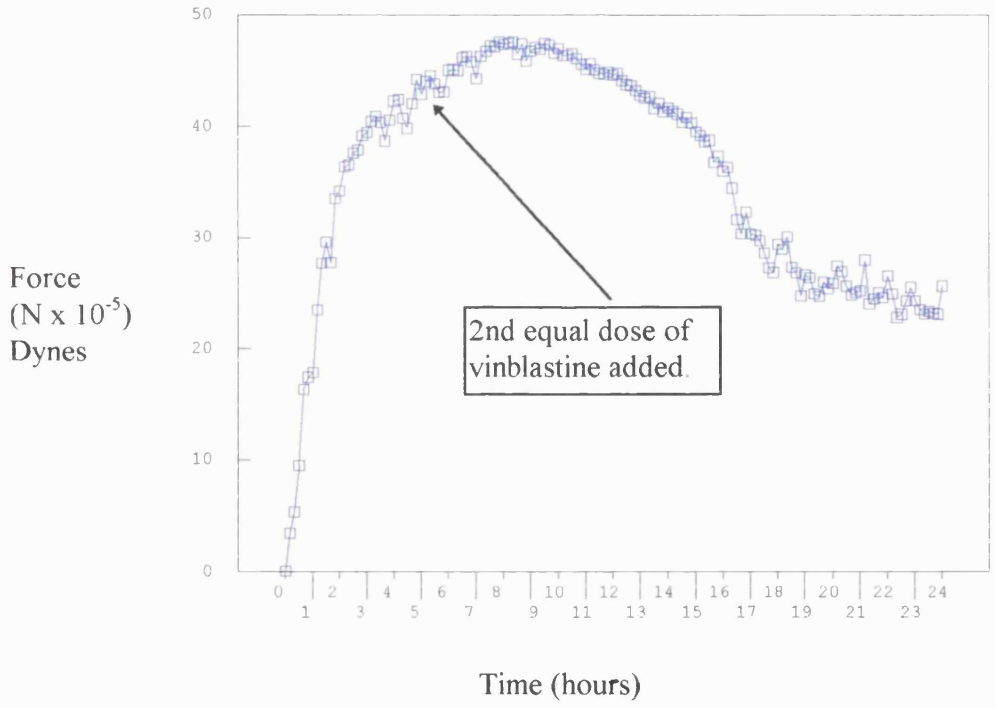

Figure 5.12) Vinblastine sulphate added to culture prior to gel forming. Second equal dose added 4.75h into the experiment.

As in the case of bolus application of the drug during the experiment, no additional effects were produced by further additions of colchicine. The addition of vinblastine sulphate prior to contraction, and a second equal dose 7.5 hours into the contraction had the same effect as the pre-treatment of colchicine (figure 5.12), i.e. no further contraction was evident. Failure of a second equal dose to elicit any further effect suggests that the initial dose was saturating.

5.9) Microtubular Stabilisation by Taxol.

Since an increase in force was elicited by microtubular disrupting agents it was important to determine the effect of microtubular stabilisation. This was achieved by addition of the drug taxol. Taxol was given near the end of the phase 1 contraction, 6 hours after the start of the experiment (figure 5.13). At this time point it was estimated that cells would have been effectively attached to the collagen lattice, though maximal contraction had not been reached. This retained at least the possibility that we could detect an increase in the rate of contraction if this was produced. In fact the effect of taxol was clearly one of reducing the level of measured force.

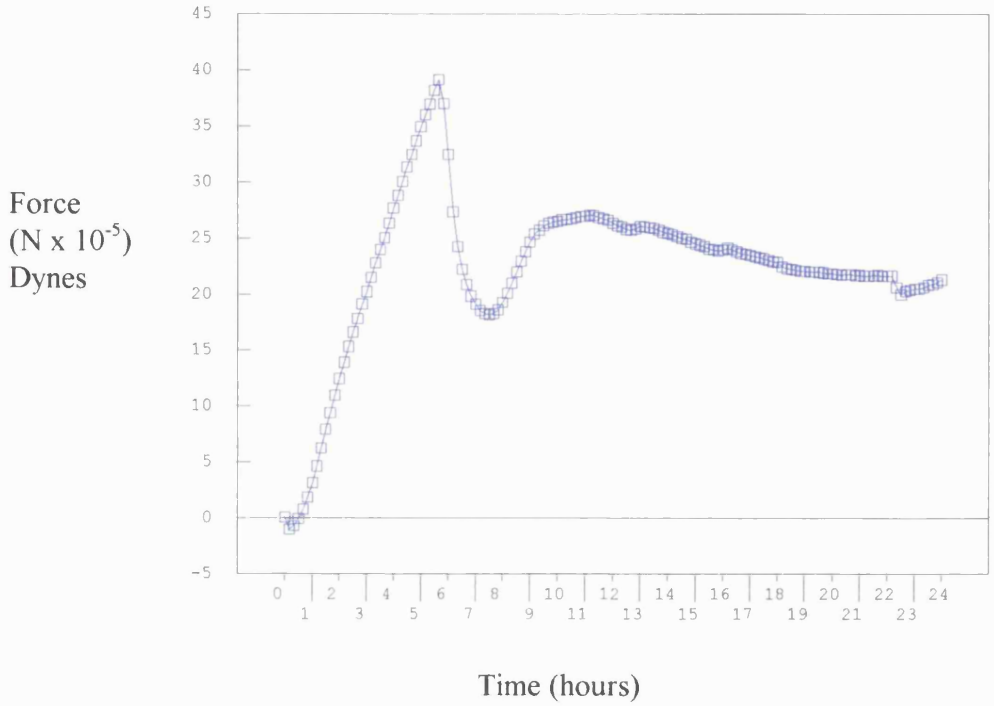

Figure 5.13) Graph showing the effect of the addition of taxol at 6 hrs. This was followed at 22 hrs with a 0.1mM dose of colchicine.

Immediately following the addition (<10 mins) there was a rapid drop in force at a rate of approximately 14 dynes/hr. This continued over 1.5 hours and was followed by a more gradual decline (at 1 dyne/hr). At 3.5 hours post treatment there was a recovery of force generated at a rate of 3 dynes/hr. It was important to note that the rate of fall following taxol was approximately the same as the rate of increase which followed colchicine treatment. A new force equilibrium persisted for 11 hours with only minimal reduction until the 2nd drug application (colchicine). Addition of colchicine (again to 0.1mM) at 22 hours did not in this case elicit a peak in contraction, indicating that stabilisation of the microtubular structure

was not reversible under these conditions. Control cultures, receiving the application vehicle only, produced no response.

5.10) Discussion.

The mechanism underlying fibroblast contraction of matrices, particularly in wounds (Ehrlich and Rajaratnam, 1990; Grinnell, 1994), is of widespread importance both clinically and as a more basic problem of cell biology. It is a process closely linked with fibroblast locomotion, shape change, collagen organisation, and the cytomechanics of connective tissues (Eastwood et al, 1996, Dennerll et al, 1988; Ingber, 1991; Chvapil, 1980). The observation that force exerted by fibroblasts increases following microtubule disruption initially seems to contradict the simple idea of cytoskeletal involvement in motor functions and cell process extension (Ehrlich and Rajaratnam, 1990; Eastwood et al, 1996). This is particularly true in view of earlier reports that, on fibroblasts, colcemid (a microtubule disrupter) produces morphological changes associated with reduced motility and persistence of motility (Gail and Boone, 1971). Detailed resolution of this is likely to prove important in clarifying the role of microtubules in locomotion and force generation.

Danowalski (1989) reported an increase in the wrinkling of silicone membranes by attached fibroblasts following treatments to disrupt microtubules. Delvoye et al, (1991) and Bell et al, (1979) appeared to find a reduction in contraction of collagen gels in their systems. In contrast, Kolodney and Wysolmerski (1992) reported an increase in force with this drug, whilst stabilisation of microtubules by the addition of taxol,

Kolodney and Elson (1995), decreased the contraction similar to that reported here. However, these two studies were complicated by the absence of serum which is known to be essential, in a complex multi-component manner, for effective FPCL contraction (Gulberg et al, 1990 and Asaga et al, 1991).

On the basis of their results, Kolodney and Elson, (1995) proposed that the increase in force was a result of chemical signals released from microtubules as they de-polymerise. This signalling event was suggested to explain a correlation identified between microtubule disruption and an increase in myosin light chain phosphorylation. Myosin light chain (LC_{20}) phosphorylation has been implicated in the control of cytoplasmic motor activity through its role in actino-myosin function. This led these authors to propose that the increase in force following microtubule disruption was, in fact, a result of stimulation of contractile microfibrillar elements.

Measurements of force changes in individual neurites in a quite different system indicated that microtubule disruption leads to an increase in the cell resting tension (Dennerll et al, 1988). Such changes in force in this system were dependent on links between functional microtubular assembly and attachment to the substrate. This is consistent with the tensigrity theory (Ingber, 1991; 1993), which links the expression of cytomechanical forces with the nature of the extracellular matrix to which

the cell (and its cytoskeleton) is attached. Functional microfilament and microtubular components have been implicated as important in the maintenance of cell shape (Gail and Boone, 1971; Madreperla and Adler, 1989) in retinal photo-receptors and in fibroblasts (Tomasek and Hay, 1985). In fibroblasts filopodial extension was microfilament-dependent, but acquisition of a bipolar morphology was additionally dependent on microtubular function.

The present study confirms the finding in other systems that disruption of microfilaments decreases the force generated (consistent with removal of contractile elements). In contrast, to the contraction peak which followed microtubular disruption, the contractile force fell on addition of taxol, which stabilises microtubules and enhances microtubule mass (Manfredi et al, 1982). These findings are consistent with the idea that there is a residual internal tension (RIT) in fibroblasts which exists as a compressive loading on the microtubules.

Cytoskeletal components are responsible for the generation and maintenance of this RIT, which is an internal cellular tension generated by the actino-myosin motor function of the microfilaments, balanced by the microtubular component of the cell. This has the effect of creating a higher energy state i.e. residual spring energy within the cell. The RIT generated in the cell is balanced by the stiffness (i.e. spring constant) of

the collagen lattice. It may be then that during the phase 1 contraction the rise in measured force to an equilibrium constant, that varies for different cell lines, is a measure of the different RIT values for different cell lines and sub-populations of these cells. The greater the value of the RIT the more the cell is capable of contracting the collagen lattice. Contraction of the collagen lattice will cause an increase in the density, and hence the stiffness (spring constant) of the lattice will also increase, this process occurs during the phase 1 contraction. Figure 5.14 shows a representation of the fibroblasts residing within the collagen lattice in terms of the spring constants for the component parts of the system.

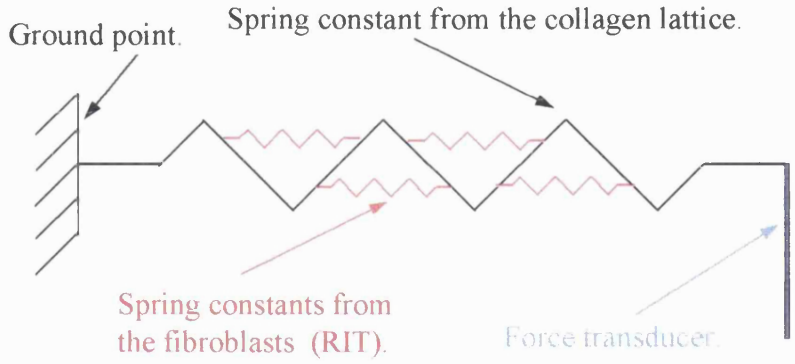

Figure 5.14) Representation of the collagen matrix and resident fibroblasts attached to the collagen lattice in terms of their spring constants.

Assuming that the value of RIT remains constant (for individual cell lines) then this force (when released) on a less stiff matrix will cause a greater reduction in matrix size, and hence greater rise in measured force. This is indeed the case, figure 5.8 shows the comparison of the rise in measured force when the RIT is released into the collagen lattice at early time points, before the phase 1 equilibrium has been reached when the lattice is less stiff. The observation that the drug induced contractions have an almost identical peak value would suggest that an identical density, and hence stiffness, had been achieved within these collagen lattices.

Since disruption of the microtubules immediately reduces the RIT, displacing this force onto the extracellular matrix (i.e. the collagen lattice), increasing the microtubule density (by stabilisation with taxol) would increase the RIT and take load off the collagen lattice. The rapid nature and direction of these changes are consistent with measurements made using the CFM. It is also important to note that comparable stimulation of contraction was seen at all stages of colchicine addition providing it was after cells had time to attach and spread through collagen fibrils in the lattice (Eastwood et al, 1996).

Pre-treatment with either colchicine or vinblastine did not stop the fibroblasts from contracting the FPCL. Figure 5.11, 5.12 show that the contraction did indeed occur, however the force profile was considerably

altered from that seen in untreated cells from both the same passage and cell line. Failure of a second dose of colchicine or vinblastine to elicit a further contraction showed that the RIT was absent. This is consistent with the idea that a RIT is placed on the microtubules, though it further indicates that the RIT may be important in regulation of force generation.

On the basis of this study it is proposed that the additional force which is generated by saturating doses of colchicine equates to the RIT for that cell type and that stage of its activity. This interpretation is central to the mechanical model proposed in figure 5.14 and visualised in figure 5.15. In this model, tensile forces are produced across fibroblasts by motor elements of the microfilaments (shown as green bands in figure 5.15) which generate intracellular tensions when attached to the extracellular matrix (through integrin based attachment plaques) or to links with other cytoskeletal elements. In order to maintain some cell shape, against the tendency of these forces to produce random distortion, an opposing element of the cytoskeleton must be present. The role proposed here for microtubules (represented as copper rods in figure 5.15) is that of maintaining cell shape against a compressive loading originating from the microfilaments.

This view of microtubular function supports previous suggestions that a compressive loading is exerted on microtubules (Dennerll et al, 1988;

Jamney et al, 1991; Rudolph and Woodward, 1978, Eastwood et al 1995) consistent with their structural rigidity. Under these circumstances, the level of intracellular compressive load on the microtubules will equal the RIT, a concealed force not expressed under normal circumstances on the ECM. This clearly represents a balancing of forces within the cell and disruption of this balanced restraint would inevitably lead to loss of cell shape and alter the nature of cellular locomotion.

Using this 'balanced' model of opposing mechanical forces in the cell it is possible to interpret a great deal of the behaviour of fibroblasts in this and other experimental systems. The model proposed here (figure 5.14, 5.15) is analogous to engineered structures based on a 'balanced space frame'. In this, the structural integrity (i.e. shape) is maintained through the action of a suspended internal frame under compressive loading from tensioning (microfilament) components. This model is comparable with the framework within an aircraft fuselage, or the guide cables tensioned across a radio mast, though in contrast to such static examples cytoskeletal elements are dynamic.

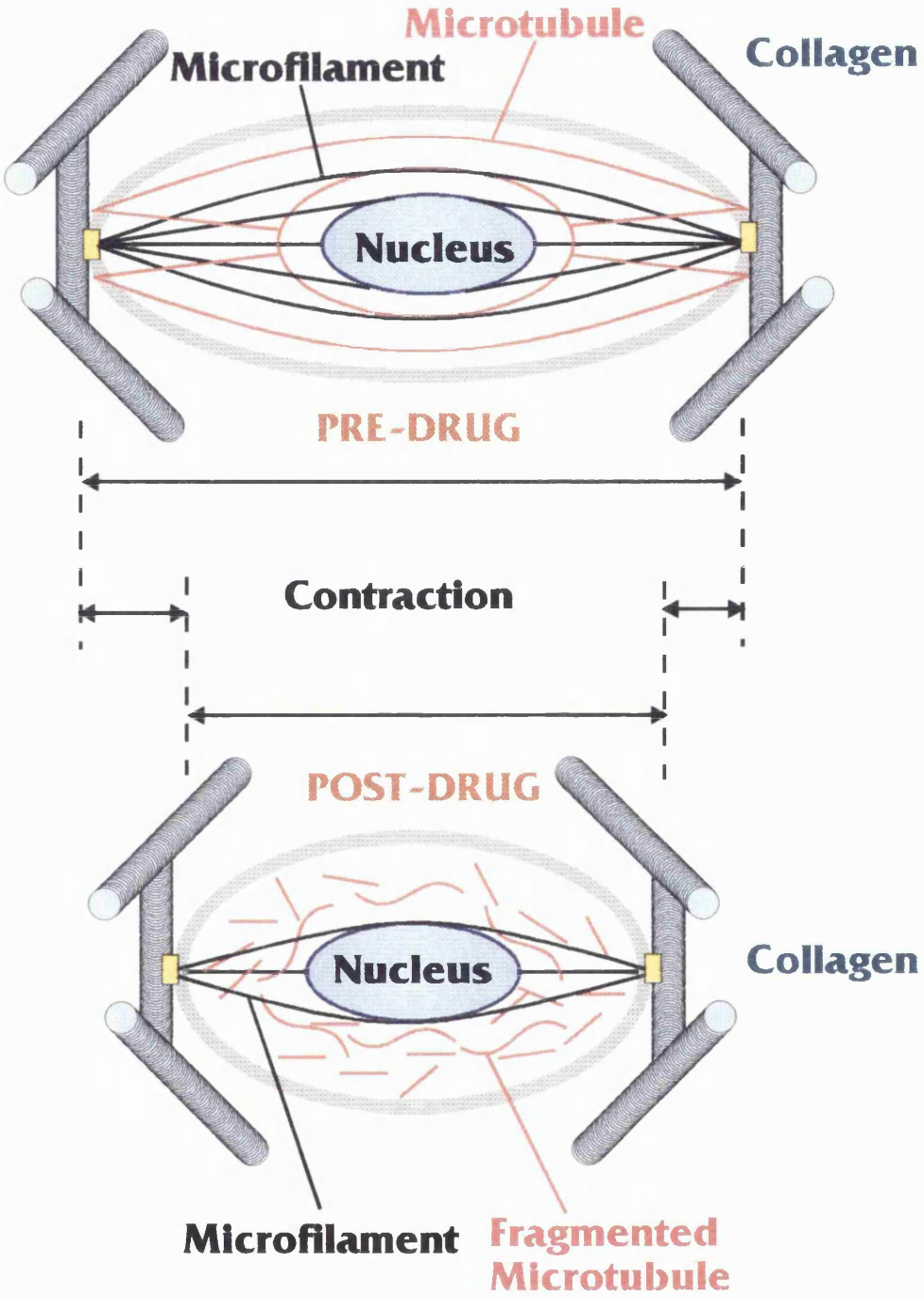

Figure 5.15) Diagram of the 'balanced space frame' model of microtubular function in fibroblasts. Indicating how fragmentation of microtubules under compressive loading would lead to an increase measured external force. Conversely, increased microtubular mass would cause a reduction in measured external force, by increasing the RIT. Yellow areas represent cell-matrix integrin-based attachment plaques, linking both microfilaments and collagen fibrils.

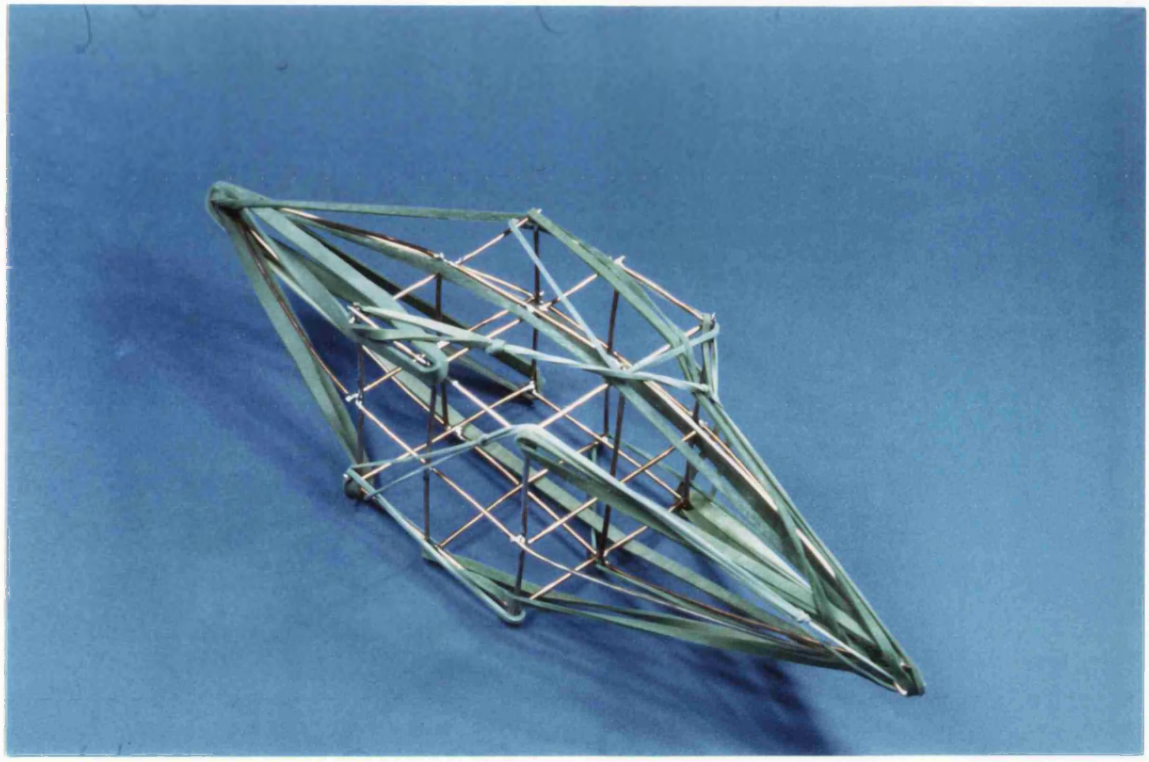

Figure 5.16) Mechanical visualisation of the 'Balanced Space Frame' model. Green bands are representative of the microfilaments and copper rods of the microtubules. The structure is highly stressed, so failure of any of the microtubules, (copper rods) will immediately overload the remaining structural members, leading to a catastrophic failure.

By this analysis, therefore, the colchicine-generated force peak is a measure of the RIT stored in the 'space frame'. Its magnitude is considerable, at around 33% of the total external contractile force at equilibrium. This would imply that the magnitude of this balanced internal force could be a characteristic for different forms of fibroblasts.

Control of the RIT would be predicted to depend on the mass of assembled microtubules and the presence of microfilament motor elements. Differences in the RIT levels between fibroblasts would determine the external force they were able to exert on their ECM. For example, the net force generated on the ECM by myofibroblasts, with their prominent and contractile cytoskeleton (Gabbiani et al, 1972; Gabbiani et al, 1978), would be modulated by density of their microtubular network. Normal dermal fibroblasts could still exert significant external stress on the ECM by having a less robust microtubular 'space frame'. Based on this interpretation myofibroblasts may represent a particular, if extreme, state of balance of the space frame which constitutes one phenotypic variable between fibroblasts. Such a view could provide a framework for understanding the varied clinical features associated with wound contraction.

One critical feature of the balanced frame system is that initial failure of a proportion of the supporting members would immediately overload the remaining intact members, potentially leading to a rapid and catastrophic structural collapse. In the case of colchicine-treated fibroblasts, retraction of cell processes would transmit force directly to the attached collagenous extracellular matrix (ECM), producing a force peak on the CFM. This rapid collapse type of failure is consistent with the rate of onset of force generation seen with colchicine, particularly as the drug

must diffuse into the collagen gel and through the cell membrane to be effective.

Dependence on two dynamic and opposed cytoskeletal elements could also explain the rapid effects of shape change and contraction. The 'balanced space frame' model proposed here on mechanical data supports earlier deductions that microtubules maintain cell shape under compressive loading (Jamney et al, 1991; Rudolph and Woodward, 1978). Given that microtubules are indeed under compressive loading, the proposal that microtubule disruption also stimulates contraction of motor elements via phosphorylation of the LC_{20} protein (Kolodney and Elson, 1995) appears to be unnecessary, or at least a secondary effect. The first and immediate consequence of disrupting microtubules under compression would be to apply load to the matrix (Eastwood et al 1995), irrespective of the contribution of multi-stage slower events which lead to contraction.

The space frame model, proposed here, complements that of tensegrity, where internal forces in the cell are balanced by loading onto the external collagenous matrix (DennerII et al, 1988; Ingber, 1992; 1993) and the suggestion of opposed forces within retinal photoreceptors (Madreperla and Alder, 1989). In a contracting collagen lattice, fibril bundling would be expected to continue until aggregation was sufficient to resist the net

external tension of attached cells (i.e. total internal tension minus the load taken by the 'space frame'). Subsequently it could deduced that the final material properties of the collagenous network, in terms of the collagen alignment, density of the packing and the extent of any cross-linking, would be determined by the type of cells and their cytoskeletal organisation. For example, fibril density achieved by normal dermal fibroblasts would be predicted to be less than that of contractile types, namely the myofibroblasts, therefore with normal dermal fibroblasts the balanced space frame would store a relatively smaller proportion of the total force generated. Hence the space frame, RIT and tensegrity models together provide a novel hypothesis of how different fibroblast populations might produce different collagen architectures.

Chapter 6: The tensioning-Culture Force Monitor, and the effect of mechanical stimulation on fibroblast populated collagen lattices.

6.1) Materials and Methods.

To determine the effect of mechanical stimulation on cellular response the tensioning-Culture Force Monitor (t-CFM) was used to perform cyclical loading and unloading on FPCLs. The loading cycles used were Cyclical Over Loading (COL), Cyclical Under Loading (CUL), Cyclical Median Loading (CML) and Cyclical Incremental Loading (CIL). These loading cycles are shown in chapter 3, figures 3.6-3.9.

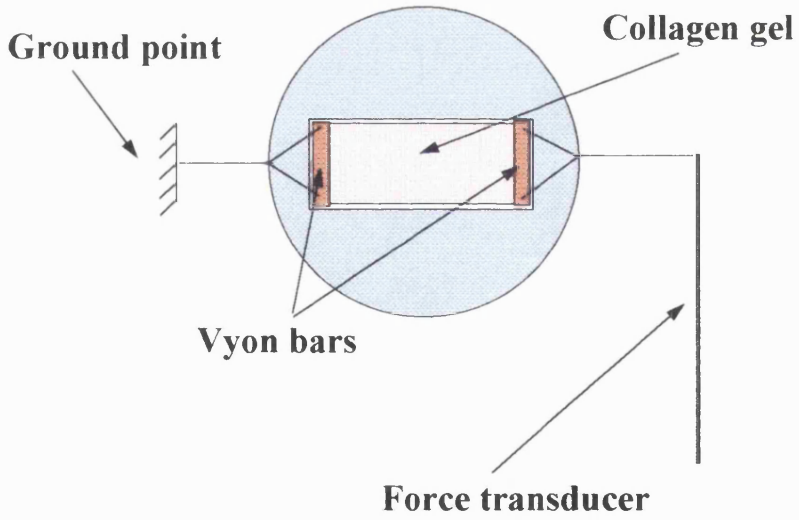

Figure 6.1) High aspect ratio culture well. In this format the aspect ratio is increased to 3:1 from 0.33:1 as shown in figure 2.3

Tissue culture, collagen gel preparation and t-CFM set-up was as previously described in chapters 2 and 3. High aspect ratio cultures (figure 6.1) were used in some of the experiments to determine the effect of different patterns of strain profile within collagen gels under identical external loading on fibroblast alignment and morphology. In this format the vyon bars were placed in the short aspect ends of the culture well. This orientation increased the aspect ratio from 0.33:1 in the previous arrangement to 3:1.

In this part of the study collagen lattices were seeded with 5 x 10^6 cells, the graphs shown are the net response of the total cell population, i.e. the results have not been normalised for 10^6 cells as the mechanical stimulation was of a fixed value. Cyclical mechanical stimulation did not start until the phase 1 equilibrium contraction had been reached i.e. there was a 8 hr delay before the loading cycle started. This meant that the whole cell-collagen lattice was under a relatively constant tensional load, which was maintained by the resident cells themselves.

The effect of mechanical stimulation on fibroblast alignment and morphology was assessed by the direct observation of un-sectioned FPCL's, on an Edge High Definition Stereo Microscope, fixed under load at the end of treatment on the t-CFM. Observation was also carried out

on cell and collagen orientation, relative to the plane of the applied load by scanning electron microscopy on freeze fractured specimens.

Results.

6.3) Cell free collagen response.

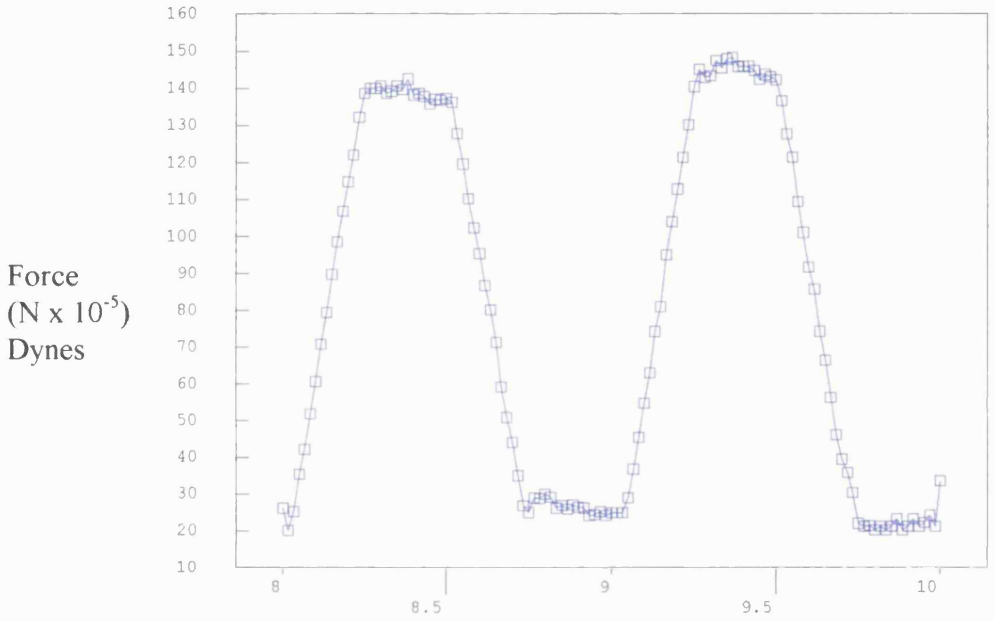

Figure 6.2) Cell free collagen gel response to mechanical stimulation (Note 1 minute data points have been used).

The response of a cell free collagen gel is shown in figure 6.2, showing the faithful reproduction of measured load following gel displacement after applied mechanical stimulation. 15 minutes of applied displacement generated a linear gradient of measured force. 15 minutes of no table

motion gave a clear plateau response followed by a sharp linear fall in measured force for 15 minutes. There was no evidence of resonance or visco-elastic responses from the cell free collagen gel.

6.4) Cyclical Over loading (COL).

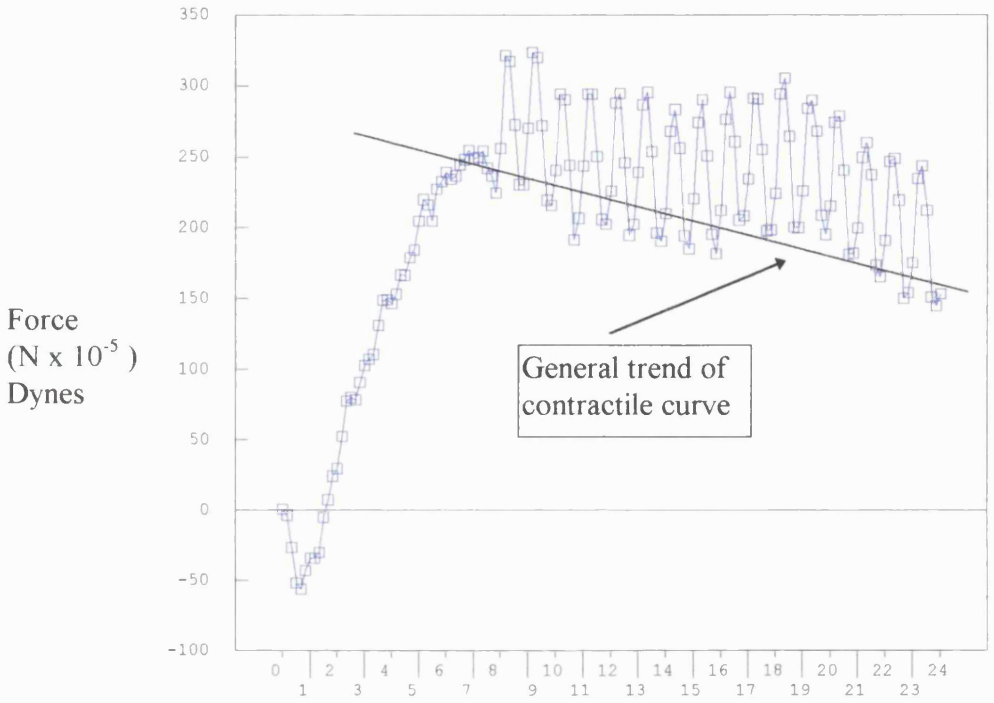

Figure 6.3) COL Gross response over 24hrs. The general trend is also indicated on the graph.

Figure 6.3 shows the response to the applied mechanical stimulation being above the resident cell population derived contractile force. The start point of the mechanical stimulation can clearly be seen at 8 hours. The general trend of the contractile curve in this case (ignoring the mechanical stimulation) was to reduce the matrix tension at a rate of

approximately 4.68 dynes/hr. The first 3 cycles of the mechanical stimulation are shown in figure 6.4, (note the data displayed in this figure is the average of 60 readings i.e. 1 min data points). This figure clearly shows the cellular response to the applied mechanical stimulation. Loading the matrix resulted in an immediate response by the resident fibroblast population of releasing matrix tension. Similarly when the matrix tension was reduced by the t-CFM the immediate cellular response was to retension the matrix.

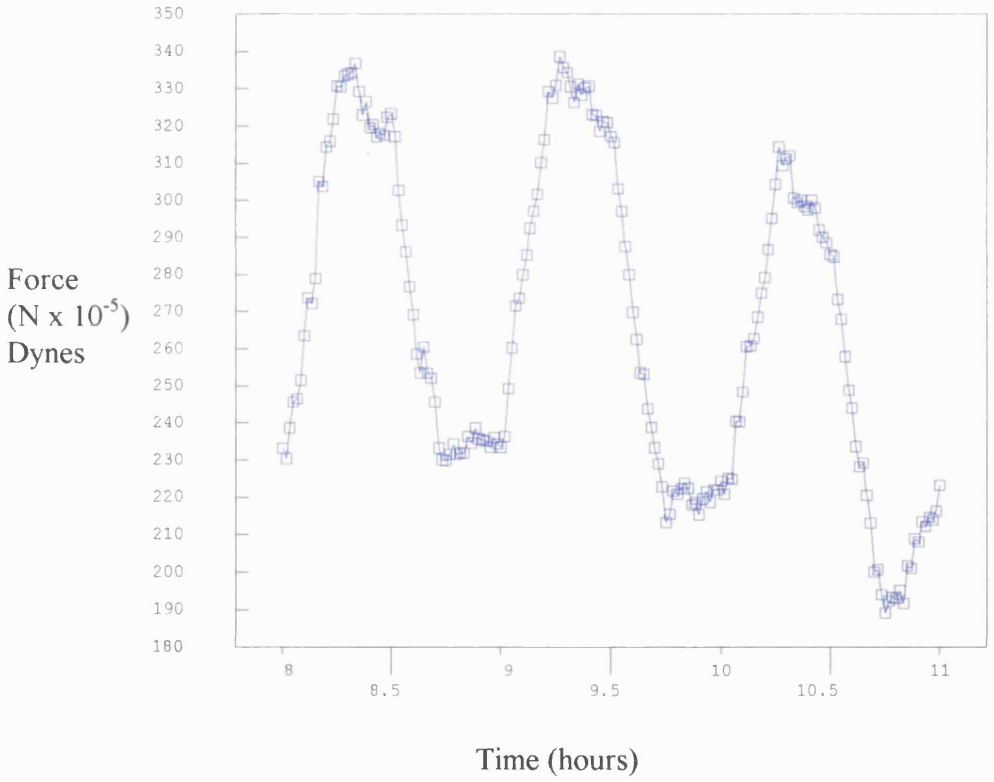

Figure 6.4) The initial 3 cycles of the COL program. Note: 1 minute data points have been used in this graph.

Figure 6.5 shows the complete analysis of the 15 cycles. The red columns above the base line show the cellular response as a rate of matrix retensioning following each unloading cycle. Cell mediated retensioning occurred over the whole 15 cycles at an average rate of 37.2 +/- 37.1 dynes/hr. The cellular response to loading the matrix is also shown in figure 6.5, (green columns). The cell mediated relaxation of the matrix, following mechanical loading, occurred at an average rate of 52.5 +/- 40.7 dynes/hr. Clearly the mean cell mediated response in both cases was opposite to the applied load but of variable magnitude (hence the high SD). However this variation was not random but appeared to be following a sinusoidal cycle. This was most pronounced in the relaxation response (green columns) following loading cycles.

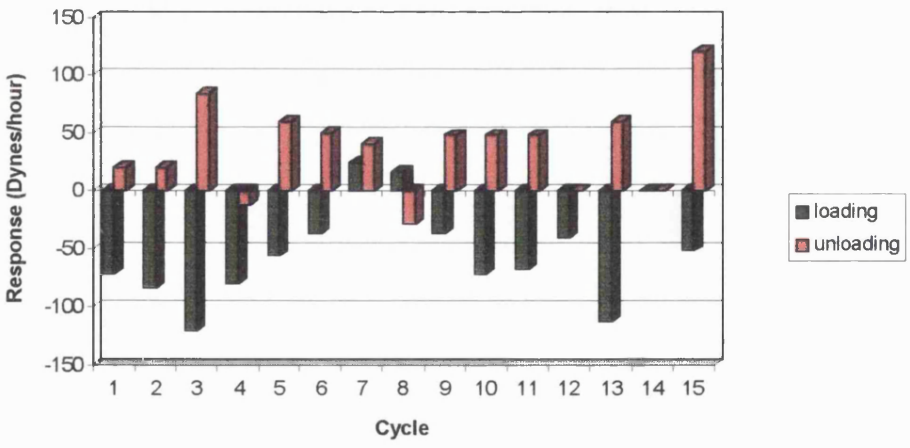

Figure 6.5) Analysis of the cellular response to the 15 cycles of the COL program.

6.5) Cyclical Under Loading (CUL).

The effect of CUL is shown in figure 6.6, the starting point of the mechanical stimulation can be seen at 8 hrs. The general trend of the contractile curve at this point was a relaxation in tension of 7.5 dynes/hr.

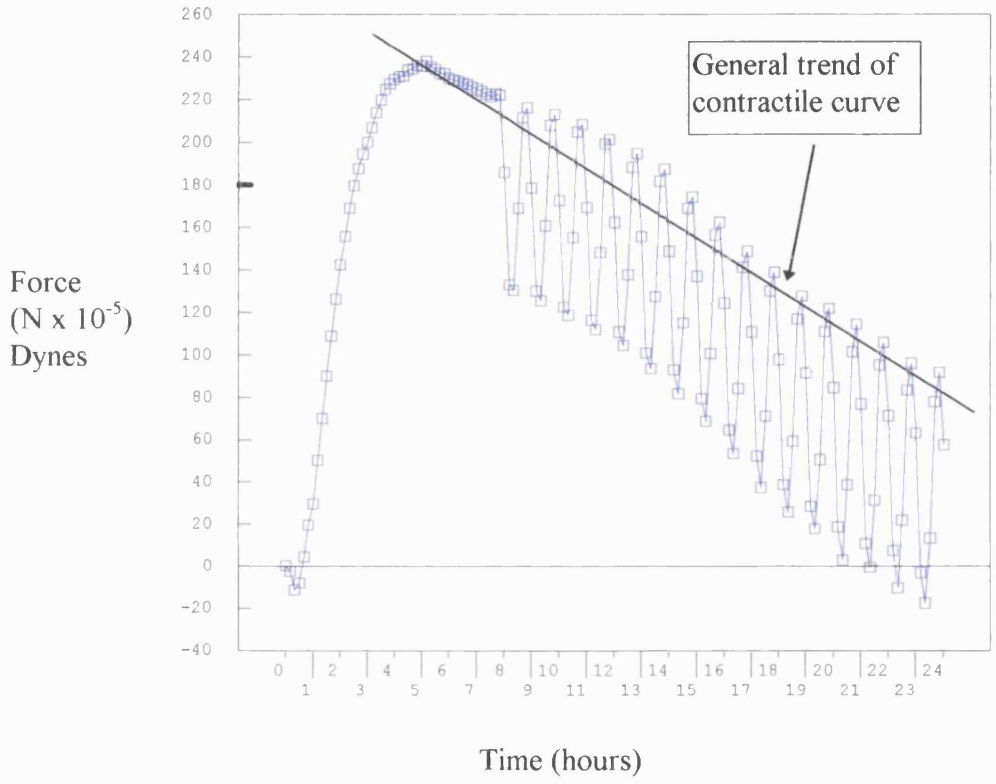

Figure 6.6) CUL. Gross response over 24 hrs. The general trend is also indicated on the graph.

The initial 3 cycles of CUL (figure 6.7) showed that the cellular response to mechanical stimulation had an identical trend to that of COL. Altering the matrix tension caused the fibroblasts to respond by immediately adjusting the matrix tension back towards the pre-stimulation level.

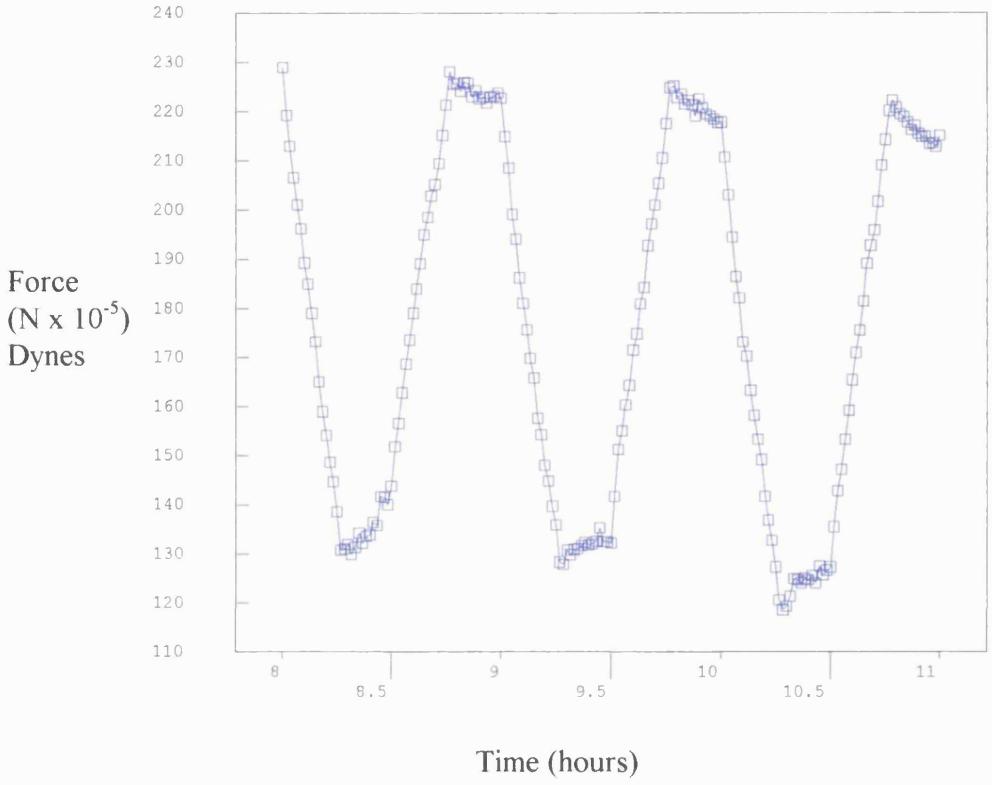

Figure 6.7) The initial 3 cycles of the CUL program. (In this graph 1 minute data points have been used.)

A complete analysis of the 15 cycles is shown in figure 6.8. Loading the matrix caused a cell-mediated reduction in matrix tension at a rate of approximately 37.2 +/- 7.9 dynes/hr (green columns). Relaxing the matrix tension caused an immediate cellular response of retensioning the matrix at an average rate of 20.3 +/- 16.1 dynes/hr (red columns). Again there was evidence of a sinusoidal level of response to loading, in this case most marked in the response to the unloading cycle. This response rose

between cycles 1 and 4, fell to a minimum at cycles 9 and 10, and rose

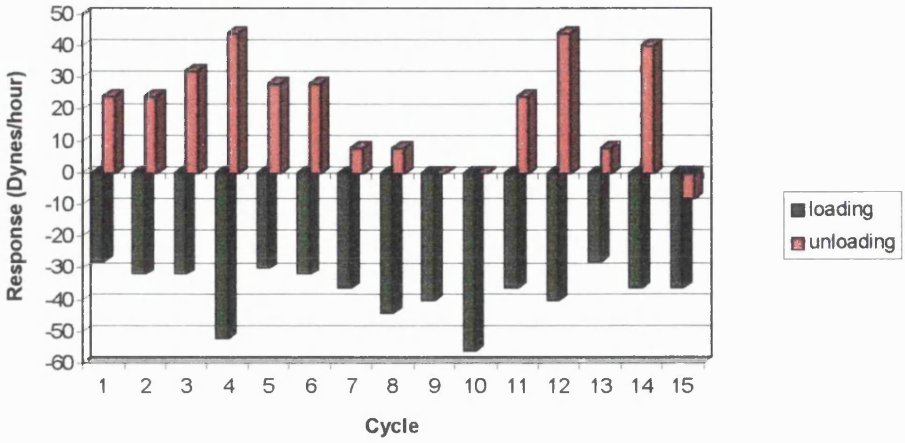

Figure 6.8) Analysis of the 15 cycles of the CUL program.

again by cycle number 12. Responses to the loading cycles were more constant, and only showed a slight indication of sinusoidal response which was not in phase with that of the unloading response.

6.6) Cyclical Median Loading (CML).

Mechanical stimulation about the cell generated force is shown in figure 6.9. During the course of the CML stimulation the general trend of the resident cell population was to increase tension in the matrix at an approximate rate of 5.6 dynes/hr. The overall fibroblast response to the mechanical stimulation was identical to that seen for the COL and CUL (figure 6.10), The cellular response was generally in the opposite

direction to the applied mechanical stimulation, but again the magnitude of this response varied.

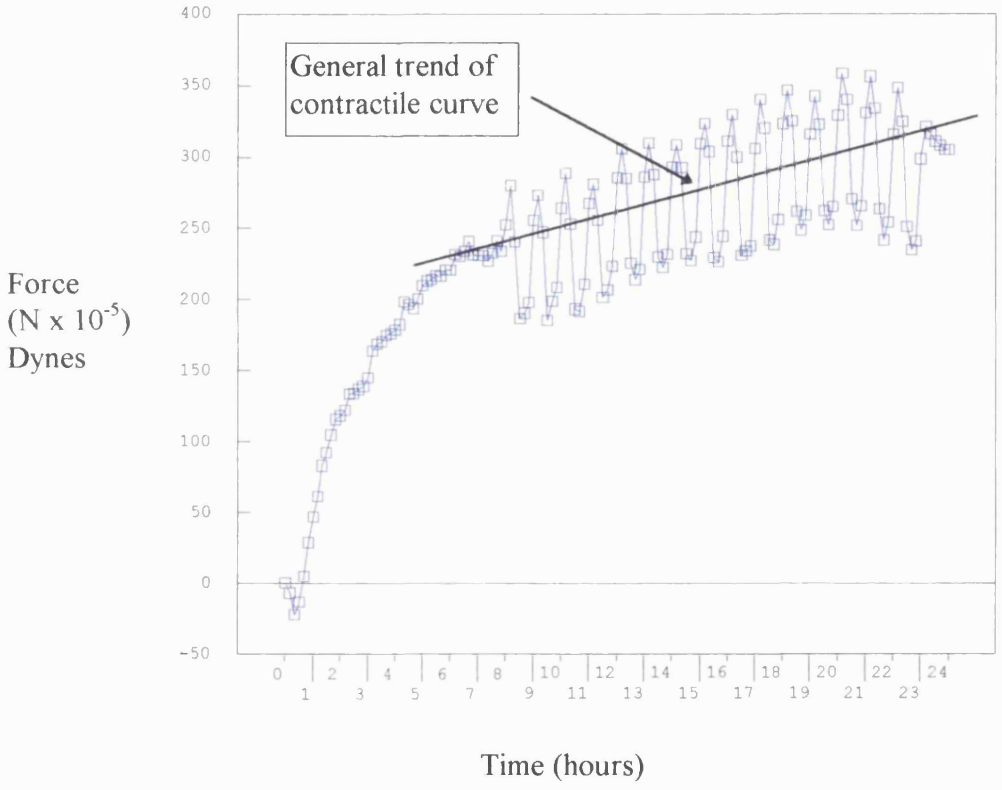

Figure 6.9) CML. Gross response over 24hrs. The general trend of the contractile curve is also indicated on the graph.

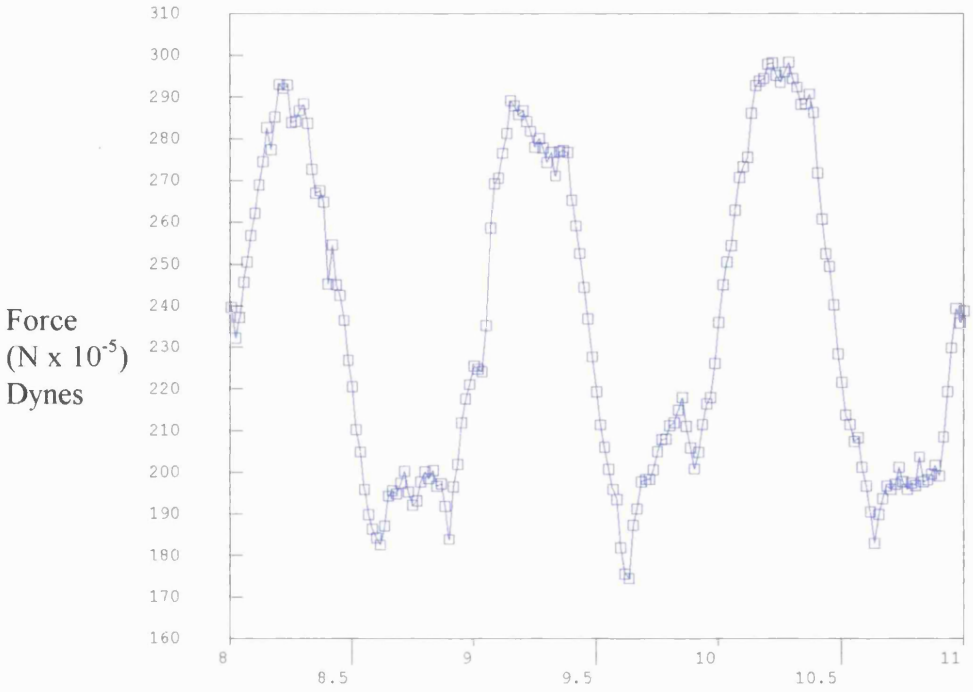

Figure 6.10) The initial three cycles of the CML program (1 minute data points have been used in this graph).

Analysis of the 15 cycles is shown in figure 6.11, following the loading phase the fibroblast response was to release matrix tension at an average rate of 37.1 +/ 39.8 dynes/hr. On mechanical unloading of the matrix the cellular response was to load the matrix at an average rate 47.5 +/- 24.7 dynes/hr. In this case neither loading or unloading responses followed such clear sinusoidal variation, though responses to loading gave the clearest indication of this effect.

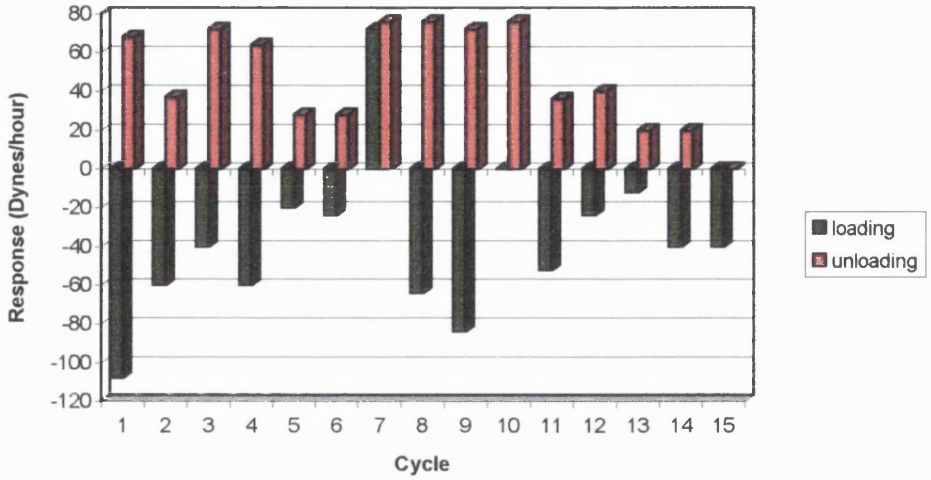

Figure 6.11) Analysis of the 15 cycles of the CML program.

Figure 6.12 shows the average response to the COL, CUL, and CML programs over the 15 cycles. In all cases the overall response was constant with increased loading of the eliciting a cell-mediated reduction in tension and unloading producing an increase in cell mediated tension. Clearly there was considerable variation in the magnitude of the response, reflecting the changing pattern of cell responses over the course of the 15 cycles.

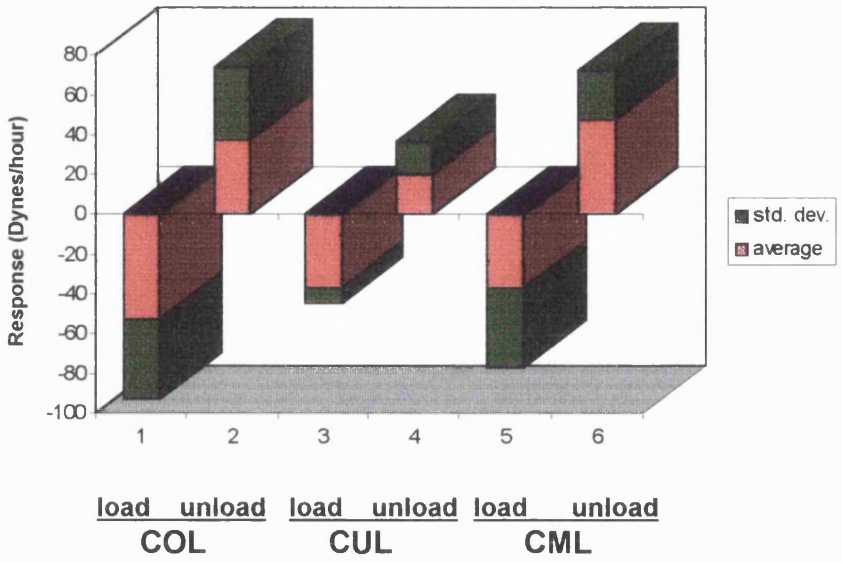

Figure 6.12) Comparison of the COL, CUL and CML mechanical stimulation programs.

6.7) Cyclical Incremental Loading (CIL).

The threshold at which cells began to respond to mechanical loading was determined by the use of the CIL program. The aim of this was to increase the magnitude of the mechanical load until a cellular response was detectable. The program did not become active until the phase 1 equilibrium had been reached i.e. 8 hours into the contraction. At this time point a 10 dyne load was applied to the matrix. Loading and unloading was at a rate of 225 dynes/hour. After the initial load the matrix was rested for 15 minutes to observe any changes prior to unloading.

After a further 15 minute rest period the matrix was unloaded, rested,

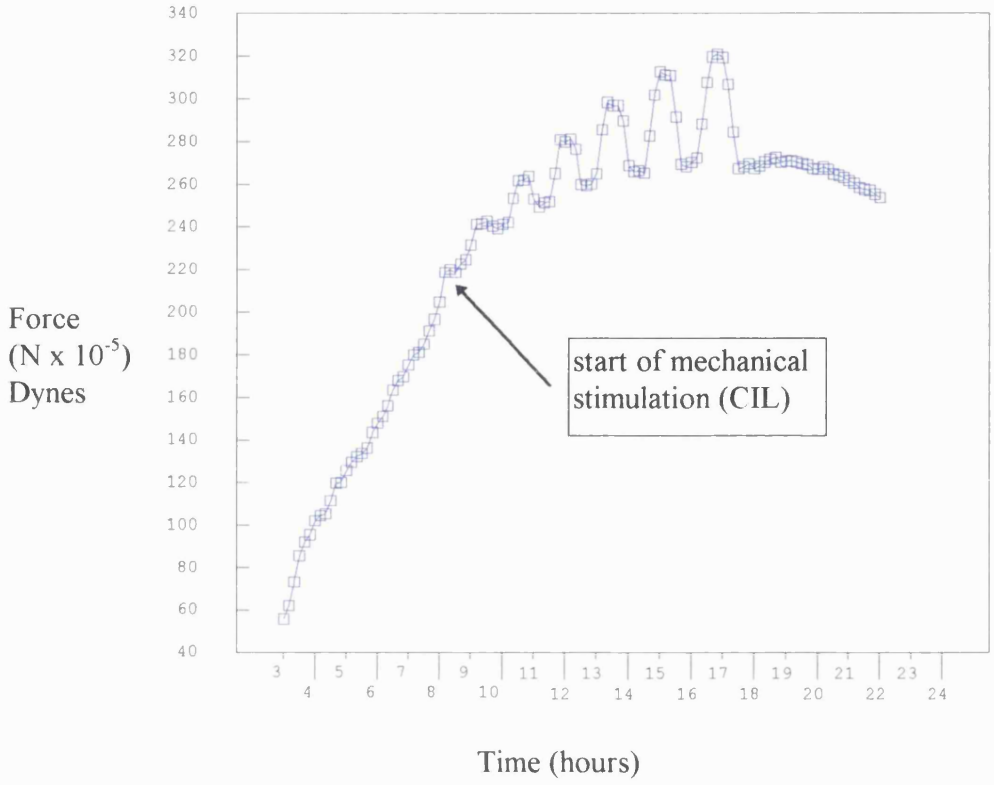

Figure 6.13) Cyclical Incremental Loading (CIL). Indicated on the graph is the start point of the seven cycles.

then loaded to 20 dynes, again with 15 minute observation periods. The cycle was repeated 7 times with 10 dyne increments The Figure 6.13 shows the response to the full 7 cycles. The start of the stimulation at 8 hrs. is indicated on the graph. Figure 6.14 shows cycles 3-5, also indicated on the graph are the gradients of the endogenous cell generated force and the cellular response to the mechanical load. Changes in gradient occurred on cycles 4 and 5 indicating that a cellular response was present. The value of the mechanical stimulation at these

points was between 16 and 20% (cycles 4 and 5 respectively) above the endogenous cell mediated tension.

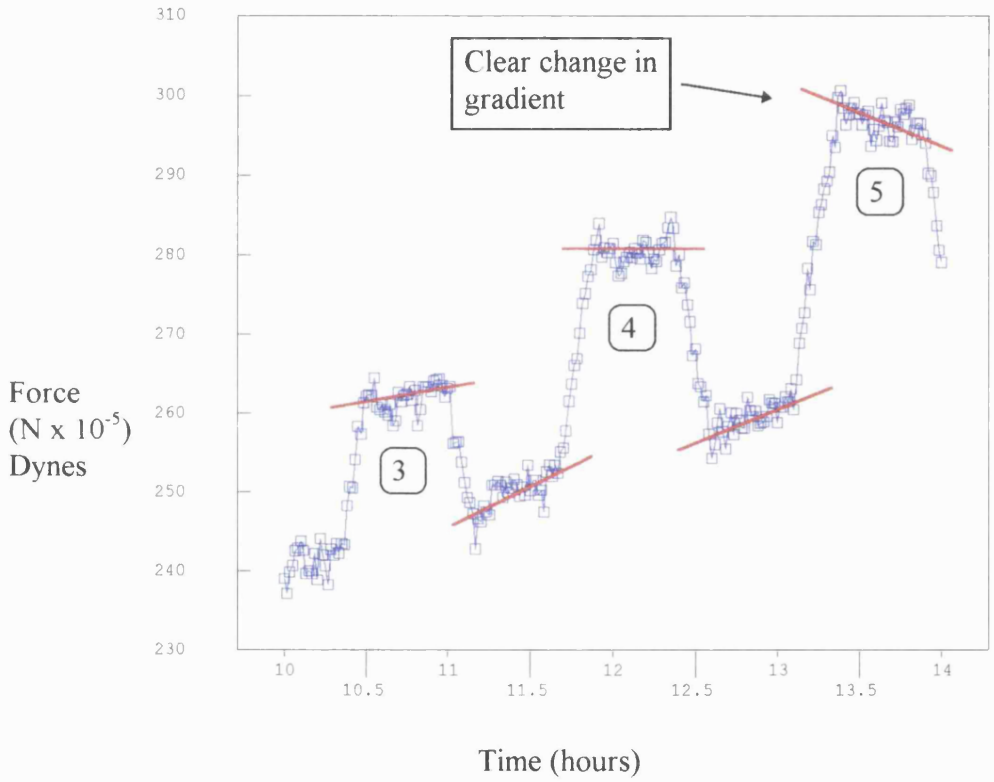

Figure 6.14) Cellular response to the CIL program. Indicated on the graph are the cycle numbers and the gradient of the contractile force during the rest periods.

6.8) Computational Finite Element Analysis.

Any increase in matrix tension resulted in a change in length of the FPCL. This change in length is known as strain (the definition of strain is:- change in length [dL]/original length [L]). In a 3D object there are strains set up in each of the 3 principal axes. These are the maximum principal strain, minimum principal strain and the minimax principal strain. (Timoshenko 1908). In the collagen lattice system the minimum and minimax principal strains are of a low order of magnitude. These strains, and the definition of strain, are shown diagramatically in figure 6.15.

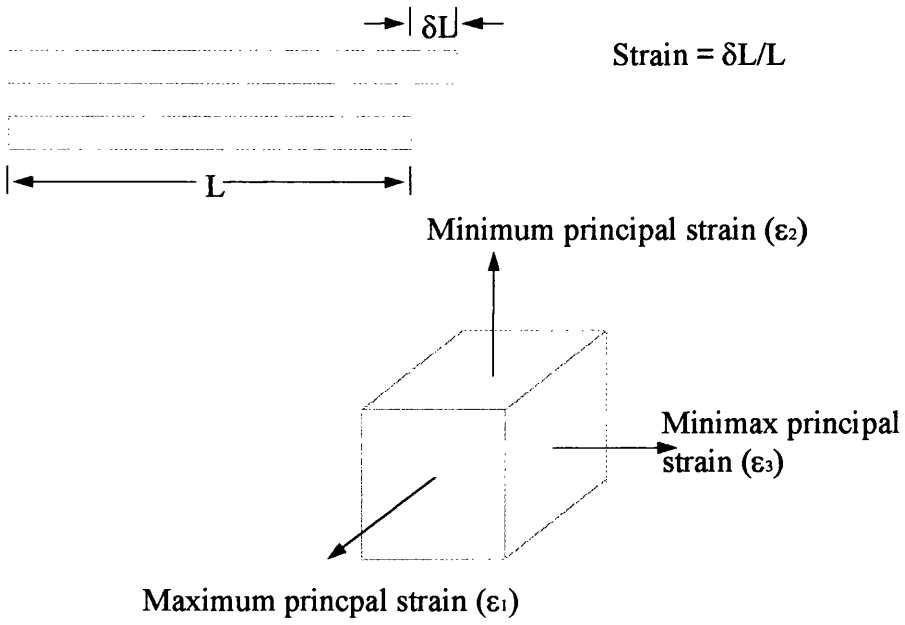

Figure 6.15) Definition of strain and 3D solid indicating principal strains and their orientation.

Mechanical loading caused strains to be developed in the tethered collagen lattices as does the force generated by the cells themselves. An investigation was undertaken on the effect of mechanical loads on the collagen matrix by a Finite Element Analysis (FEA) to determine the strain gradients that were present in the FPCL, in both the high and low aspect ratio gels. The resultant strain gradients generated by the application of the mechanical stimulation are shown in figure 6.16a, b. The FEA performed on the low aspect ratio gel (figure 6.16a) showed that the strain gradients were of a low order of magnitude with no regions of high gradient and orientated parallel with the long axis of the gel, i.e. at 90° to the direction of the applied mechanical stimulation. By contrast the strain gradients in the high aspect ratio gels (figure 6.16b) were highly condensed, aligned parallel with the long axis, of a higher value due to the reduced cross sectional area, and orientated in the direction of the applied load. Figure 6.16b also showed that all regions within the gel had high strain gradients except for the delta zone starting 4mm back from the vyon bars. This zone had minimal strain due to the stiffness imparted into the collagen gel by the close proximity to the rigid vyon bar.

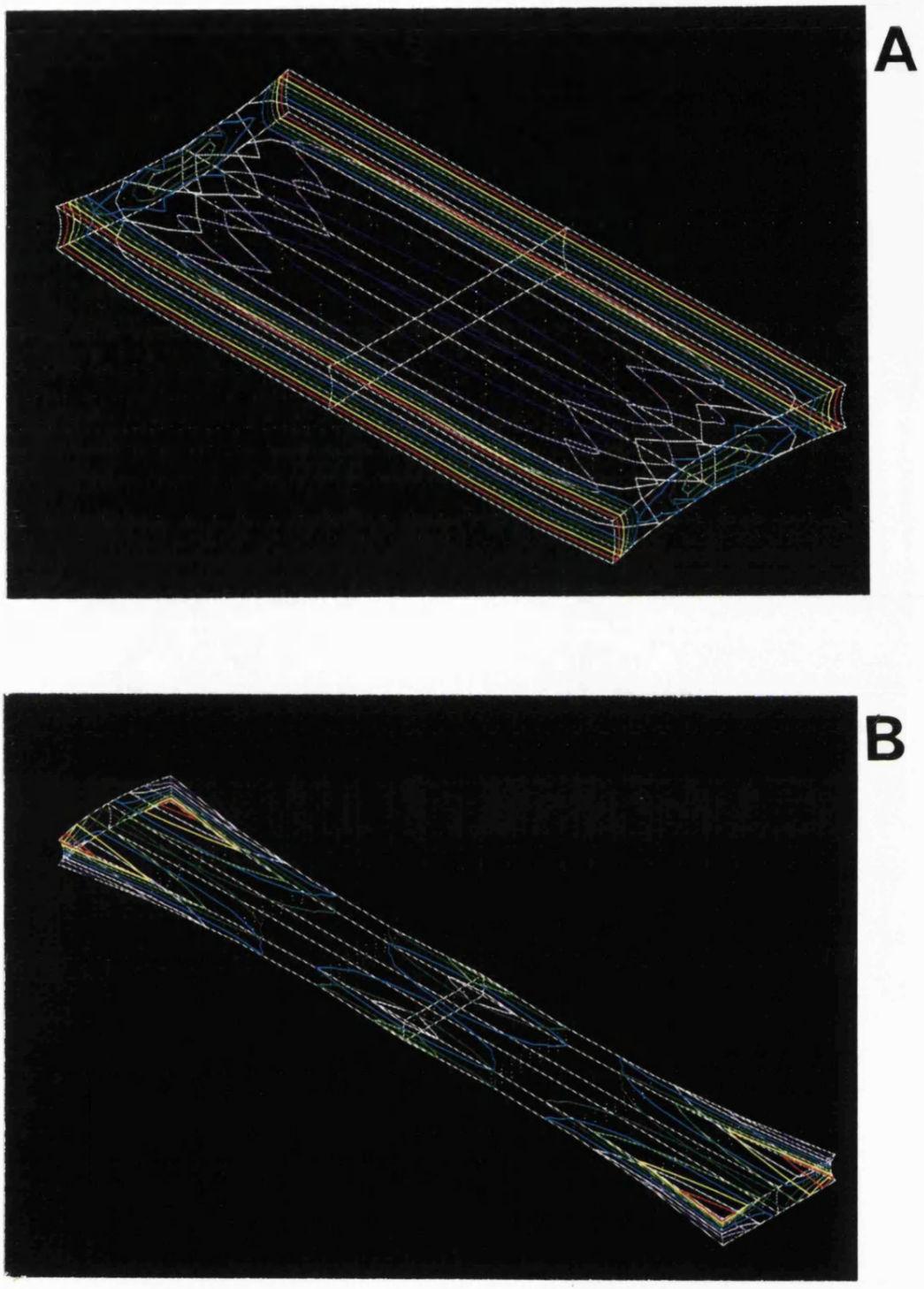

Figure 6.16) Finite element analysis of, a-low aspect ratio collagen gel, and, b-high aspect ratio collagen gel. Lines in the pictures represent the iso-strains, close lines indicate high strain gradients.

6.9) Fibroblast Orientation.

Figure 6.17 shows a typical FPCL after 24 hours in culture connected to the CFM. Cells had a mixture of stellate and bipolar morphologies in appearance, with no preferred orientation. FPCL's were loaded with the COL program as this had shown previously to cause maximum cellular response. Figure 6.18 showed the effect of mechanical loading on a low aspect ratio FPCL, (aspect ratio 0.33:1, loading along the long edge of the gel). Comparison between this and figure 6.17 indicated that the effect of mechanical loading was minimal. Fibroblasts displayed only limited alignment which was at 90^0 to the direction of the applied load. The change in morphology (stellate to bipolar) was also only slight.

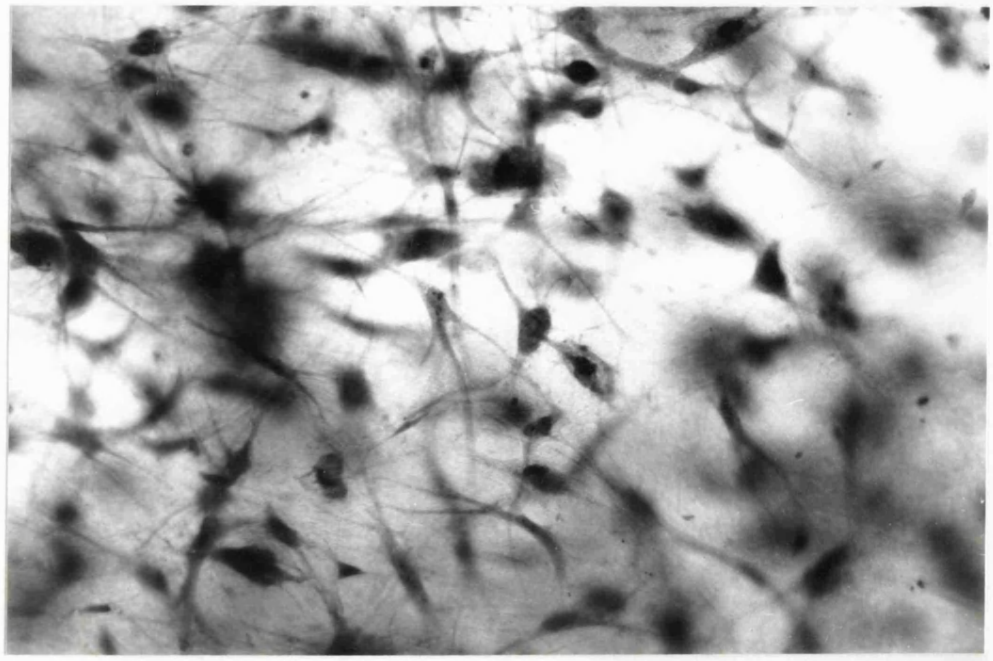

Figure 6.17) Low aspect ratio FPCL after 24 hours in culture. Note the mixture of stellate and bipolar morphologies.

Comparing figure 6.18 to the FE analysis for the low aspect ratio gel (figure 6.16a) showed that the cells appeared to have followed the predicted strain gradients, i.e. there was a correlation between the direction of the maximum principal strain and the slight amount of alignment observed.

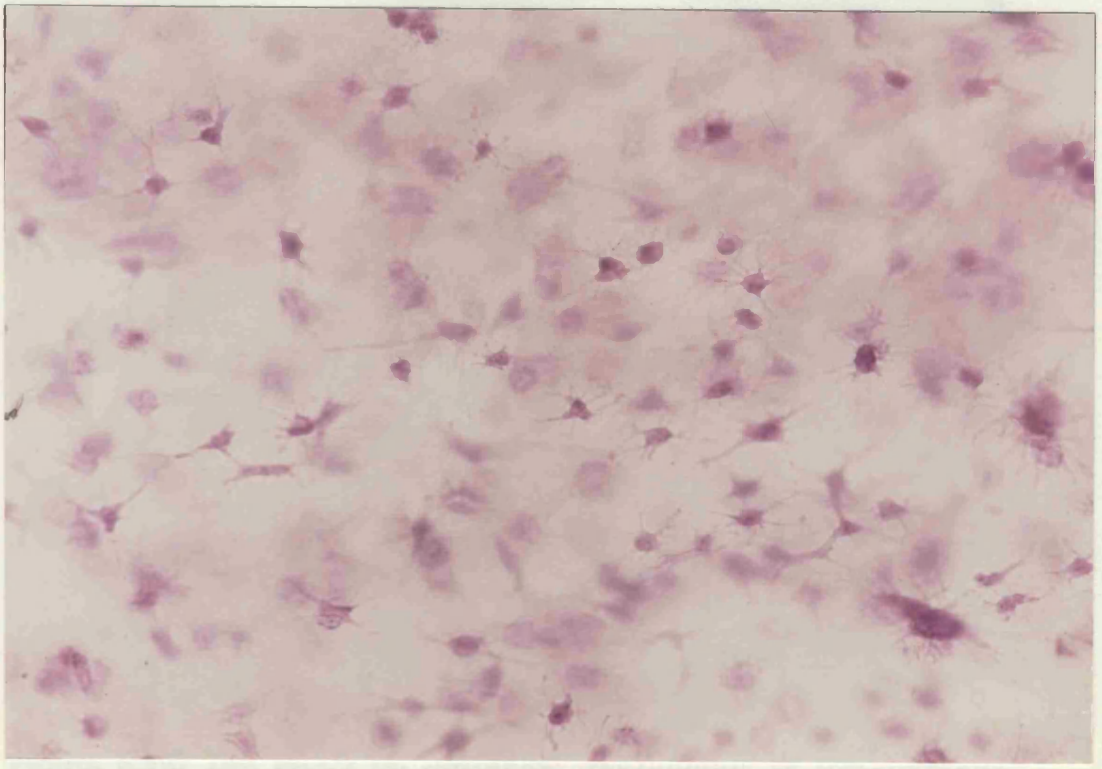

Figure 6.18) The effect of mechanical loading on a low aspect ratio FPCL. Note the slight amount of cellular alignment.

Figure 6.19 shows the effect of altering the aspect ratio to 3:1, with the load applied in the direction of the long axis i.e. the load was applied perpendicular to the short side (as shown in figure 6.1). Elongate and

bipolar cells are aligned with the long axis of the FPCL, i.e. in the direction of the applied mechanical load. Again comparison between figure 6.19 and 6.16b (FEA on the high aspect ratio gel) showed that the cells had aligned along the predicted iso-strain lines.

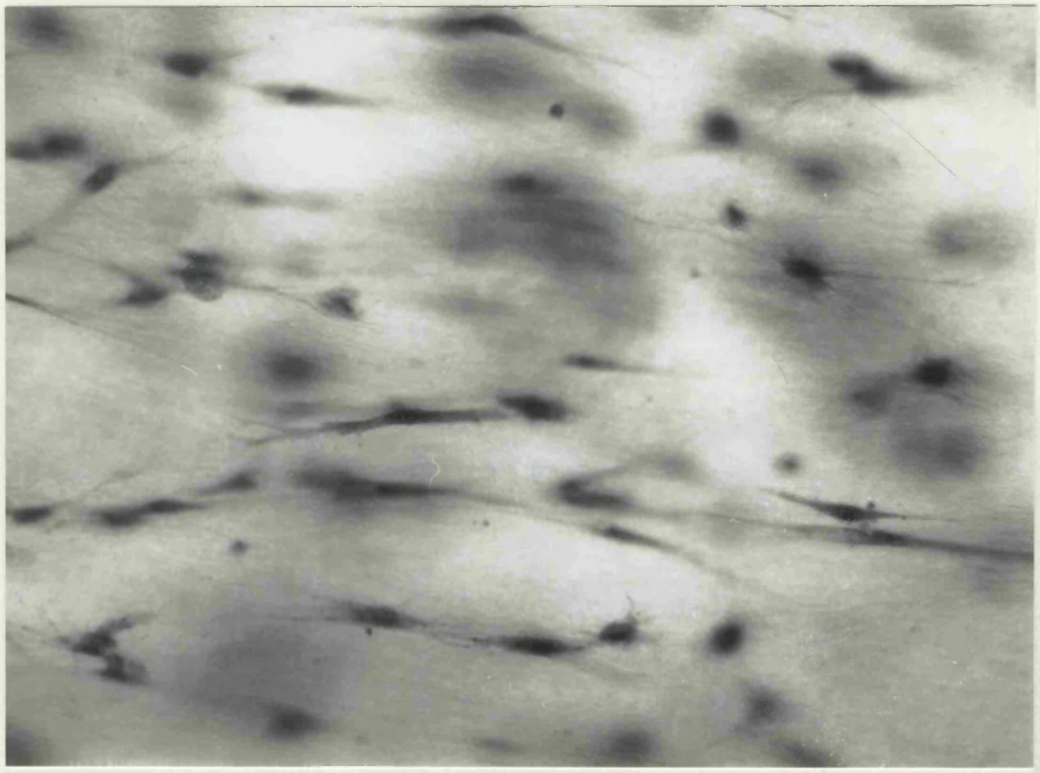

Figure 6.19) The effect on fibroblast morphology of mechanically loading a high aspect ratio FPCL. Note the highly aligned bipolar fibroblasts.

From the FEA it was predicted that non aligned stellate cells would be found in areas of constant strain, i.e. areas of low strain gradients. Figure 6.20 shows regions of low strain gradients bordered by high strain

gradients. From this model it would be expected to find aligned cells in areas 1 and 3 and non aligned cells in area 2, also shown in figure 6.20

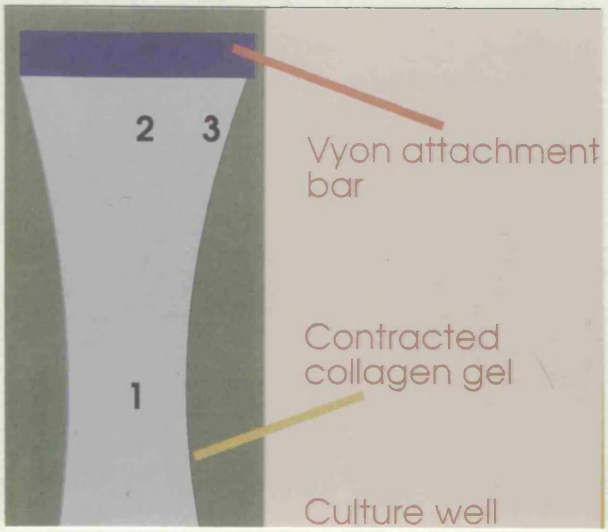

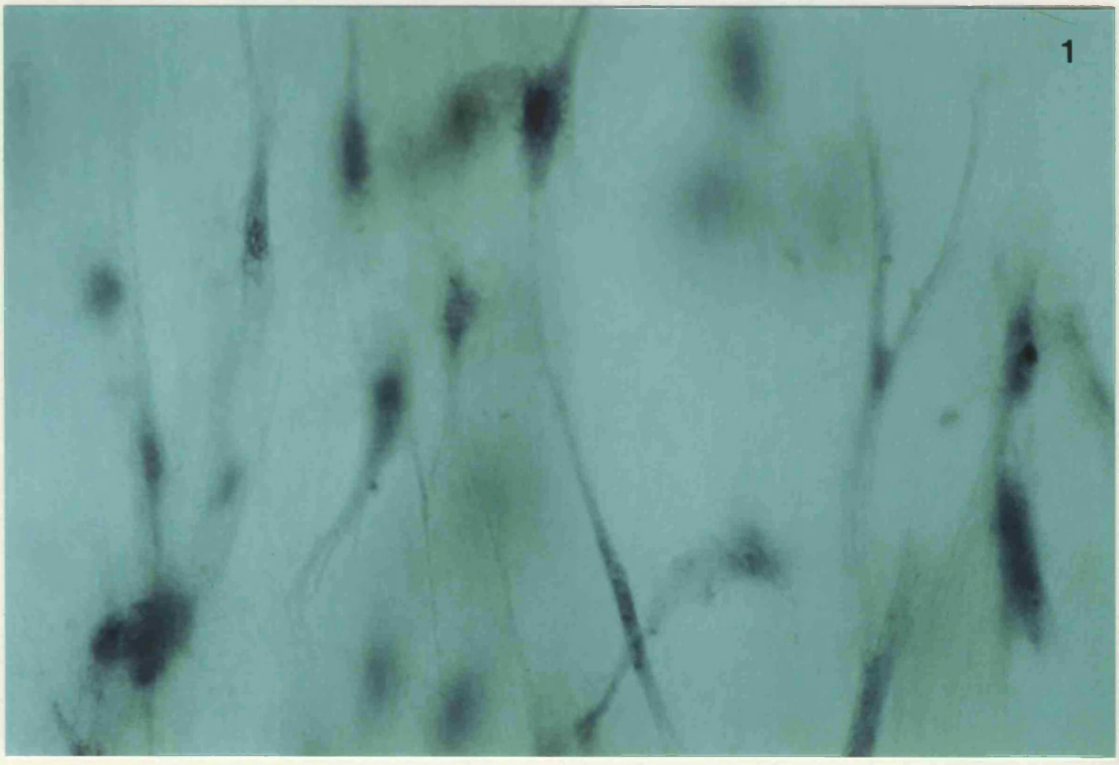

Figure 6.20) Diagram of a high aspect ratio FPCL and the morphologies of cells from 3 regions.

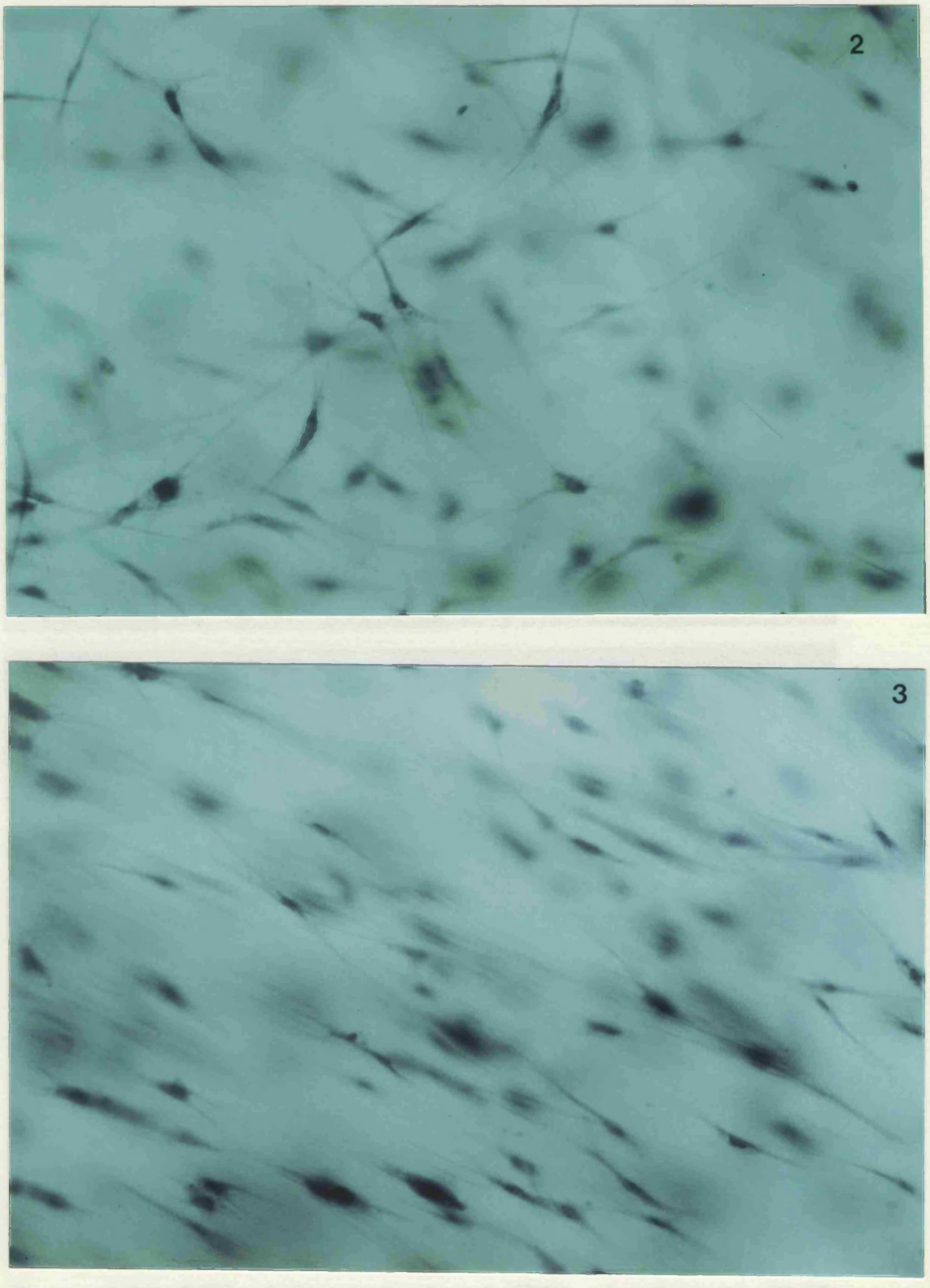

Figure 6.20 cont.) Diagram of a high aspect ratio FPCL and the morphologies of cells from 3 regions.

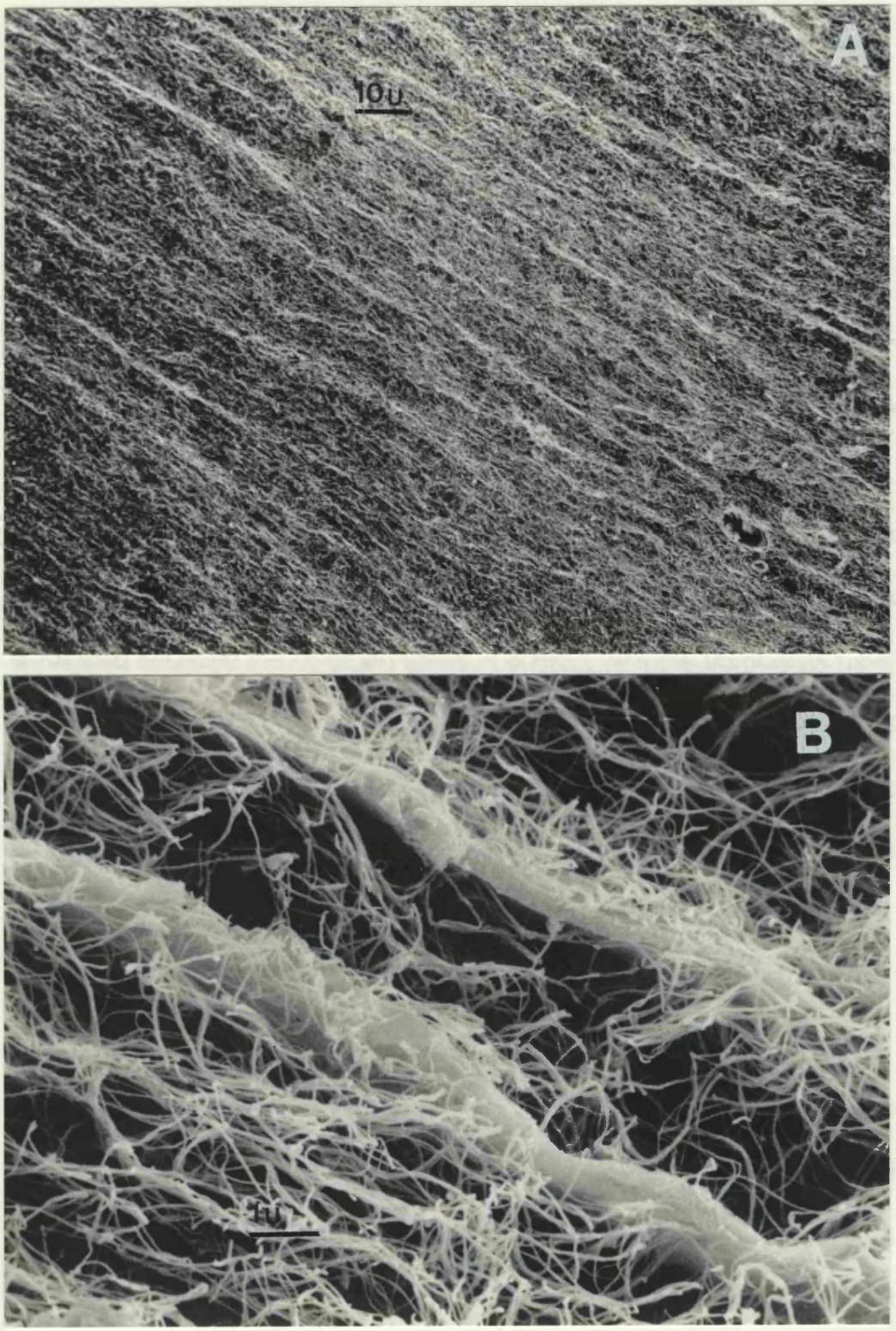

Figure 6.21) SEM of freeze fractured FPCL showing: a:- highly aligned fibroblasts and b:- random orientation of collagen fibrils in-between cells. Microscopy courtesy of Miss K. Smith.

are the corresponding micrographs of the resident cells in those areas. As expected non aligned cells were found in area 2 and elongate bipolar cells aligned along the predicted principal iso-strains in areas 1 and 3.

Scanning EM of freeze fractured gels (figure 6.21a,b) showed the bipolar nature of the fibroblasts and their parallel alignment relative to each other. Figure 6.21a also shows the collagen matrix surrounding the cells, which at low magnification appears to have some alignment in the direction of the cells. The appearance of this collagen alignment is enhanced because the collagen fibrils in contact with the fibroblasts have become orientated in the direction of the long axis of the cell on the cell surface. However, higher powered magnification, figure 6.21b shows that there is little evidence of collagen fibril alignment away from the cells even after 24 hours in culture.

Figure 6.22 shows a culture that had the same high aspect ratio of 3:1 initially, but was allowed to contract as a free floating collagen lattice after 7 hrs in the t-CFM, i.e. the endogenous tension generated by the fibroblasts was removed at the time point when the test gels were being loaded. The collagen gel contracted, and the fibroblasts assumed the morphology associated with free floating collagen lattices, i.e. small and stellate with no alignment.

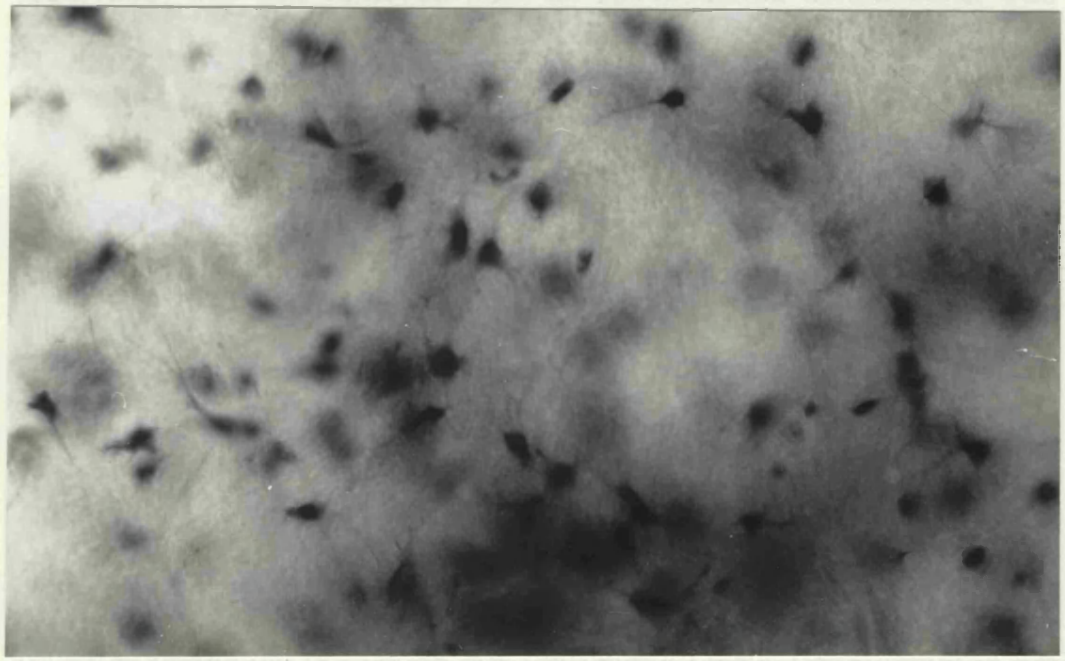

Figure 6.22) High aspect ratio FPCL allowed to contract for 7 hours before mechanical load removed and allowed to contract as a free floating gel.

Discussion.

The maturation of the cell free collagen matrix itself produced a small endogenous internal tension to be created (figure 3.1) (Eastwood et al, 1994,1996) this was removed from all cell-mediated contractions. The level of this internal tension is also evident from figure 6.2, Mechanical loading caused the cell free matrix to become stretched, which during the rest periods this level of force was maintained showing that there were no visco-elastic effects, as suggested by Delvoye (1991), at this level of mechanical loading and from our data can be discounted. Unloading of the collagen matrix resulted in a complete return to the original tension, indicating that all the elastic strain energy had been recovered. Hence control experiments showed that levels of mechanical stimulation used in the experiments did not cause any permanent plastic deformation of the collagen lattice. This demonstrated that the changes in matrix tension following mechanical stimulation were indeed cell mediated and establishes this technique as a means of assessing mechanical responses of cells to mechanical stimulation.

This series of experiments was performed to quantitate the cellular response to mechanical stimulation. Two aspects were studied, effects of external loading on cell contraction (tensional homeostasis), and the effect on cell shape and alignment (morphology). The response to

mechanical stimulation by the resident fibroblast population had constant features.

In the experiments reported here cells responded to reduce or minimise the externally applied tensional loading i.e. decreasing contraction after increased loading and increasing contraction after unloading. This response was seen following both single, static loads and during cyclical loading. Furthermore, comparable responses were produced by cells in mechanically weak, 1.75% collagen gels and somewhat stronger collagen-GAG sponges (data not shown). Together, these data demonstrate that cellular mechanisms operate to maintain tensional homeostasis. In the present t-CFM model the tensional equilibrium is a balance between fibroblast contraction and deformation of the tethered collagen gel. In vivo the cell mediated tension would involve a more complex balance due to material properties of other components which make up the composite extracellular matrix structure, such as elastin and proteoglycans.

Delvoye et al, (1991) made direct force measurements from contracting FPCLs using a non motorised force measurement instrument, with a chart recorder data capture. They reported the effects of increasing or decreasing the externally applied tension by manual movement of the gel. Within an hour of this change, measured tension in the FPCL had

returned to near its original value. It was suggested that in this case the gel behaved as a visco-elastic material, with indications of cell involvement. The findings reported here have shown that the material itself i.e. cell free collagen gel is not visco-elastic under these conditions. Rather the restoration of equilibrium tension, following external changes is entirely due to the cells themselves. This is a critical distinction since extracellular matrices in vivo do have complex mechanical properties which would tend to obscure the identification of this cell-mediated maintenance of tension.

Identification of tensional homeostasis in connective tissue leads to further questions:

-by what mechanisms do fibroblasts increase or decrease matrix tension so quickly?

-by what means do they monitor tensional changes in the extracellular matrix? and

-by what method do fibroblasts become aligned in the orientation of mechanical loading?

The mechanism by which fibroblasts generate externally applied force has attracted much attention (Tomasek and Hay, 1984; Elsdale and Bard, 1972, Bell, Iversson and Merrill, 1979, Ehrilch and Rajaratnam, 1990). Previous studies on the contraction of FPCLs (chapter 4) have shown

that the generation of tension is indeed rapid (Eastwood et al, 1994, 1996; Delvoye et al, 1991). The action of cytoskeletal elements in generating, maintaining and even storing forces has been shown through the action of cytoskeletal disrupters (chapter 5), which again can elicit rapid increases and decreases in tension (Kolodney and Wysolmerski 1992; Kolodney and Elson 1995: Brown et al, in press) depending on the cytoskeletal element disrupted.

It has been proposed that external tensional forces generated by fibroblasts onto collagen are the result of an internal balance between contractile forces of actino-myosin motor elements in microfilaments and compressive loading onto the microtubular elements which maintain cell shape (see chapter 5) (Brown et al, in press). The amount of contractile force which is 'stored' as an internal force by compression of microtubules would then be a function of the requirement of a cell to maintain a particular shape.

A comparable balance of cytoskeletal functions has been suggested for neurites (Letourneau et al, 1987, Dennerll et al, 1988; Avila et al 1994; Madreperla and Alder 1989). The importance and interdependence of cell shape (itself dependant on cytoskeletal function see chapter 5) and force generation has been established previously (Eastwood et al, 1996; Tomasek and Hay, 1984). It seems reasonable to propose then, that

decreases in external force generated by these cells (to maintain the matrix tension) are produced by a combination of a decrease in microtubule assembly (hence a fall in the tension within the cells) and an increase in the microfilament actino-myosin assembly or activity. The resultant of these balanced cytoskeletal functions would be applied to the matrix via attachment plaques at the cell surface. Decreases in forces generated by fibroblasts to compensate for increases in tension in the matrix would be brought about by the opposite processes.

With regard to the second question it is rather less clear how resident cells in the FPCL monitor changes in the tension across the matrix to maintain an equilibrium. Parallels are possible to draw with mechanisms by which nerve growth cones respond to mechanical tension (Bray 1979,1984), stress-related microtubule polymerisation and myocardial function (Tsuitsui et al, 1993) and vascular endothelial cell function by shear through cytoskeletal rearrangement and selective ion channel function (Ohno et al, 1995, Girard and Nerem, 1993). Mechanical stimulation of fibroblast activity has previously been correlated with calcium dependant, cyclic AMP signalling (van Bockxmeer et al, 1984; He and Grinnell 1995). It is possible then that a tensional mechano-receptor system is linked with the assembly of microtubules (Brown et al, in press; Kolodney and Elson 1995; Dennerll et al, 1988; Joshi et al, 1985; Madreperla and Alder 1989) or with deformation of the microfilament-

integrin assembly site and may be mediated via familiar intracellular signalling pathways involving cyclic AMP and, in smooth muscle cells, through changes in intracellular calcium levels (Ohata et al, 1995). The present model of tensional homeostasis in a connective tissue provides an important quantitative means of assessing these mechanisms.

As to the third question, a mechanism by which fibroblasts orientated themselves in response to applied mechanical load, it seems that fibroblasts orientated along lines of iso-strains. In effect these cells are hiding from the 3D strain, and only perceive the strain in one direction, i.e. the maximum principal strain. Mechanical loading of FPCLs has been seen to cause morphological changes i.e. stellate to elongate bipolar, which in the present model of tensional homeostasis and alignment along iso-strains, would present a minimal cell aspect to the perceived strain in the two other directions, i.e. the cells become bipolar.

Cell processes can be induced by the action of a local force. Margolis and Popov (1991) induced cell processes in rounded mouse embryo fibroblasts that had been cultured on coverslips by 'pulling' the cells with two tungsten microelectrodes. These electrodes were placed either side of the cell and a force was created (Margolis and Popov 1988) that acted on the cell membrane. According to the present model this force would

alter the tensional homeostasis, which would result in a cellular compensation as previously described. Indeed cell processes were reported to be created within 20 seconds of the application of the mechanical load. The model of Margolis and Popov (1991) also supports the hypothesis of cells being aligned along the maximum principal iso-strains. The application of the tensile force would cause a principal strain to be generated. Cell processes formed were in the direction of the applied force, which would also be the direction of the maximum principal strain.

The observation reported here of fibroblasts being aligned 'nose to tail' rather than in a staggered formation has analogies with slip planes, common place in engineering materials (John 1984). Engineering materials fail along these slip planes as it represents the minimum energy requirement for failure to occur. When fibroblasts become aligned due to mechanical load it creates 'minimum potential energy wells' between the two aligned fibroblasts in a similar manner to slip planes. It may be then that any cell with processes encompassed in this region would detect the energy well and migrate towards it, eventually becoming aligned with the two other cells, and so further increasing the alignment.

Removal of the mechanical load would also remove the 'minimum potential energy wells' leading to loss of cellular orientation and bipolar

morphology as has been seen. Indeed it has been reported by others (Tomasek et al, 1992) that removal of tension in FPCLs caused bipolar fibroblasts to become stellate.

Tests on other cell and tissue types are needed to establish whether there is an interplay between the cell-mediated, intrinsic tension within a connective tissue and the function of that tissue. For example, there may be analogies here between the control of tissue tension by smooth muscle cells in a blood vessel wall and the tension in skin, with the contractile force being balanced, in each case, by matrix components such as elastin and collagen. In view of this, defects in cell-mediated tensional homeostasis may be important factors in age related diseases and tissue regeneration. Also an understanding of the means by which cells can be aligned and activated is fundamental to the understanding of the mechanisms involved in ligament and tendon repair. The implications of tensional homeostasis and cell alignment with principle iso-strains have far reaching consequences for future research into organ repair by surgery and tissue engineering in general.

Chapter 7: General Discussion.

In the course of this study mechatronic devices have been developed, the CFM and t-CFM (chapters 2 and 3). These devices have enabled quantitative studies to be performed on cells residing within a collagen matrix, both these systems use highly sensitive force transducers capable of measuring to 10^{-5}N. Data is captured on computer at a rate of 1 reading/second, which is later processed to give data points on a graph that are the average of 600 readings. The use of a computer enables the removal of base line responses if required, so that only the net effect of the cells is plotted. The t-CFM, a development of the CFM, enables high positional accuracy to be obtained by the use of a computer controlled microdriver, which activates a microstepping motor. This system applies precisely controlled loads to collagen matrices whilst simultaneously measuring the overall effect.

Using the CFM it has been shown that collagen gel alone causes a small force to be developed whilst the gel matures (chapter 4, Eastwood et al 1994, 1996), possibly due to fibril maturation and growth. The initial phase of contraction (0-8hrs) has been related to the size and shape of the cell (chapter 4, Eastwood et al 1996), showing that cell shape change and process growth can cause a force of contraction to be generated. Further phases of contraction during the initial 24hrs have also been

identified, these have been hypothesised to be due in part to fibroblast sub-populations and changes in cell shape and orientation.

The disruption of cytoskeletal components within the cells (Chapter 5, Eastwood et al 1995, Brown et al in press) causes a change in measured force. The addition of microtubule poisons, such as colchicine and vinblastine sulphate, elicited an immediate rise in force, whilst addition of the microfilament poison cytocholasin B induced an immediate fall in force. This data has led to a new hypothesis of the function of cytoskeletal components based on a 'balanced space frame', which explains the increase or decrease in measured force when these components are disrupted.

The 'residual internal tension' of a cell has been quantitated based on the data derived from the disruption of the cytoskeletal components. The addition of microtubule disrupters to cells prior to being suspended in pre-polymerised collagen gel, cast then set up in the CFM, has shown that a contractile force can be generated, although small and substantially altered. This limited contraction represents the force generated purely the action of attachment into the collagen matrix (Eastwood et al 1996), as the normal cell processes cannot be extended due to the non formation of microtubules (hence the altered contractile curve).

Mechanical loading of a FPCL with the t-CFM, and the subsequent cellular response (chapter 6, Eastwood et al 1996a, Brown et al 1996), has shown that the residual internal tension and balanced space frame models can be used to explain this response. Resident fibroblasts, when mechanically shifted from their normal resting tension will strive to return back to the pre-loading value, giving rise to the hypothesis of mechanical homeostasis within cell lines (chapter 6, Brown et al 1996). The shape of the culture is also important for fibroblast orientation, as altering this shape can dictate the direction and magnitude of the maximum principle strain. Fibroblasts attempt to 'hide' from this maximum principle strain by altering the orientation of the cell and morphology to align along one of the maximum principle isostrains (Eastwood et al 1996a). Reducing the diameter of the cell also reduces the perceived force in the direction of the other two principle strains.

The way in which fibroblasts in vivo behave in an organ, and respond to injury and the associated increase or decrease in tension can be speculated on, based upon the data generated in the course of this study. It could be then that the normal dermal fibroblast, when confronted with increased tension following injury and subsequent wound contraction, attempt to reduce the perceived force by altering the morphology and changing the cellular orientation to that of the iso-strains of the maximum

principle stress. If the tension generated is still very high so that the fibroblasts cannot 'hide' then the load could be further reduced by the increased synthesis of collagen matrix. Increasing the extra cellular matrix would reduce the load carried by the matrix, and hence the load on the fibroblasts.

The high directional orientation of the extra cellular matrix observed in organs such as ligaments and tendons can be explained by the high aspect ratio of these organs. Fibroblasts residing within these organs would favour orientation along the major axis, which would be the direction of the maximum principle strain (Eastwood et al 1996a). It may be then that the variation in contractile force produced from fibroblasts from different organs (chapter 4, Eastwood et al 1996) reflects the fibroblast activity within these organs.

The implications for surgeons, when operating on organs such as ligaments and tendons, are immense. Removing the tension from a ligament would also imply that a major signal for directional orientation of the repairing cells, the fibroblasts, had also been lost. The removal of tension from an aligned fibroblast, as seen in chapter 6, causes an immediate change in morphology and loss of orientation. This would imply that the freshly synthesised collagen in the repair area would also be non aligned and hence weaker. The suturing of a damaged area

would also tend to remove the load from the very place where tension is required to effect alignment of the fibroblasts.

Numerous fibroblast growth factors have been investigated previously e.g. PDGF, bFGF, TGF-beta, EGF, IGF-I, IGF-II (Shah et al 1995, Khaw et al 1995). These growth factors have been assessed on free floating collagen lattices, under these conditions the fibroblasts are quiescent and have stellate morphologies (Grinnell 1994). Using the t-CFM the effect of these growth factors could be quantitated on fibroblasts whilst under a known mechanical load, and hence more representative of granulation tissue. It may be then that fibroblasts under mechanical load will react differently to these growth factors than fibroblasts in a free floating collagen lattice. Drugs have been tested that are supposed to inhibit wound contraction (Khaw et al 1995) others that inhibit the action of growth factors (Chamberlain et al 1995) have also been tested on free floating collagen lattices and animal models, however a truly quantitative analysis is not presently available.

Tissue and cellular engineering are becoming regarded as new fields in their own right (Langer and Vaccanti 1993). The lack of donor organs has far reaching consequences on terminally ill patients. Improved surgical technique has enabled many life saving procedures to be developed, but this has in many cases highlighted a serious shortage of graft or donor

tissues. The advantages of "engineered" organs prepared in the tissue culture laboratory from patients own cells are clear. Use of such autologous material has the added advantage of requiring no immunosupressive agents to prevent rejection (Badger 1984).

Current research in the field of cellular and tissue engineering has shown advances in the areas of skin, liver, pancreas (Cima et al 1991, Dixit 1994, Tziampazis 1995, Mooney et al 1995, Ronabhia et al 1995) and tubular structures such as trachea, oesophagus, intestine, bladder and urethra (Mooney et al 1994). Other high strength organs are also being researched, ligament, tendon, cartilage, bone, muscle (Kanda and Mutsuda 1993, Cao et al 1994, Freed et al 1994, Reddi 1994). One underlying theme with all of this research is the need to be able to guide cells by either contact guidance or by mechanical stimulation. Contact guidance requires either a biodegradable scaffold such as polyglycolic or polylactic acid (Dunkelman et al 1995), or an absorbable biomaterial, such as a fibronectin mat (Brown et al 1994, Ejim et al 1994) for the cells to become attached to, however, in an unloaded state the fibroblasts will adopt a stellate morphology and remain quiescent (Grinnell 1994). Mechanical stimulation with the t-CFM provides many of the answers, by loading the culture fibroblast morphology can be changed (see chapter 6, Eastwood et al 1996a).

The appearance and strength of a scar is dependant upon the architecture of the connective tissue within the scar (De-Viris et al 1995, Shah et al 1995 Ferdman et al 1993). The CFM and t-CFM can be used to analyse the optimal cellular stimulation within the wound which will control the architecture of the resulting scar. Mechatronic devices described in this thesis can be used to test some of the principles involved in this form of control.

REFERENCES

Abercrombie, M, Flint, M.H. and James, D.W. (1956) Wound contraction in relation to collagen formation in scorbutic guinea pigs. *J. Embryol. Exp. Morph.* 4:167-175

Abercrombie, M., James, D.W. and Newcombe, J.F. (1960) Wound contraction in rabbit skin, studied by splinting the wound margins. *J. Anat.* 94:170-182.

Afzelius, B.A. Dallai, R. Lanzavecchia, S. and Bellon, P.L. (1995) Flagellar structure in normal human spermatozoa and in spermatozoa that lack dynein arms. *Tissue. Cell.* 27(3): 241-7

Akalin, E. Hancock, W.W. Perico, N. Remuzzi, G. Imberti, O. Carpenter, C.B. and Sayegh, M.H. (1995) Blocking cell microtubule assembly inhibits the alloimmune response in vitro and prolongs renal allograft survival by inhibition of Th1 and sparing of Th2 cell function in vivo. *J. Am. Soc. Nephrol.* 5(7): 1418-25

Arem, A.J and Madden, J.W. (1976) Effects of stress on healing wounds, I. Intermittent noncyclical tension. *J. Surg. Res.* 20:93-102.

Arora, P.D. Bibby, K.J. and McCulloch, C.A. (1994) Slow oscillations of free intracellular calcium ion concentration in human fibroblasts responding to mechanical stretch. *J. Cell. Physiol.* 161(2):187-200

Asaga, H, Kikuchi, S, and Yashizato, K. (1991) Collagen gel contraction by fibroblasts requires cellular fibronectin but not plasma fibronectin. *Exp. Cell Res.,* 193:167-174.

Avila, J. Ulloa, L. Gonzalez, J. Moreno, F. and Diaz-Nido, J. (1994) Phosphorylation of microtubule-associated proteins by protein kinase CK2 in neuritogenesis. *Cell. Mol. Biol. Res.* 40(5-6): 573-9

Badger, A.M. (1984) Detection of biological response modifiers of natural origin: a review, *Dev.Ind.Microbiol.* 25: 277-91

Bell, E. (1995) Deterministic models for tissue engineering. *J. Cell. Eng.* 1:28-34.

Bell, E., Iverson, B. and Merrill, C. (1979) Production of a tissue like structure by contraction of collagen lattice by human fibroblast of different proliferative potential in vitro. *Proc. Nat. Acad. Sci.* 76:1274-1278

Bellows, C. Melcher, A. Aubin, J. (1982) Association between tension and orientation of peridontal ligament fibroblasts and exogenous collagen fibres in collagen gels in-vitro. *J. Cell Sci.* 58:125-138.

Bellows, C. Melcher, A. Bhargava, U. Aubin, J. (1982) Fibroblasts contracting three-dimensional collagen gels exhibit ultrastructure consistent with either contraction or protein secretion. *J Ultrastruct Res* 78: 178-192.

Bergman, J.E. Kupfer, A. Singer S.J. (1983) Membrane insertion at the leading edge of motile fibroblasts. *Proc.Natl.Acad.Sci.* 80:1367-1371.

Bershadsky, A..D. and Vasiliev, J.M. (1988) *Cytoskeleton,* Plenun Press, New York,

Bouvard, V. Germain, L. Rompre, P. Roy, B. Auger, F.(1992). Influence of dermal equivalant maturation on the development of a cultured skin equivalent. *Biochem Cell Biol* 70: 34-42

Bray, D. (1979) Mechanical tension produced by nerve cells in tissue culture. *J. Cell. Sci.* 37: 391-410

Bray, D. (1984) Axonal growth in response to experimentally applied mechanical tension. *Dev. Biol.* 102(2): 379-89

Brown, R.A.. Blunn, G.W. and Ejim, O.S. (1994) Preparation of orientated fibrous mats from fibronectin: composition and stability. *Biomaterials* 15:457-461.

Brown, R.A. Talas, G. Porter, R.A. McGrouther, D.A. and Eastwood, M. (1996) Balanced mechanical forces and microtubule contribution to fibroblast contraction. *J. Cell Physiol* In Press.

Brown R. Porter, R. McGrouther, D and Eastwood, M. (1996) Fibroblast responses within mechanically loaded collagen matrices: Mechanical homeo-stasis. *Wound Repair and Regeneration.* 4.1:146 (ab).

Burges, L.P.A., Morin, G.V., Rand, M., Vossughi, J. and Hollinger, J.O. (1990). Wound healing: Relationships of wound closing tension to scar width in rats. *Arch. Otolaryngol. Head & Neck Surg.* 116:798-802.

Burt, A. M. and McGrouther, D. A. (1992). Production and use of skin cell cultures in theraputic situation. In *Animal Cell Biotechnology* pp 150-168. Academic Press, New York.

Butt, R.P. Laurent, G.J. and Bishop, J.E. (1995) Mechanical load and polypeptide growth factors stimulate cardiac fibroblast activity. *Ann. N. Y. Acad. Sci.* 752: 387-93

Cao, Y. Vacanti, JP. Ma, X. Paige, KT. Upton, J. Chowanski, Z. Schloo, B. Langer, R. and Vacanti, CA. (1994) Generation of neo-tendon using synthetic polymers seeded with tenocytes.: *Transplant. Proc.* 26(6): 3390-2

Carter, S.B. (1967) haptotaxis and the mechanism of cell motility. *Nature.* 213:256-260

Carver, W. Nagpal, M.L. Nachtigal, M. Borg, T.K. and Terracio, L. (1991) Collagen expression in mechanically stimulated cardiac fibroblasts. *Circ. Res.* 69(1):116-22

Chamberlain, J. Shah, M. and Ferguson, M.W. (1995) The effect of suramin on healing adult rodent dermal wounds *J. Anat.* 186:87-96

Chen, Y. Centonze, V.E. Verkhovsky, A. and Borisy, G.G. (1995) Imaging of cytoskeletal elements by low-temperature high-resolution scanning electron microscopy. *J. Microsc.* 179 (Pt 1): 67-76

Chvapil, M. Peacock, E.E, Carlson, E.C. Blau, S. Steinbronn, K. Morton, D. (1980) Colchicine and wound healing. *J. Surg. Res.* 49-56.

Chiquet-Ehrismann, R. Tannheimer, M. Koch, M Brunner, A. Spring, J. Martin, D. (1994) Tenasci C expression by fibroblasts is elevated in stressed collagen gels. *J. Cell. Biol.* 127: 2093-2101.

Cima, L.G. Vacanti, J.P. Vacanti, C. Ingber, D. Mooney, D. and Langer, R. (1991) Tissue engineering by cell transplantation using degradable polymer substrates. *J. Biomech. Eng.* 113(2): 143-51

Clark, RA.(1989) Wound repair. *Curr. Opin. Cell. Biol.* 1(5): 1000-8

Cockburn, C.G. and Barnes, M.J. (1991) Characterization of thrombospondin binding to collagen (type I) fibres: role of collagen telopeptides. *Matrix.* 11(3):168-76

Danowalski, B.A. (1989) Fibroblast contractility and actin organisation are stimulated by microtubule inhibitors. *J. Cell. Sci.* 93:255-266.

Danowski, B.A. and Harris, A. (1988) Changes in fibroblast contractility, morphology and adhesion in response to a phorbol ester tumor promoter. *Exp. Cell Res.* 177:47-59.

De-Vries, H.J. Zeegelaar, J.E. Middelkoop, E. Gijsbers, G. Van-Marle, J. Wildevuur, C.H. and Westerhof, W. (1995) Reduced wound contraction and scar formation in punch biopsy wounds. Native collagen dermal substitutes. A clinical study. *Br. J. Dermatol.* 132(5): 690-7

Delvoye, P. Wiliquet, P. Leveque, J. L. Nusgens, B. V. and Lapiere, C. M. (1991). Measurement of mechanical forces generated by skin fibroblasts embedded in a three-dimensional collagen gel. *J. Invest. Dermatol.* 97:898-902.

Dennerll T.J, Joshi V.L, Steel R.E, Buxaum R.E, Heidemann S.R. (1988) Tension and compression in the cytoskeleton of PC-12 neurites II: Quantitative measurements. *J.Cell Biol.* 107:665-674.

Dixit, V. (1994) Development of a bioartificial liver using isolated hepatocytes. *Artif. Organs.* 18(5): 371-84

Dunkelman, N.S. Zimber, M.P. LeBaron, R.G. Pavelec, R. Kwan, M. and Purchio, A.F. (1995) Cartilage production by rabbit articular chondrocytes on polyglycolic acid scaffolds in a closed bioreactor system. *Biotechnol.Bioeng.* 46, 4: 299-305

Eastwood, M., McGrouther, D. A. and Brown, R. A. (1994) A culture force monitor for measurement of contraction forces generated in human dermal fibroblast cultures: evidence for cell-matrix mechanical signalling. *Biochim. Biophys. Acta.* 1201:186-192.

Eastwood, M. Prajapati, R.T. McGrouther, D.A. and Brown, R.A. (1995) Effects of microtubule disruption on collagen contraction by human dermal fibroblasts: a quantitative study. *Wound Repair and Regeneration.* 3.1:88 (ab).

Eastwood, M., Porter, R., Khan, U., McGrouther, D.A., Brown, R.A. (1996) Quantitative Analysis of Collagen Gel Contractile Forces Generated by Dermal Fibroblasts and the Relationship to Cell Morphology.*J Cell Physiol.* 166: 33-45

Eastwood, M. Prajapati, R.T. McGrouther, D.A. and. Brown. R.A. (1996) Fibroblast responses within mechanically loaded collagen matrices: Morphological changes. *Wound Repair and Regeneration.* 4.1:150 (ab).

Ehrlich, H. P. and Rajaratnan, J. B (1990). Cell locomotion forces versus cell contraction forces for collagen lattice contraction: An in vitro model of wound contraction. *Tissue. Cell.* 22, 407-417.

Ehrman, R. and Grey, G. (1956) The growth of cells on a transparent gel of reconstituted rat-tail collagen *J. Natl. Cancer Inst.* 16:1375-1403.

Elsdale, and Bard (1972) Collagen substrata for studies on cell behaviour. *J. Cell Biol.* 54:626-637.

Ejim, O.S. Blunn, G.W. Brown, R.A. (1993) Production of artificial-orientated mats and strands from plasma fibronectin: a morphological study. *Biomaterials* 14: 743-748

Farsi, J. and Aubin, J. (1984). Microfilament rearrangements during fibroblast-induced contraction of three-dimensional hydrated collagen gels. *Cell. Motil.* 4:29-40.

Ferdman, A.G. and Yannas, I.V. (1993) Scattering of light from histologic sections: a new method for the analysis of connective tissue. *J.Invest.Dermatol.* 100(5): 710-6

Finesmith, T. H., Broadley, K. N. and Davidson, J. M. (1990). Fibroblasts from wounds of different stages of repair vary in their ability to contract a collagen gel in response to growth factors. *J. Cell. Physiol.* 144, 99-107

Freed, LE. Vunjak-Novakovic, G. Biron, RJ. Eagles, DB. Lesnoy, DC. Barlow. SK. and Langer, R. (1994) Biodegradable polymer scaffolds for tissue engineering. *Biotechnology. N. Y.* 12(7): 689-93

Gabbani, G., Hirschel, B. J., Ryan, G. B., Statkov, P. R. and Majno, G. (1972) Granulation tissue as a contractile organ: A study of structure and function. *J. Exp. Med.* 135: 719-725.

Gabbiani, G., Chaponnier, C. and Huttner, I. (1978) Cytoplasmic filaments and gap junctions in epithelial cells and myofibroblasts during wound healing. *J. Cell. Biol.* 76: 561-568.

Gail M.H. Boone CW. (1971) Effect of colcemid on fibroblast motility *Exp.Cell Res.* 65:221-227.

Garana, R. M. Petroll, W. M. Chen, W. T. Herman, I. M. Barry, P. Andrews, P. Cavanagh, H. D. and Jester, J.V. (1992). Radial keratotomy II. The role of the myofibroblast in corneal wound healing. *Invest. Ophthalmol. Vis. Sci.* 33: 3271-3282

Girard, P.R. and Nerem, R.M. (1993) Endothelial cell signaling and cytoskeletal changes in response to shear stress. *Front. Med. Biol. Eng.* 5(1): 31-6

Greenberg, G. and Boyde, A. (1993). Novel method for stereo imaging in light microsocpy at high magnifications. *Neuroimage.* 1: 121-128.

Grinnell, F. (1994). Fibroblasts, myofibroblasts, and wound contraction. *J. Cell. Biol.* 124: 401-404.

Grinnell, F. and Lamke, C.R. (1984). Reorganisation of hydrated collagen lattices by human skin fibroblasts. *J. Cell. Sci.* 66: 51-63

Guidry, C. and Grinnell, F. (1985). Studies on the mechanism of hydrated collagen gel reorganisation by human skin fibroblasts. *J. Cell. Sci.* 79, 67-81.

Guidry, C. Grinnell, F. (1986) Contraction of hydrated collagen gels by fibroblasts: evidence for two mechanisms by which collagen fibrils are stabilized. *Collagen Rel Res* 6: 515-529

Gullberg, D. Tingstrom, A.. Thuresson, A.C. Olsson, L. Terracio, L. Borg, T.K. and Rubin, K. (1990) Beta-1 integrin-mediated collagen gel contraction is stimulated by PDGF. *Exp. Cell Res.* 186:264-272.

Gross, J. (1958) Collagen substrata for studies on cell behaviour. *J Exp Med* 107: 265.

Harris, A.K. (1973) Behavior of cultured cells on substrata of variable adhesiveness, *Exp Cell Res.* 77:285:297

Harris, A. K., Wild, P.and Stopak, D. (1980).Silicon rubber substrata: A new wrinkle in the study of cell locomotion. *Science.* 208:177-179.

Harris, A. K., Stopak, D. and Wild, P. (1981). Fibroblast traction as a mechanism for collagen morphogenesis. *Nature.* 290: 249-251.

Harris, A. (1988) *Methods in Enzymology* Vol 163.

He, Y. and Grinnell, F. (1994) Stress relaxation of fibroblasts activates a cyclic AMP signaling pathway. *J. Cell. Biol.* 126(2): 457-64

Herrick, S.E. Sloan, P, McGurk, M. Freak, L. McCollum, C.N. and Ferguson, M.W. (1992) Sequential changes in histologic pattern and extracellular matrix deposition during the healing of chronic venous ulcers. *Am. J. Pathol.* 141(5): 1085-95

Hennessey, E.S. Drummond, D.R. and Sparrow, J.C. (1991) Post-translational processing of the amino terminus affects actin function. *Eur. J. Biochem.* 197(2): 345-52

Higton, D. and James, D. (1964). The contraction of full thickness wounds of rabbit skin. *Br. J. Surg.* 51:462-466.

Hodge, A.J. Highberger, J.H. Deffner, G.G.J. Schmitt, F.O. (1960) The effects of proteases on the tropocollagen macromolecule and on its aggregation properties. *Proc Nat Acad Sci 46*: 186

Ingber, D.E. (1993) Cellular tensigrity: defining new rules of biological design that govern the cytoskeleton. *J. Cell Sci.* 104:613-627

Ingber. D. Integrins as nechanochemical transducers. (1991) *Curr. Opin. Cell Biol.* 3:841-848.

Ingber, D.E. (1990) Fibronectin controls capilary endothelial cell growth by modulating cell shape. *Proc. Nat. Acad. Sci.* 87: 3579-3583.

Jamney P.A., Euteneuer, U., Traub, P., Schliva, M. (1991) Viscoelastic properties of vimentin compared with other filamentous biopolymer networks. *J. Cell. Biol.* 113;155-160.

John, V.B. (1972) In *An introduction to engineering materials.* Published by McMillian.

Kanda, K. and Matsuda, T. (1993) Behavior of arterial wall cells cultured on periodically stretched substrates.*Cell. Transplant.* 2(6): 475-84

Kasugai, S., Suzuki, S., Shibata, S., Amano, H,. and Ogura, H. (1990) Measurements of the isometric contractile forces generated by dog periodontal ligament fibroblasts in vitro. *Archs oral Biol.* 35: 597-601.

Kerstein, M.D. (1995) Moist wound healing: the clinical perspective *Ostomy. Wound. Manage.* 41(7A Suppl): 37S-44S; discussion 45S

Khaw, P. T., Occleston, N. L., Schultz, G., Grierson, I., Sherwood, M. B. and Larkin, G. (1994) Activation and suppression of fibroblast function. *Eye.* 8, 188-195.

Kischer, CW. Shetlar, MR. and Shetlar CL. (1975) Alteration of hypertrophic scars induced by mechanical pressure. *Arch. Dermatol.* 111:60-64.

Kolodney, M. S. and Wylsolmerski, R. B. (1992) Isometric contraction by fibroblasts and endothelial cells in tissue culture: A quantitative study. *J Cell Biol* 117: 73-82.

Kolodney, M.S. and Elson, E.L. (1995) Contraction due to microtubule disruption is associated with increased phosphorylation of myosin regulatory light chain. *Proc. Natl.Acad.Sci.* 92:10252-10256.

Lambert, C. A., Soudant, E. P., Nusgens, B. V. and Lapiere, C. M. (1992). Pretranslational regulation of extracellular matrix molecules and collagenase expression in fibroblasts by mechanical forces. *Lab. Invest.* 66, 444-451.

Lampidis, T.J. Kolonias, D. Savaraj, N. and Rubin, R.W. (1992) Cardiostimulatory and antiarrhythmic activity of tubulin-binding agents. *Proc. Natl. Acad. Sci*; 89(4): 1256-60

Larson,D. Abston, B., Dobrkovsky, M. and Linares, A. (1971) Techniques for decreasing scar formation and contractures in the burned patient. *J. Trauma.* 11:807-823.

Leibovich, S.J. and Weiss, J.B. (1970) Electron microscope studies of the effects of endo- and exopeptidase digestion on tropocollagen. A novel concept of the role of terminal regions in fibrillogenesis. *Biochim. Biophysica. Acta.* 214:445-454.

Lewis-Alberti, L. (1989) Altering the vector of polarity of BHK syncytia changes their motile behavior. *Cell. Motil. Cytoskeleton.* 14(2): 187-93

Letourneau, P.C (1975) Cell-to-substratum adhesion and guidance of axonal elongation. *Dev. Biol.* 44(1): 92-101

Letourneau, P.C. (1975) Possible roles for cell-to-substratum adhesion in neuronal morphogenesis. *Dev. Biol.* 44(1): 77-91

Letourneau, P.C. Shattuck, T.A. and Ressler, A.H. (1987) "Pull" and "push" in neurite elongation: observations on the effects of different concentrations of cytochalasin B and taxol. *Cell. Motil. Cytoskeleton.* 8(3): 193. 209

Luduena, R.F., Roach, M.C. (1981) Contrasting effects of maytansine and vinblastine on the alkylation of tubulin sulphydrls. *Arch. Biophys. Biochem.* 210:498-504.

Madreperla, S.A. and Alder, R. (1989) Opposing microtubular and actin dependent forces in the development and maintenance of structural polarity in retinal photoreceptors. *Dev.Biol.* 131:149-160.

Manfredi, J.J. Parness, J. Horowitz, S.B. (1982) Taxol binds to cellular microtubules. *J.Cell Biol.* 94:688-696.

Margolis, L.B. and Popov, S.V. (1991) Induction of cell processes by local force. *J.Cell.Sci.* 98 (Pt 3): 369-73

Mauch, C. and van der Mark, K. (1988) A defective cell surface collagen binding protein in dermatosparactic sheep fibroblasts. *J Cell Biol* 106: 205-211

Mayne, R. and Brewton, RG. (1993) New members of the collagen superfamily. *Curr.Opin.Cell.Biol.* 5(5): 883-90

Millis, A. J., Hoyle, M., McCue,H. M. and Martin, H. (1992) Differential expression of metalloproteinase and tissue inhibitor of metalloproteinase genes in aged human fibroblasts. *Exp. Cell. Res.* 210: 373-379.

Mochitate, K., Pawelek, P. and Grinnell. F. (1991) Stress-relaxation of contracted collagen gels: Disruption of actin filament bundles, release of surface fibronectin, and down-regulation of DNA and protein synthesis. *Exp. Cell. Res.* 193:198-207.

Mooney, D.J. Organ, G. Vacanti, J.P. and Langer, R. (1994) Design and fabrication of biodegradable polymer devices to engineer tubular tissues. *Cell. Transplant.* 3(2): 203-10

Mooney, J. Park, S. Kaufmann, P.M. Sano, K. McNamara, K. Vacanti, J.P. and Langer, R. (1995) Biodegradable sponges for hepatocyte transplantation.*J. Biomed. Mater. Res.* 29(8): 959-65

Nakagawa, S. Pawelek, P. and Grinnell, F. (1989) Long-term culture of fibroblasts in contracted collagen gels: effects on cell growth and biosynthetic activity. *J. Invest. Dermatol.* 93(6): 792-8

Nishiyama, T. Tommaga, N. Nakayama, Y. and Hayashi, T. (1988). Quantitative evaluation of the factors affecting the process of fibroblast-

mediated collagen gel contraction by separating the process into three phases. *Coll. Rel. Res.* 8:259-273.

Nishiyama, T. Tsunenaga, M. Nakayama, Y. Adachi, E. and Hayashi, T. (1989). Growth rate of human fibroblasts is repressed by the culture within reconstituted collagen matrix but not by the culture on the matrix. *Matrix.* 9:193-199.

Parry, J.M. (1993) An evaluation of the use of in vitro tubulin polymerisation, fungal and wheat assays to detect the activity of potential chemical aneugens. *Mutat. Res.* 287(1): 23-8

Peacock K.C. Hanna D.P. Kirkpatrick K. Breidenbach W.C. Lister G.D. and Firrell, J (1988) Efficacy of perioperative cefamandole with postoperative cephalexin in the primary outpatient treatment of open wounds of the hand. *J. Hand. Surg. Am.* 13(6): 960-4

Pollard, T. Fujiwari, K. Niederman, R. and Maupin-Szamier, P. (1976). In *Cell Motility.* (Goldman. R., Pollard, T. & Rosenbaum, J. Eds) pp 689-724 Published by Coldspring Harbour Laboratory Press, New York.

Rasmussen, C.D. and Means, A.R. (1992) Increased calmodulin affects cell morphology and mRNA levels of cytoskeletal protein genes. *Cell. Motil. Cytoskeleton.* 21(1): 45-57

Reddi, AH. (1994) Symbiosis of biotechnology and biomaterials: applications in tissue engineering of bone and cartilage. *J.Cell.Biochem.* 56, 2: 192-95

Rockwell, W. Cohen, I. and Ehrilch, H. (1989) Keloids and hypertrophic scars: A comprehensive review. *Plastc Reconstr. Surg.* 84:827-837.

Rudolph, R. Woodward, M. (1978) Spatial orientation of microtubules in contractile fibroblasts in vivo. *Anat.Rec.* 191:169-182.

Rudolph, R. (1980) Contraction and the control of contraction. *World J. Surg.* 4:279-287

Rudolph, R., Vande Berg, J. and Ehrlich, H. P. (1992). Wound contraction and scar contracture. In *Wound Healing: Biochemical and Clinical Aspects.* pp 96-114. W.B. Saunders Co., Philadelphia.

Rubin, A.L. Pfahl, P. Speakman, P.T. Davison, P.F. Schmitt, F.O. (1963) *Science* 139: 37

Schwienbacher, C. Magri, E. Trombetta, G. and Grazi, E. (1995) Osmotic properties of the calcium-regulated actin filament. *Biochemistry.* 34(3): 1090-5

Shah, M. Foreman, D.M. and Ferguson, M.W. (1995) Neutralisation of TGF-beta 1 and TGF-beta 2 or exogenous addition of TGF-beta 3 to cutaneous rat wounds reduces scarring. *J. Cell. Sci.* 108:985-1002

Slichenmyer, W.J. and Von-Hoff, D.D. (1991) Taxol: a new and effective anti-cancer drug. *Anticancer. Drugs.* 2(6): 519-30

Stopak, D. and Harris, A. K. (1982). Connective tissue morphogenesis by fibroblast traction. I Tissue culture observations. *Dev. Biol.* 90:383-398.

Tomasek, J. J. Haaksma, C. J. Eddy, R. J. and Vaughan, M. B. (1992). Fibroblast contraction occures on release of tension in attached collagen lattices: Dependancy on an organised actin cytoskeleton and serum. *Anat. Rec.* 232:359-368.

Tomasek, J. J. and Hay, E. D. (1984) Analysis of the role of microfilaments and microtubles in acquistion of bipolarity and elongation of fibroblasts in hydrated collagen gels. *J. Cell. Biol.* 99:536-549.

Torry, D. J. Richards, C. D. Podor, T. J. and Gauldie, J. (1994). Anchorage-independent colony growth of pulmonary fibroblasts derived from fibrotic human lung tissue. *J. Clin. Invest.* 93:1525-1532.

Trinkaus, J. (1984) *Cells into Organs*. Prentice Hall Inc. New Jersey. USA.

Tranquillo, R. T. and Murray, J. D. (1992) Continuum model of fibroblast-driven wound contraction: inflamation-mediation. *J. Theor. Biol.* 158: 135-172.

Tziampazis, E. and Sambanis, A. (1995) Tissue engineering of a bioartificial pancreas: modeling the cell environment and device function. *Biotechnol. Prog* 11(2): 115-26

Van Winkle. W. Jnr. (1967). Wound contraction. *Surg. gynecol. Obstet.* 125:131-142.

Vande Berg, J. S. Gelberman, R. H. Rudolph, R. Johnson, D. and Sicurello, P. (1984). Dupuytrens disease: comparitative growth dynamics and morphology between cultured myofibroblasts (nodule) and fibroblasts (cord). *J. Orth. Res.* 2:247-256

Vandenburgh, H.H. (1988) A computerised mechanical cell stimulator for tissue culture: effects on skeletal muscle organogenesis. *In. Vitro. Cell. Dev. Biol.* 24:609-619.

Vandenburgh, H.H. and Karlisch, P. (1989) Longitudinal growth of skeletal myotubes in vitro in a new horizontal mechanical cell stimulator. *In. Vitro. Cell. Dev. Biol.* 25:607-616.

Vandenburgh, H.H. Shansky, J. Solerssi, R. and Chromiak, J. (1995) Mechanical stimulation of skeletal muscle increases prostraglandin F2 alpha production, cylclooxygenase activity, and cell growth by a toxin sensitive mechanism. *J. Cell. Physiol.* 163:285. 294.

Ward, R.S. (1991) Pressure therapy for the control of hypertrophic scar formation after burn injury. A history and review. *J-Burn. Care. Rehabil.* 12(3): 257-62

Weihrauch, D. Zimmermann, R. Arras, M. and Schaper, J. (1994) Expression of extracellular matrix proteins and the role of fibroblasts and macrophages in repair processes in ischemic porcine myocardium *Cell. Mol. Biol. Res.* 40(2): 105-16

Weiss, J.B and Ayad, S. (1982) An introduction to collagen. In *Collagen in Health and Disease.* Published by Churchill Livingstone. Eds. J. B. Weiss and M.V. Jayson.

Wood, G. Keech, K. (1960) The formation of fibrils from collagen solutions. (1) The effect of experimental conditions: Kinetics and electron microscope studies. *J Biochem* 75: 588-597.

Wood, G. (1960) The formation of fibrils from collagen solutions. (2) Mechanisms of collagen-fibril formation *J Biochem* 75: 598-605.

Wood, G. (1960) The formation of fibrils from collagen solutions. (3) Effects of chondroitin sulphate and some naturally occuring pollyanions on the rate of formation. *J Biochem* 75: 605-612.

Appendix. Publications, oral papers, poster presentations and other output generated as a result of this study

Publications.

M. Eastwood, D. Gus McGrouther, R.A. Brown,
"A Culture Force Monitor for Measurement of Contraction Forces Generated in Human Dermal Fibroblast Cultures: Evidence for cell-matrix mechanical signalling". Published in *Biochima Et Biophysica Acta* November 1994 1201 186-192.

M. Eastwood, R. Porter, U. Khan, G. McGrouther, R. Brown.
"Quantitative analysis of collagen gel contractile forces generated by dermal fibroblasts and the relationship to cell morphology." Published in the *Journal of Cellular Physiology* vol. 166 pg. 33-42 January 1996

C. Cacou, M. Eastwood, D. McGrouther, R. Brown.
"A culture force monitor for investigating the function of adhesions between tissue interfaces in vitro". Published in the *Journal of Cellular Engineering.* vol. 1 pg. 109-114. April 1996.

A. Wilson, D. McGrouther, M. Eastwood, R. Brown.
"The effect of burn blister fluid on fibroblast contraction" In press, *British Journal of Plastic Surgery.*

R. Brown, G. Talas, R. Porter, D. McGrouther, M. Eastwood.
"Balanced mechanical forces and microtubule contribution to fibroblast contraction." In press *Journal of Cellular Physiology.*

Oral Papers

M. Eastwood, R.A. Brown.
"Development of a Sensitive Robust Device for Measurement of Forces Generated by the Contraction of Human Fibroblasts in Culture". presented at the International Conference of The Wound Healing Society and The European Tissue Repair Society. Amsterdam, August 23-26 1993, also published in *Wound Repair and Regeneration* June 1993: vol. 1:(2) 102

U. Khan, N. Occleston, M. Eastwood, P. Khaw, D.A. McGrouther.
"The Behaviour of Endotenon and Synovial Sheath Fibroblasts in Collagen Gels" Presentation at The European Tissue Repair Society. Oxford 5-8 September 1994.

R. Brown, M. Eastwood, R. Porter, C. Cacou, R. Prajapati.
"Tensile forces in fibroblast cultures and models of tissue repair". Presented at the Society for Experimental Biology meeting, St. Andrews, Scotland 3-4 April 1995.

M. Eastwood, R.T. Prajapati, D.A. McGrouther, R.A. Brown.
"Effects of microtubule disruption on collagen contraction by human dermal fibroblasts: a quantitative study". Presented at the Wound Healing Society meeting Minniapolis Minnesota USA April 27-30 1995, also published in *Wound Repair and Regeneration.* vol. 3.1 pg. 88 March 1995

M. Eastwood, R. Prajapati, G, Mcgrouther, R. Porter, and R. Brown.
"Mechatronic devices for the measurement and precise application of mechanical loads onto fibroblast populated collagen lattices". Presented at the International conference of Cellular Engineering. 19-22 August, 1995. San Diego California USA.

G. Talas, M. Eastwood, Z. Ahmed, D. McGrouther, R. Brown. "Quantitative measurement of contractile forces generated by fibroblasts from normal and pathologic skin." Presented at the International conference of the European Tissue Repair Society. Padova, Italy. September 1995.

C. Cacou, R. Brown, K. Smith, R. Prajapati, M. Eastwood, D.A. McGrouther "An in-vivo model for studying adhesion formation". Presented at the International conference of the European Tissue Repair Society. Padova, Italy. September 1995.

R. Brown, R. Porter, R. Prajapati, B. Idowu, and M. Eastwood. "Cell-substrate contact and mechanical loading as organisational cues in tissue repair and graft engineering". Presented at the n+n Cellular Engineering meeting. Corronado, California, USA. August 23-24 1995.

R. Brown. M. Eastwood. R. Porter. R. Prajapati. G. Terenghi. G. McGrouther. "Substrate guidance and mechanical cues in cellular engineering". Presented at the n + n Cellular Engineering meeting. Japan, March 1996.

M. Eastwood, R. Prajapati, D. McGrouther, R. Brown. "Fibroblast responses within mechanically loaded collagen matrices: Morphological changes". Presented at the Joint European Tissue Repair Society and Wound Healing Society meeting Boston USA. May 15-19 1996 also published in *Wound Repair and Regeneration.* vol. 4.1 pg. 150 March 1996.

R. Brown R. Porter, D. McGrouther, M. Eastwood.
"Fibroblast responses within mechanically loaded collagen matrices: Mechanical homeo-stasis". Presented at the Joint European Tissue Repair Society and Wound Healing Society meeting Boston USA. May 15-19 1996 also published in *Wound Repair and Regeneration.* vol. 4.1 pg. 146 March 1996.

Poster presentations.

M. Eastwood, R.A. Porter, K. Smith, D.A. McGrouther, R.A. Brown.
"Force Measurement and Fibroblast Morphology during early phase Collagen Gel Contraction." Presented at The European Tissue Repair Society. Oxford 5-8 September 1994.

M. Eastwood, R. Porter, U. Khan, D. McGrouther, R. Brown
"Fibroblast contraction of a collagen gel is a multiphase process, evidence for fibroblast subpopulations." Presented at The European Tissue Repair Society. Oxford 5-8 September 1994.

M. Eastwood, R. Porter, U. Khan, D. McGrouther, R. Brown
"Collagen gel contraction phases and fibroblast morphology". Presented at the Federation of European Connective Tissue Societies. Lyon, France. 1-3 September 1994.

R. Prajapati, M. Eastwood, R. Brown.
"Induction of proteases by mechanically loaded fibroblasts during contraction". Presented at the British Connective Tissue Society meeting, Bristol, April 10/11 1996.

K. Sethi, M. Eastwood, I. Yannas, R. Brown.
"Quantitation of cell-matrix interaction during contraction." Poster presented at the British Connective Tissue Society meeting, Bristol, April 10/11 1996.

Other Output.

M. Eastwood.
"In vitro measurement of cell contraction". Invited lecture at the Massachusetts Institute of Technology, Boston, Massachusetts, USA 2 May 1995.

D. McGrouther, M. Eastwood, P. Khaw, G. Schultz, P. Martin, and R. Brown
"Wound contraction - why do wounds grow smaller?" Exhibitor at the Royal Society Summer Exhibition "New Frontiers in Science", London 21-22 June 1995.